FEASIBILITY STUDY OF A STEP SCANNED OMNIDIRECTIONAL COMMUNICATIONS ANTENNA FOR AN INTERNATIONAL MAGNETOSPHERIC EXPLORER SPACECRAFT

Prepared By:

Richard E. Herskind
Avco Corporation Systems Division
201 Lowell Street
Wilmington, Massachusetts 01887

October 22, 1974
Final Report (1 April 1974 - 22 July 1974)

Prepared For:

Goddard Space Flight Center
Greenbelt, Maryland 20771

TECHNICAL REPORT STANDARD TITLE PAGE

1. Report No.	2. Government Accession No.	3. Recipient's Catalog No.

4. Title and Subtitle	5. Report Date
Feasibility Study of a Step Scanned Omni-directional Communications Antenna for An International Magnetispheric Explorer Spacecraft	October 28, 1974
	6. Performing Organization Code: -
7. Author(s): Richard E. Herskind	8. Performing Organization Report No.: AVSD-0298-74-RR
9. Performing Organization Name and Address: Avco Corporation Systems Division, 201 Lowell Street, Wilmington, Massachusetts 01887	10. Work Unit No.: -
	11. Contract or Grant No.: NAS5-20020
12. Sponsoring Agency Name and Address: Goddard Space Flight Center, Greenbelt, Maryland 20771, Robert Jackson, Technical Monitor	13. Type of Report and Period Covered: Final Report, 1 Apr. - 22 July 1974
	14. Sponsoring Agency Code: -

15. Supplementary Notes

16. Abstract

The results of the subject study has indicated that omnidirectional antennas requiring directive gains steered off broadside are limited by the feed system efficiencies. The directive gain can be increased to offset the feed losses, but this approach leads quickly to diminishing returns. While gains of 4.8 db appear feasible, a system gain of 3.0 db is considered practical. These results apply to antenna configurations limited in packaging volume to 10 cm diameter by 61 cm length.

17. Key Words (Selected by Author(s))	18. Distribution Statement
step scanned array, omnidirectional antenna, antenna feed efficiency	-

19. Security Classif. (of this report)	20. Security Classif. (of this page)	21. No. of Pages	22. Price*
Unclassified	-	133	

*For sale by the Clearinghouse for Federal Scientific and Technical Information, Springfield, Virginia 22151.

Preface

A) Objective:

The objective of this report was to investigate the feasibility of design of an omnidirectional communication antenna which could be step scanned to ± 30° from the broadside position. The antenna gain desired of this antenna was 6.0 db peak. The results of the study is to recommend a laboratory feasibility demonstration leading to a flight development program.

B) Scope:

The scope of the work was limited to theoretical analysis utilizing Avco computer codes for aperture configuration definition. Layouts and estimated efficiencies of antenna feed and phase switching networks were made to provide a selection of a preferred approach to the antenna design.

C) Conclusions:

The results of this study has shown that the physical implementation of the desired design goals including packaging volume can not be met in their entirety. Directive gains of 6.0 db can easily be achieved but the real world of feed configuration and losses limit the peak gain to approximately 4.8 db with a 5 row axial arrayed aperture. The gain at the off boresight angles of ± 30° decrease to 4.5 db. With only 2 beam positions off broadside, the gain at the crossover points decreases to -2.50 db.

To achieve 6.0 db gain over a sector ± 30° from broadside, requires increased directive gain by increased axial length of aperture. This requirement in turn increases feed system complexity which increases total feed system losses, reducing the realizable gain. The increased directivity with its narrow pattern, requires finer incremental stepping to maintain the desired gain, thus further complicating the feed system phase steering design. A point of diminishing returns occurs and limits the practical gains achievable.

D) Summary of Recommendations:

The results of this study suggest that a review be made of the communication system requirements to determine if the antenna system gain can be relaxed from the 6.0 db. A practical gain over the sector of ± 30° would be in the order of 3.0 db.

Should the peak gain of 4.8 db be acceptable, a detail investigation should then be made to define a specific aperture configuration and feed distribution network. A laboratory evaluation of the feed network efficiency should be made to more accurately estimate the system losses due to discontinuities, mutual coupling, and normal insertion loss. Should the system losses be found acceptable, a full-up electrical prototype including aperture radiating element and feed system is recommended to establish the expected system gain of a flight unit.

CONTENTS

Preface		v
Illustrations		viii, ix
Tables		x
Para. No.	Title	Page No.
1.0	Introduction	1
2.0	Scope	1
3.0	Summary	2
3.1	Radiating Aperture	2
3.2	Feed Networks	2
4.0	Antenna Configuration Candidates	7
4.1	Cylinder Array Element	13
5.0	Conclusions for Aperture Study	25
6.0	Feed Design	25
6.1	Feed System Components	27
6.2	MXN Array Matrix	28
6.3	Corporate Feed Network	29
6.4	Phase Shifter	34
6.5	Switching Matrix	35
7.0	System Gain Summary	41
8.0	Antenna Configuration 9.0 db	43
9.0	Recommendations for Electrical Design Prototype	49

List of Illustrations

Figure No.	Figure Title	Page No.
1	LA 14767 - IME Antenna - Slot/Dipole Configuration	3
2	LA 14766 - IME Antenna - Cirranslot Configuration	4
3a	LA 14805 - IME Antenna Feed Network - 5 Row x 5 Element Aperture Configuration	5
3b	LA 14806 - IME Antenna Feed Network - Tapered Transformer Option for Corporate Feed (6 Row Feed)	6
4	Cirranslot Radiation Pattern - RHC - Circumferential Plane, 5 Element Circumferential Array x 4 Row Axial Array - $d/\lambda = .53$	9
5	Cirranslot Radiation Pattern - RHC - Axial Plane 5 Element Circumferential Array x 4 Row Axial Array - Broadside Beam 90° $d/\lambda = .53$	10
6	Cirranslot Radiation Pattern - RHC - Circumferential Plane, 5 Element Circumferential Array x 4 Row Axial Array - $\theta = 60^\circ$, $d/\lambda = .53$	11
7	Cirranslot Radiation Pattern, Axial Plane 5 Circumferential Elements x 4 Row Axial Array - $\theta = 60^\circ$ $d/\lambda = .53$	12
8	Cirranslot Radiation Pattern - Axial Plane 5 Circumferential Elements x 4 Row $\theta = 60^\circ$ $d = .7\lambda$	15
9	Peak to Peak Ripple vs Cylinder Radius (Circumferential Plane)	17
10	Radiation Pattern Slot/Dipole Typical E (Slot) Response vs ϕ	18
11	Radiation Pattern Slot/Dipole - Typical E (Dipole) Response vs ϕ	19
12	Radiation Pattern - Slot/Dipole Element in Axial Plane	21
13	Typical Radiation Pattern - Slot/Dipole - Axial Plane (Broadside Pointing)	22
14	Radiation Pattern - Slot/Dipole - Axial Plane (Pointing Angle = 30° From Broadside)	23

List of Illustrations (Cont'd)

Figure No.	Figure Title	Page No.
15	Directivity vs Element Spacing - Slot/Dipole Configuration	24
16	Directivity vs Number of Elements in Axial Plane	26
17	Corporate Feed Configurations	27
18	Corporate Shunt Network Relative Phase of Elements in Circumferential Plane	33
19	Diode Phase Shifter Layout	37
20	Beam Forming Matrix	38
21	SP3T Microstrip R.F. Switch	40
22	Integrated Beam Forming Matrix and Phase Shifters for 7 Row Array	44
23 a	Radiation Pattern - 15 Row Design, $\theta = 90^{\circ}$ ϕ Variable	46
23 b	Radiation Pattern - 15 Row Design, $\phi = 0$ θ Variable	47
24	Schematic - Feed System of 3 Cascaded 6.0 db IME Arrays	48

List of Tables

Table No.	Title	Page No.
1	Specification Design Goals for Antenna System	1
2	Candidate Antenna Configuration	8
3	Stripline/Microstrip Considerations	29
4	Parameter Values for Shunt Coupled Corporate Feed Network (Configuration C)	32
5	Candidate Diode Phase Shifter Approaches	36
6	Beam Forming Matrix Relative Phase of Row vs Beam Position	38
7	Microstrip Switch Diode Logic	39
8	RF Microstrip Switch-Insertion Loss and Isolation	41
9	System Gain Summary	42
10	Truth Table for 7 Row Beam Forming Matrix	45

FINAL REPORT

AN OMNIDIRECTIONAL STEP SCANNED ARRAY

COMMUNICATIONS ANTENNA

1.0 INTRODUCTION

This report describes work performed under contract towards the definition of a spacecraft communications antenna. The design specification goals for this antenna are listed in Table 1 below.

Table 1

Specifications Design Goals for Antenna System

Frequency:	2.1 and 2.3 GHz
Gain:	6.0 ± 0.5 dBi
Main Beamwidth:	360° steerable to 30° from broadside of antenna
Size:	Cylindrical approx. 10.15 cm x 25.4 cm long
Weight:	1.8 kg or less
Material:	No magnetic material to be used
Polarization:	RHC - 2 dB circularity
VSWR:	1.2:1 or less

The antenna system to be described is to be part of the communications subsystem on the International Magnetospheric Explorer Spacecraft (IME). Amongst the key design goals for the antenna is the requirement to point its main beam perpendicular to the spacecraft spin axis, and at certain orbital locations to skew the beam at the discreet angles of ± 30° from broadside.

The work performed herein has resulted in a design approach suitable for laboratory evaluation.

2.0 SCOPE

The scope of this work was to perform theoretical analysis and tradeoffs which would lead to a preferred design approach. The tradeoffs included the following antenna parameters:

- Array size and form factor
- Array radiating element configuration
- Number of radiating elements required in circumferential plane for roll plane gain uniformity

- Number of radiating elements in axial plane
- Feed network
- Phase shifter considerations

3.0 SUMMARY

The study described in this report is summarized in these paragraphs. There are two viable options differing first in the configuration of the radiating aperture, and secondly in the approach to locating the integrated feed network assembly.

3.1 RADIATING APERTURES

From pattern analysis studies using Avco computer codes for slot and wire antennas, two basic configurations are viable. The first is the slot-dipole configuration shown in Figure 1. Here the dipole and slot fields provide the space and time quadrature signals required for circular polarization. This arrangement has the potential of being most efficient from an aperture illumination viewpoint in that there is no energy being radiated in the axial direction of the elements due to the slot and dipole element patterns having nulls in the axial direction. The disadvantage is that the dipole must sit on a radius larger than the slot, increasing the overall antenna diameter. (A 10 cm diameter design goal was imposed.) The center volume of the antenna is void so as to accommodate a spacecraft subsystem antenna at another frequency. The second aperture option is given in Figure 2. This configuration consists of a circularly polarized annular slot flush mounted on a 10 cm diameter cylinder. The advantage of this configuration is its geometrical simplicity and its maximum diameter of 10 cm. A potential disadvantage is the decreased efficiency due to energy being radiated in the axial direction. Calculations, however, have shown that in an array, the array factor minimizes radiation in the axial direction.

Both of these apertures are prime candidates and are to be investigated in parallel in a subsequent electrical design phase to insure optimum selection.

3.2 FEED NETWORKS

The feed system alternatives are best described by reference to Figure 3.

Figure 3a describes a fully integrated μ -strip feed arrangement which provides individual element excitation via a corporate power divider network. Beam position steering is accomplished by a passive integrated hybrid "beam forming matrix". This phase shifting approach has been chosen to provide increased reliability by eliminating the active components (diodes) required to steer the beam to the required positions. The quadrature time phase signals are provided by μ -strip quadrature hybrids which allow both right and left circular polarization. Finally, a single pole 3 throw μ -strip diode switch (a separate package) is provided to select beam position and polarization.

ENGR CHG	REVISIONS				
	ZONE	LTR	DESCRIPTION	DATE	APPROVED

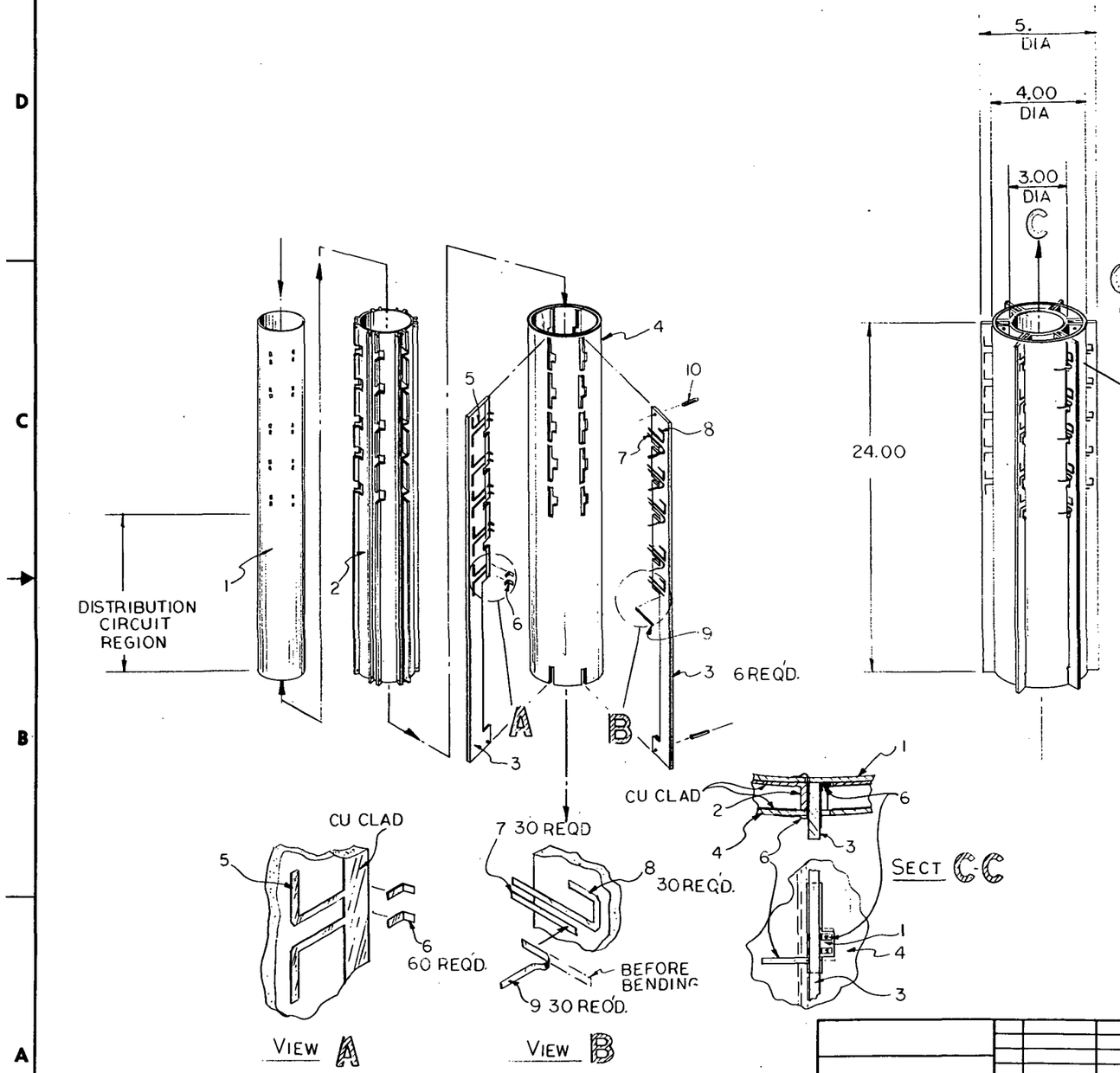

1. INNER CIRCUIT TUBE
2. SPACER
3. DIPOLE BOARD
4. SLOT CYLINDER
5. PRINTED DIPOLE AND BALUN
6. BALUN GROUNDING TABS
7. SLOT FEED STRIP
8. DIPOLE FEED STRIP
9. SLOT FEED STRIP TAB
10. DIPOLE BOARD LOCK

QTY REQD	CODE IDENT	PART OR IDENTIFYING NO.	NOMENCLATURE OR DESCRIPTION	MATERIAL OR NOTE	SPECIFICATION	ZONE	ITEM NO.
	ASSY NO.						

LIST OF PARTS

PART CLASS:	DASH NO.	NEXT ASSY	USED ON	QTY PER NHA	END ITEM NUMBER	SERIAL NO.
DWG CLASS:		APPLICATION			EFFECTIVITY	
ASG BY:						

UNLESS OTHERWISE SPECIFIED
TOLERANCE AND DRAWING INTERPRETATION PER D143
X ± .08 XX ± .04 XXX ± .020
MACHINED ANGLES ± 0° 30'
SHEET METAL BEND ANGLES ± 2°
P10001
SURFACE ROUGHNESS ✓

CONTR NO.	
RELEASE	
DWG APPD	
CHECKED	
DRAWN	Saul McLean 7-8-76
DESIGN APPROVAL	
MANAGER	
SECT CH	
DESIGNER	

AVCO SYSTEMS DIVISION WILMINGTON, MASSACHUSETTS 01887

TITLE
FIGURE 1
IME ANTENNA
DIPOLE/SLOT APERTURE

SIZE	CODE IDENT NO.	DWG NO.
D	04614	LA-14767
SCALE	WT	SHEET

DO NOT SCALE DRAWING

ENGR CHG	REVISIONS				
	ZONE	LTR	DESCRIPTION	DATE	APPROVED

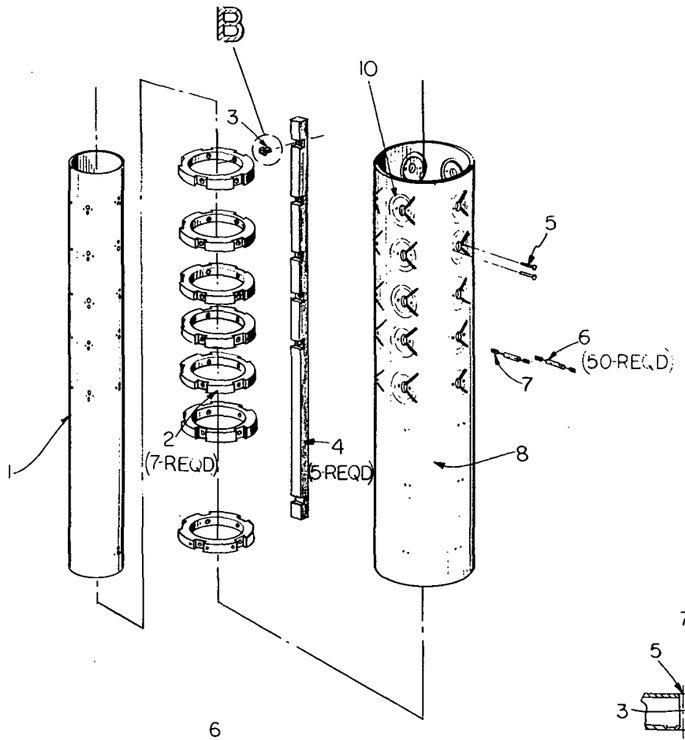

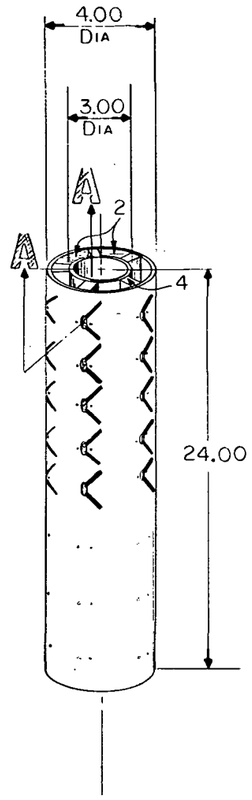

1. INNER CIRCUIT TUBE
2. CAVITY LIMIT RINGS
3. FEED SUPPORT
4. CIRRAN SLOT CIRCUIT TUBE
5. RIVET
6. INSULATOR
7. COAXIAL OUTER CONDUCTOR
8. CONDUCTOR
9. MICROSTRIP SLOT EXCITER
10. CIRRAN SLOT RADIATING APERTURE

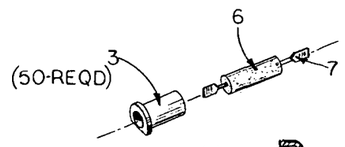

VIEW B

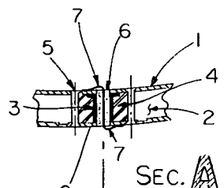

SEC. AA

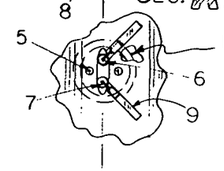

RADIATING CIRCULARY POLARIZED ANNULAR SLOT

QTY REQD	CODE IDENT	PART OR IDENTIFYING NO.	NOMENCLATURE OR DESCRIPTION	MATERIAL OR NOTE	SPECIFICATION	ZONE	ITEM NO.
	ASSY NO.						

LIST OF PARTS

PART CLASS:
DWG CLASS:
ASG BY:

DASH NO.	NEXT ASSY	USED ON	QTY PER NHA	END ITEM NUMBER	SERIAL NO.
	APPLICATION			EFFECTIVITY	

UNLESS OTHERWISE SPECIFIED-
TOLERANCE AND DRAWING INTERPRETATION PER D143
.X ± .08 .XX ± .04 .XXX ± .020
MACHINED ANGLES ± 0° 30'
SHEET METAL BEND ANGLES ± 2°
P10001 _____
SURFACE ROUGHNESS ✓

CONTR NO.	
RELEASE	
DWG APPD	
CHECKED	
DRAWN	7-8-74
DESIGN APPROVAL	
MANAGER	
SECT CH	
DESIGNER	

AVCO SYSTEMS DIVISION WILMINGTON, MASSACHUSETTS 01887

TITLE
FIGURE 2.
I.M.E. ANTENNA
CIRANN SLOT APERTURE

SIZE	CODE IDENT NO.	DWG NO.
D	04614	LA-14766

SCALE WT SHEET

DO NOT SCALE DRAWING

The Draftboard, Inc.

ENGR CHG	REVISIONS				
	ZONE	LTR	DESCRIPTION	DATE	APPROVED

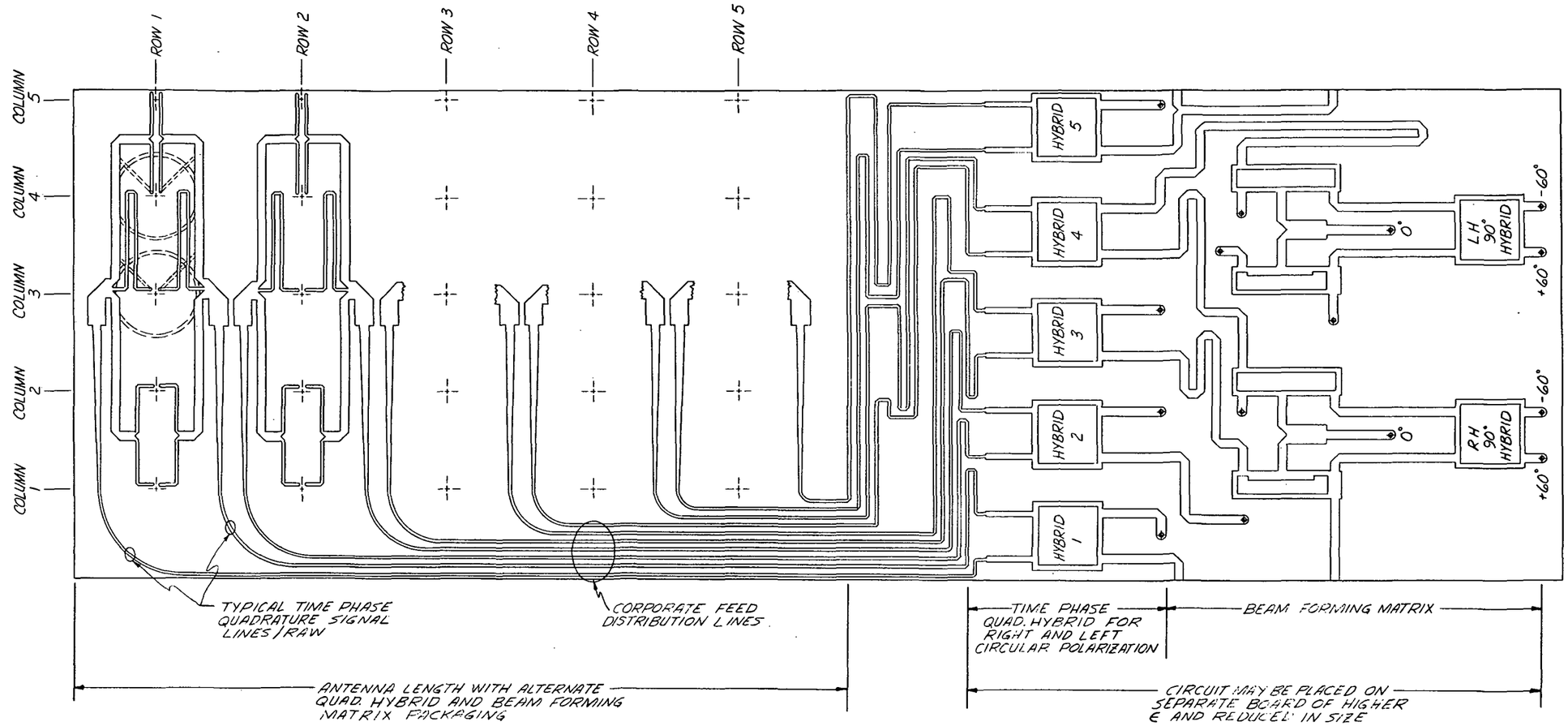

QTY REQD	CODE IDENT	PART OR IDENTIFYING NO.	NOMENCLATURE OR DESCRIPTION	MATERIAL OR NOTE	SPECIFICATION	ZONE	ITEM NO.
	ASSY NO.						

LIST OF PARTS

PART CLASS:	DASH NO.	NEXT ASSY	USED ON	QTY PER NHA	END ITEM NUMBER	SERIAL NO.
DWG CLASS:		APPLICATION			EFFECTIVITY	
ASG BY:						

UNLESS OTHERWISE SPECIFIED
TOLERANCE AND DRAWING INTERPRETATION PER D143
.X ± .08 .XX ± .04 .XXX ± .020
MACHINED ANGLES ± 0° 30'
SHEET METAL BEND ANGLES ± 2°
P10001 _____
SURFACE ROUGHNESS ✓

CONTR NO.	
RELEASE	
DWG APPD	
CHECKED	
DRAWN	
DESIGN APPROVAL	
MANAGER	
SECT CH	
DESIGNER	

AVCO SYSTEMS DIVISION WILMINGTON, MASSACHUSETTS 01887

TITLE
IME ANTENNA FEED NETWORK
FIGURE 3a

SIZE	CODE IDENT NO.	DWG NO.
D	04614	LA 14805

SCALE 1/1 | WT | SHEET

DO NOT SCALE DRAWING

LA 14805 REV.

ENGR CHG	REVISIONS LTR	DESCRIPTION	DATE	APPROVED

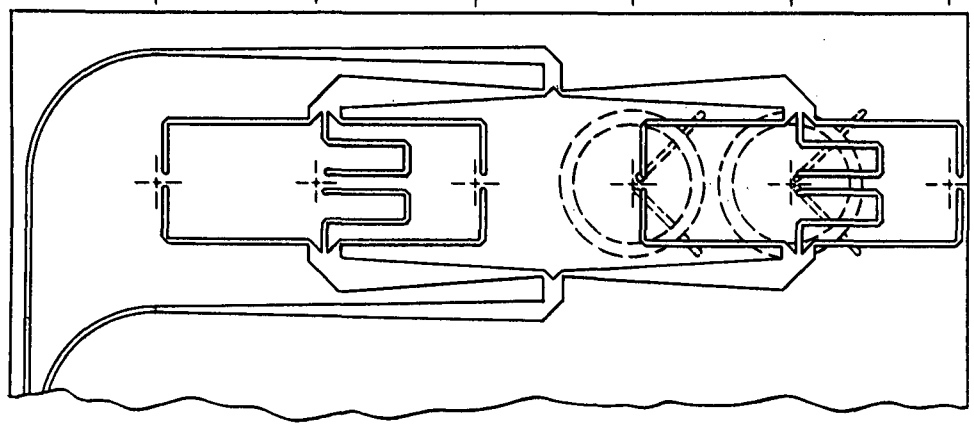

6 ELEMENT CONFIGURATION FOR USE WITH SLOT / DIPOLE OPTION

FIGURE 3b
TAPERED TRANSFORMER DESIGN

PART OR IDENTIFYING NO.	MATERIAL OR NOTE	SPECIFICATION

LIST OF PARTS

DASH NO.	NEXT ASSY	USED ON	QTY PER NHA	END ITEM NUMBER	SERIAL NO.
	APPLICATION			EFFECTIVITY	

UNLESS OTHERWISE SPECIFIED
TOLERANCE AND DRAWING INTERPRETATION PER DM3
.X ± .08 .XX ± .04 .XXX ± .020
MACHINED ANGLES ± 0° 30'
SHEET METAL BEND ANGLES ± 2°
P 10001
SURFACE ROUGHNESS ✓

CONTR NO.	
RELEASE	
DWG APPD	
CHECKED	
DRAWN	
DESIGN APPROVAL	
MANAGER	
SECT CH	
DESIGNER	

AVCO M S D / WILMINGTON, MASSACHUSETTS

TITLE IME ANTENNA FEED NETWORK

SIZE	CODE IDENT NO.	DWG NO.
B	04614	LA 14806

SCALE 1/1	WT	SHEET

DO NOT SCALE DRAWING

The basic advantage of the integrated feed is that the complete circuit is printed on a single μ -strip board, hence manufacturability of this component will be relatively straightforward. A disadvantage of the total integrated feed is the 17.8cm length required to accommodate the circuitry.

The second feed option places the quadrature hybrids for polarization selection, the beam forming matrix, and single-pole, three-throw switches on a single board of dielectric constant $\epsilon = 9.0$. The R.F. connection between this package and the individual rows of elements in the array is accomplished by 10 identical low loss coaxial lines, representing 5 rows and two polarizations. There is the distinct possibility that the coaxial lines can double as structural support members for the array in its operationally deployed configuration. This requires, however, a detail investigation from a spacecraft integration viewpoint.

The estimates for expected insertion loss have been made based on a μ -strip package for the feed system. These losses at 2.3 GHz are given in Table 9, along with the expected antenna system gains.

4.0 ANTENNA CONFIGURATION CANDIDATES

The first task in this study was to investigate the most likely conceptual antenna candidates for conducting tradeoff studies. Due to the requirements of omnidirectionality about the spin axis of the spacecraft, the antenna form factor was required to be rotationally symmetric. A bicone design (Table 2, Configuration A) was considered very early in the study but was found to require considerable volume in order to achieve the gain required. The additional requirement for discreet beam steering suggested that the bicone approach would require more vertical aperture at the feed region to provide proper phase taper. Alternate means of phase taper such as phase shifting at the outer aperture region was judged an inferior approach and the bicone was eliminated from further investigation.

The second candidate considered was an array of dipole-loops in a vertical configuration as shown in Table 2, Configuration B. Here the collinear dipoles provide the axial component of the circularly polarized field, while the loops provide the horizontal component in phase quadrature. This design approach had potential from a weight and volume viewpoint, but the requirement of beam steering and the occupation of the volume which includes spacecraft spin axis does not allow the use of a low frequency antenna coaxial with the communications antenna as desired. The concept was therefore discarded.

The antenna configuration study led to a cylindrical form factor as shown in the remainder of Table 2, CDEF. Utilization of a cylinder allows the possibility that a low frequency experiment antenna be mounted coaxial with the Communications Antenna. Further, it is amenable to theoretical parametric analysis which allows trade studies to be performed relative to the performance desired.

Table 2

Candidate Antenna Configurations

Configuration	Comment		
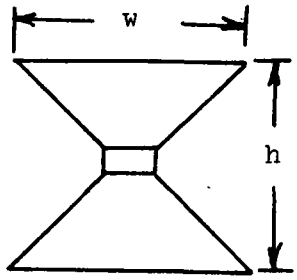 Bicone	**Configuration A** • Large Aperture Dimensions Required for 6.0 db Gain • Beam Steering Difficult • Efficiency Potential High		
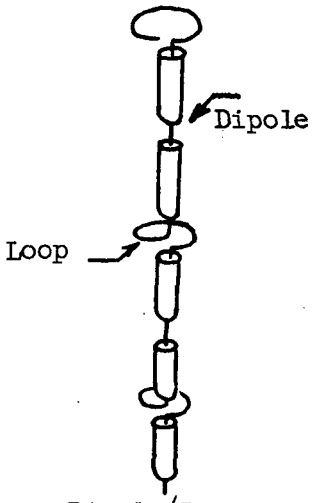 Dipole/Loop	**Configuration B** • Potential for Mechanical Simplicity • Frequency Sensitive • No Capability for Coaxial Compatibility with L.F. Experiment Antenna		
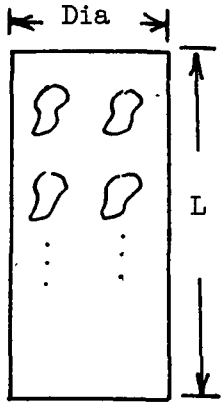 Cylinder	 Config. C  Config. D  Config. E  Config. F	Cirranslot Crossed Slot Microstrip Slot/Dipole	**Applies to All** • Good Form Factor • Compatible with Coaxial Antenna • Length A Factor of Feed Net. • Efficiency Main Concern

Cirranslot Radiation Pattern - RHC -
Circumferential Plane, 5 Element Circumferential
Array x 4 Row Axial Array - d/λ = .53

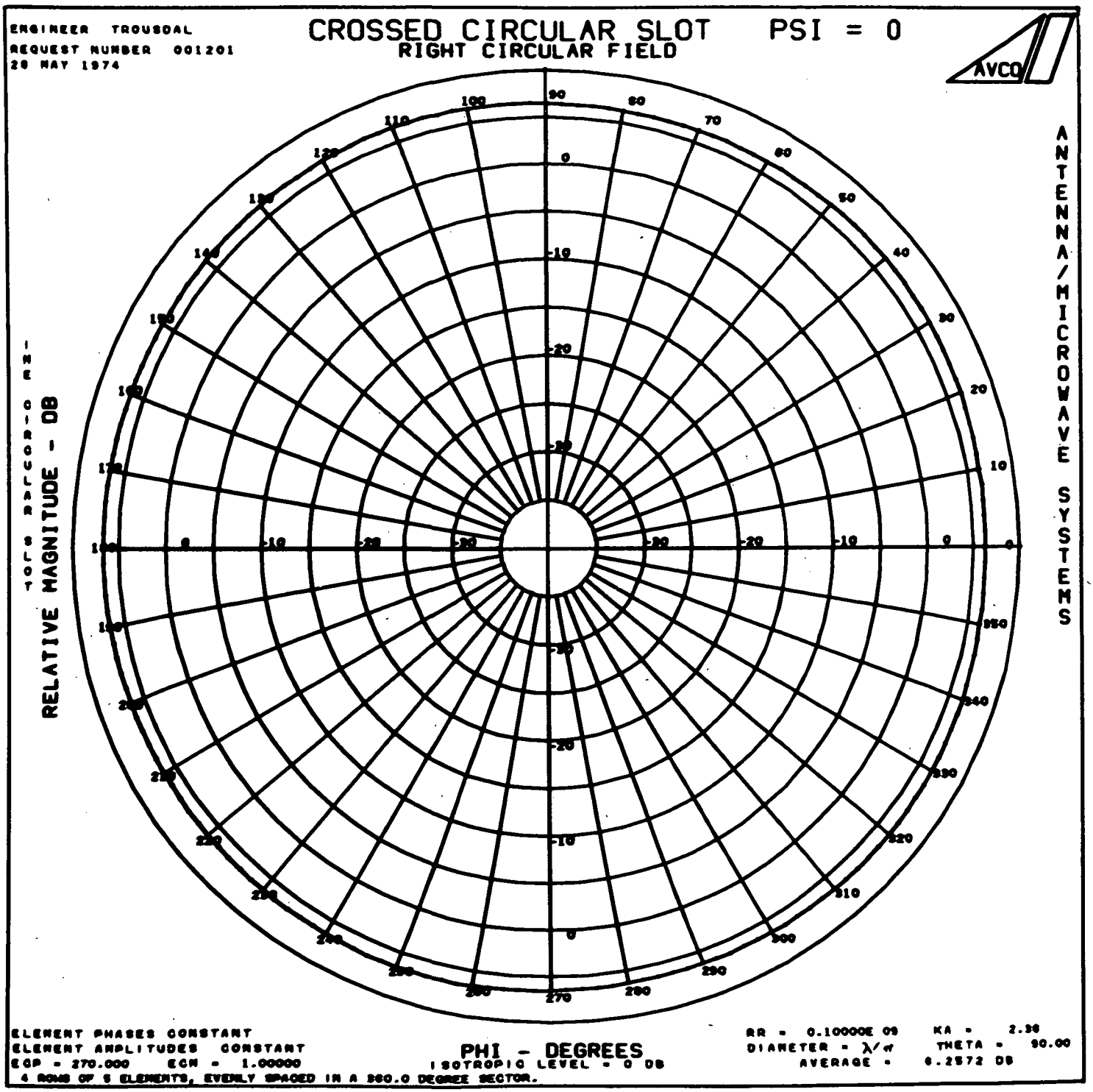

Figure 4

Cirranslot Radiation Pattern - RHC -
Axial Plane 5 Element Circumferential Array x 4
Row Axial Array - d/λ = .53

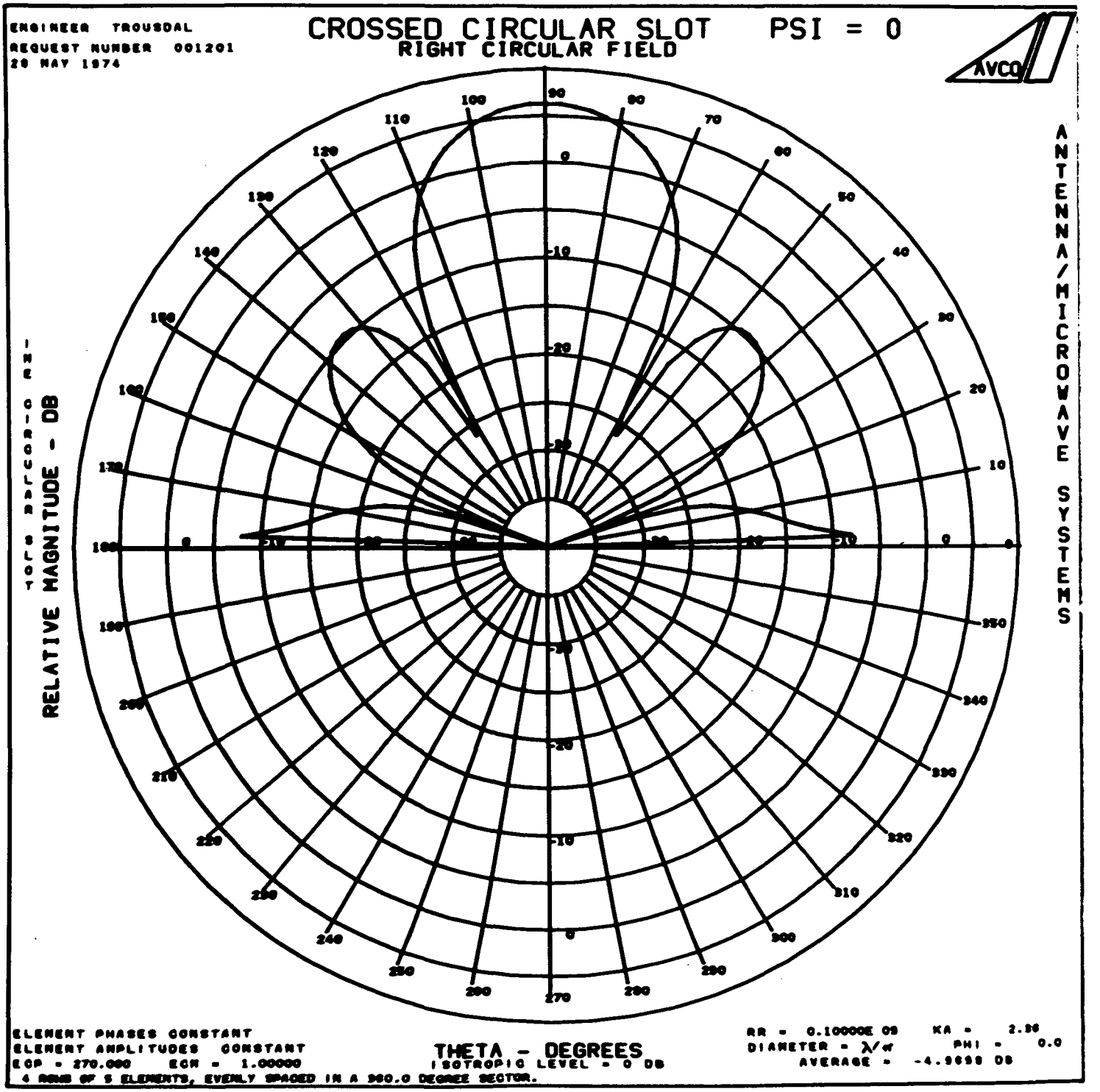

Figure 5

Cirranslot Radiation Pattern - RHC -
Circumferential Plane, 5 Element Circumferential
Array x 4 Row Axial Array - $\theta = 60^{\circ}$, $d/\lambda = .53$

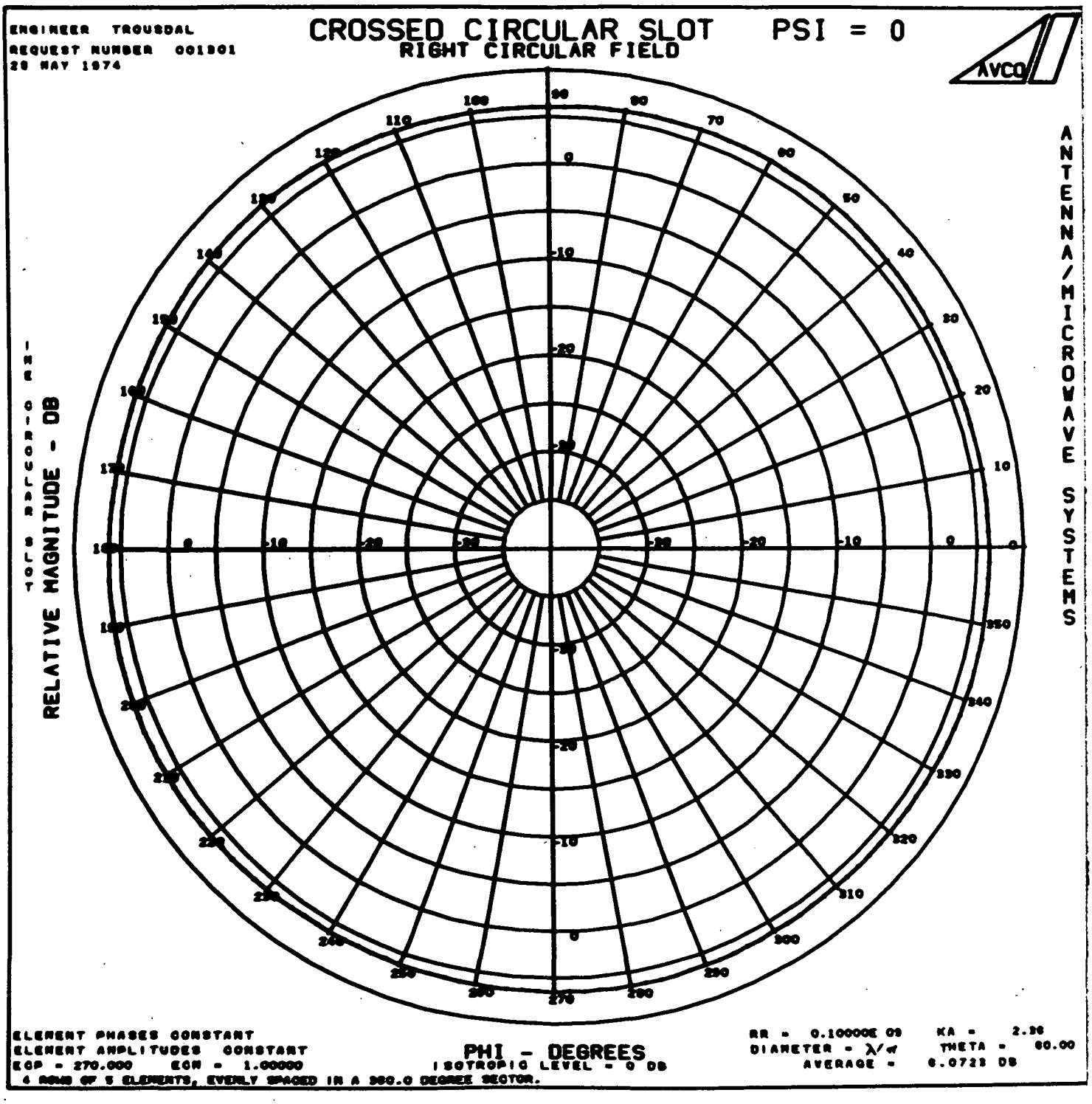

Figure 6

Cirranslot Radiation Pattern, Axial Plane

5 Circumferential Elements x 4 Row Axial

Array - $\theta = 60^{\circ}$ $d/\lambda = .53$

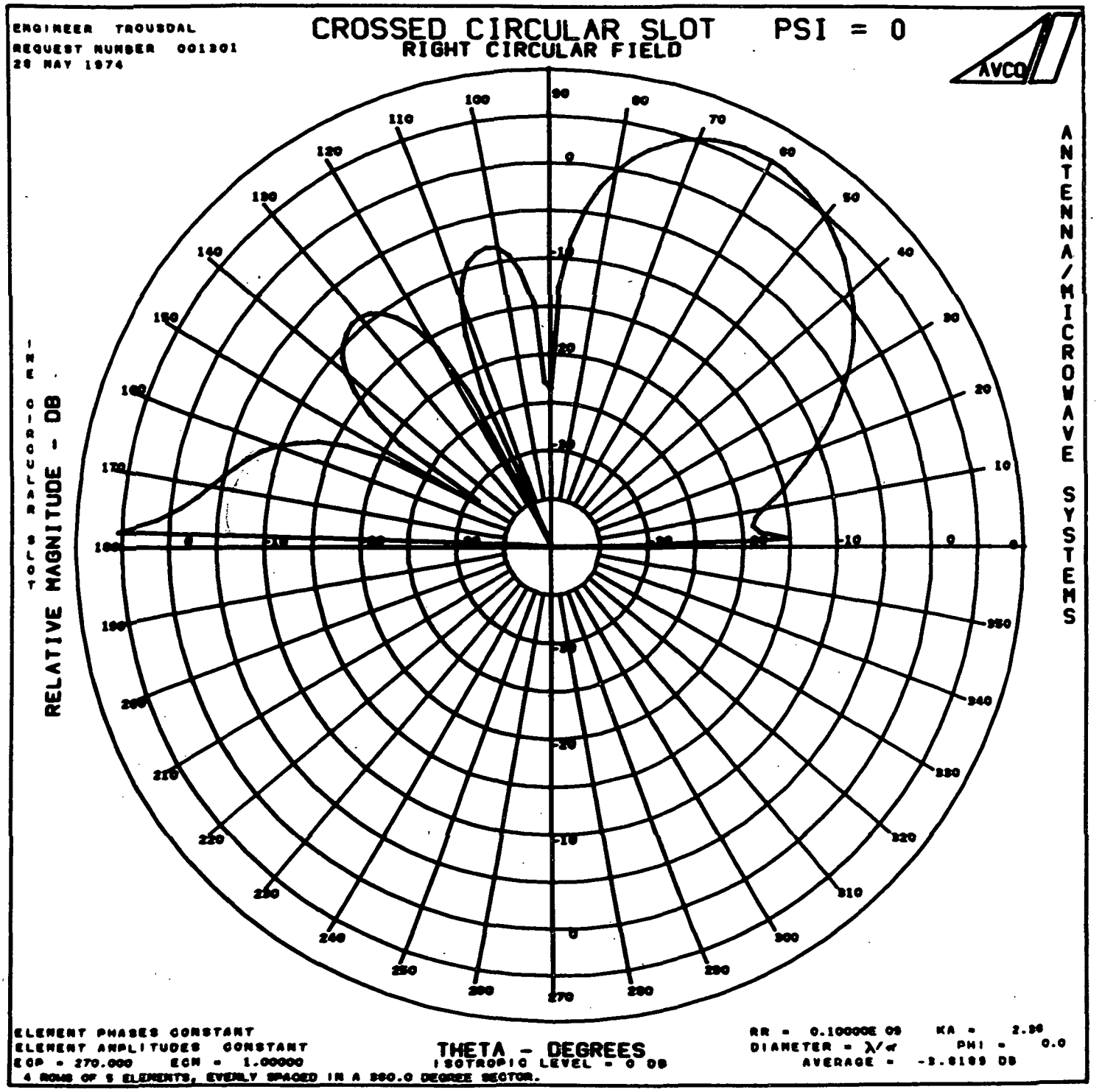

Figure 7

4.1 CYLINDER ARRAY ELEMENT

Table 2 shows array element configurations studied. While the array performance for these configurations can be expected to be similar, the method of implementing the feed is different and provides several candidates from the feed viewpoint. In the paragraphs below, the configurations of Table 2 are discussed and theoretical performance illustrated.

4.1.1 Configuration C - Cirranslot (Circularly Polarized Annular Slot)

From previous experience at S-band, a cylinder array with axial polarization required 1 element per inch of cylinder diameter to achieve uniform roll plane coverage. However, for circular polarization, it turns out to require an additional aperture. This is due to the fact that the circumferential polarized component of the circular polarized field requires a higher density of elements in the circumferential plane to provide uniformity.

Having defined the circumferential array element requirements (5 elements), the axial array configuration requirements were studied.

Avco computer code 2712 (See Appendix A) was utilized to determine the far field radiation in the axial plane of the cylinder. The patterns are described in terms of directivity, beamwidth, ellipticity ratio, and side lobe characteristics versus the number of elements, and spacing between elements. A plot of the radiation characteristics for 4 axial elements with spacing $d/\lambda = .53$ (f_o = 2.3 GHz) is shown in figures 4 and 5. Figures 6 and 7 show the radiation characteristics steered off broadside by 60°. For the element spacing considered the required phase taper was found from the simple relationship:

$$\delta = \frac{-2\pi nd}{\lambda} \cos\theta$$

θ = angle measured from cylinder axis

d = element spacing

λ = operating wavelength

n = incremental phase integer

Although sidelobe levels have not been specified in Table 1, the aperture distribution was tapered in a Dolph-Chebyshev manner to yield 15 db sidelobes. In addition, the axial spacing of $.53\lambda$ was chosen to constrain the grating lobes of the array to a level not greater than the natural sidelobes when the array is steered in the ± 30° steered directions. (θ = 60, 120).

It is seen from these plots that the beamwidth is 27° (30° design goal) at both broadside and θ = 60, 120. The directional gain is greater than 6.0 db.

The directionality achieved by this array configuration must be considered together with the losses of a feed network required to excite the array. These losses will reduce the directive gain by a factor depending on the feed network configuration selected. Feed distribution network considerations are discussed fully in Section 6.

The need for more directive gain suggests that the element spacing be increased to achieve an effective increase in the array aperture length, thereby increasing the directive gain. This of course, would cause a proportional decrease in beamwidth in the axial plane. The other possibility of increasing directive gain is to add a fifth element in the axial dimension.

To test these various approaches for increased directivity the element spacing was increased to 0.7λ which by rough calculation appeared to provide a directive gain increase of approximately 1 db. The pattern for the predominant polarization is given in figure 8. Here we see the disastrous effects of the grating lobe. The net gain is seen to be 5.75 db and is judged not satisfactory in achieving the objectives.

The second alternative of five elements arrayed axially was investigated. In addition, the spacing was put at $.53\lambda$ to prevent the appearance of any grating lobes. The results show the expected improvement in the directional gain of $\sim$ 1.0 db.

The above results basically represent the expected performance of the aperture element configurations shown in Table 2, CDE and can be used to describe the far field characteristics of each. This is due to the fact that the element pattern for these configurations are virtually identical.

4.1.2 Crossed Linear Slot Array Element - Table 2D

In terms of practical application, the crossed linear slot element was considered only as a back-up to the circular slot. The latter being considered prime candidate due to its geometrical circular symmetry, a feature which can be exploited as discussed in Section 6.0.

4.1.3 Microstrip Array Element - Table 2E

The microstrip package of Table 2E, while requiring no cavity in the conventional sense, has a very narrow bandwidth, in the order of 2%. In addition, the problem of getting the required corporate feed integrated with the microstrip radiators decreases the viability of this approach in a practical system requiring 10% bandwidth. It was therefore eliminated from further consideration.

The slot/dipole configuration was considered a prime candidate and is considered next.

4.1.4 Slot/Dipole Array Element

The next step in the analytical trade-off task was to investigate the characteristics of the circularly polarized slot/dipole configuration depicted

Cirranslot Radiation Pattern - Axial Plane

5 Circumferential Elements x 4 Row $\Theta = 60^{\circ}$ $d = .7\lambda$

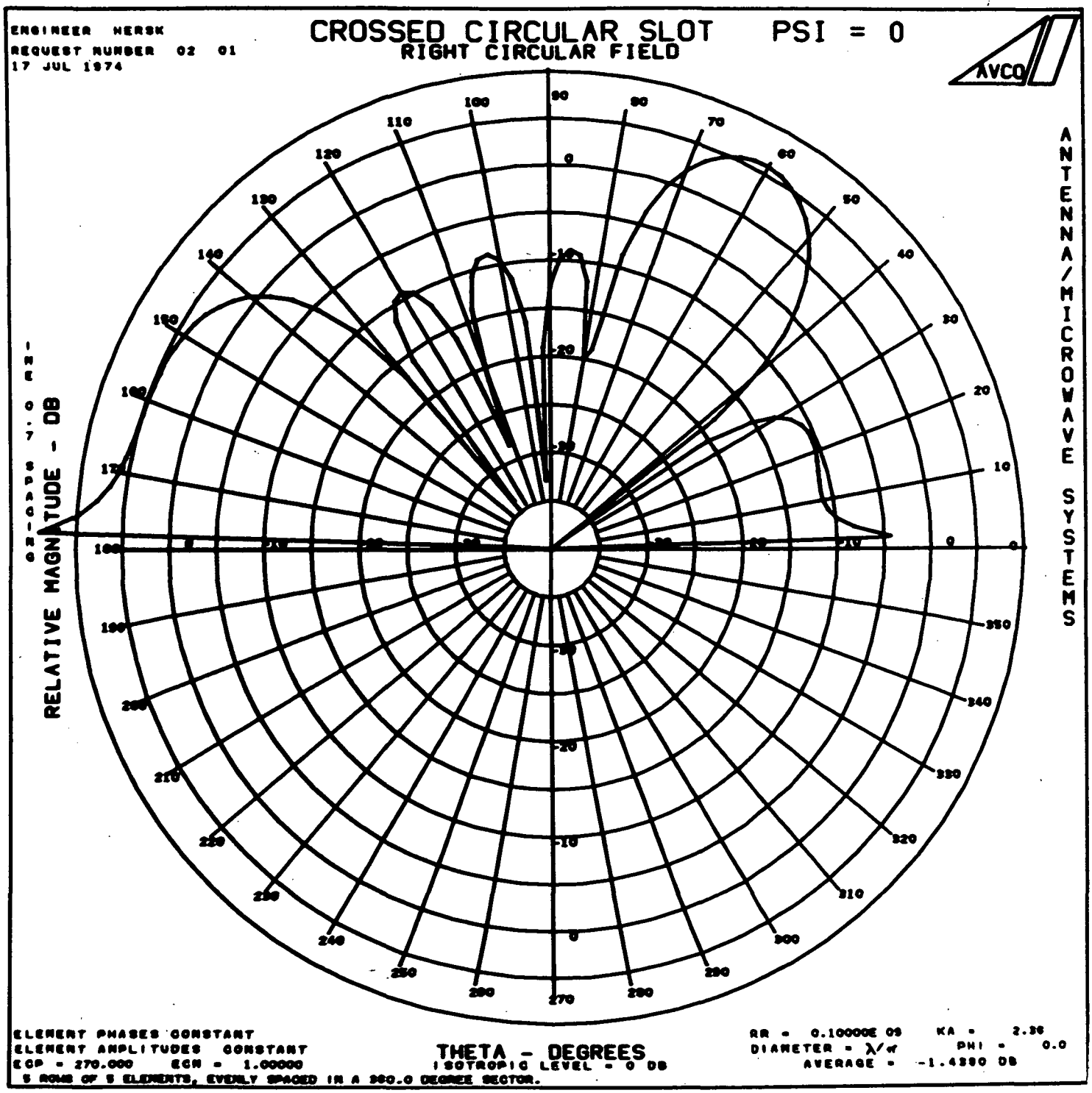

Figure 8

in Table 2F.

It is well known[1] that element patterns with nulls in the direction of the array axis allow larger spacing before grating lobes appear. The limits in element spacing are given by the expression taken from reference 1.

$$d/\lambda \leqslant \frac{1}{1 + \cos \theta}$$

where θ = Beam Angle Off Array Axis

Thus for a steered angle of $\theta = 60^{\circ}$, d must be less than or equal to $.66\,\lambda$.

The slot/dipole configuration was pursued to examine the benefits to be derived in directive gain vs. element spacing, while keeping a four element axial configuration.

The mathematical model for the dipole array was that derived in reference 2. The slot array radiation characteristics were derived from expressions found in reference 3. For purposes of documentation, the computer program listed in Appendix B was used to describe the far field pattern characteristics of the slot/dipole configuration shown in Table 2F.

The major parameters of interest in the slot/dipole investigation were the following:

a) cylinder radius
b) dipole position radius
c) relative amplitude between slot and dipole
d) relative phase between slot and dipole
e) number of elements in circumferential plane
f) axial spacing between elements
g) relative phase and amplitude between axially arrayed rows

The computer code was checked out by comparison with published data. The slot program checked out exactly. There was some small discrepancy between the dipole version as computed by Avco and that in reference 2. After careful rechecking of Avco subroutine accuracies, however, it was concluded that the reference paper probably does not have the accuracy available in today's scientific subroutines. The coding accuracy was therefore accepted, and the program was exercised.

The first task was to determine the number of elements required in the circumferential plane to achieve uniform roll plane coverage. Figure 9 summarizes the peak-to-peak amplitude variation of orthogonal polarized fields in the roll plane, as a function of cylinder radius for 5 and 6 elements equally spaced in the circumferential plane. Figures 10 and 11 show a typical roll plane variation of the $E\phi$ (slot) field, and the E_θ (dipole) field. It is clear that the dipole is the prime contributor to roll plane gain variation. Subsequent calculation revealed that 8 slot/dipole elements will produce a uniform field in the circumferential plane.

Peak to Peak Ripple Vs Cylinder Radius - Circumferential Plane

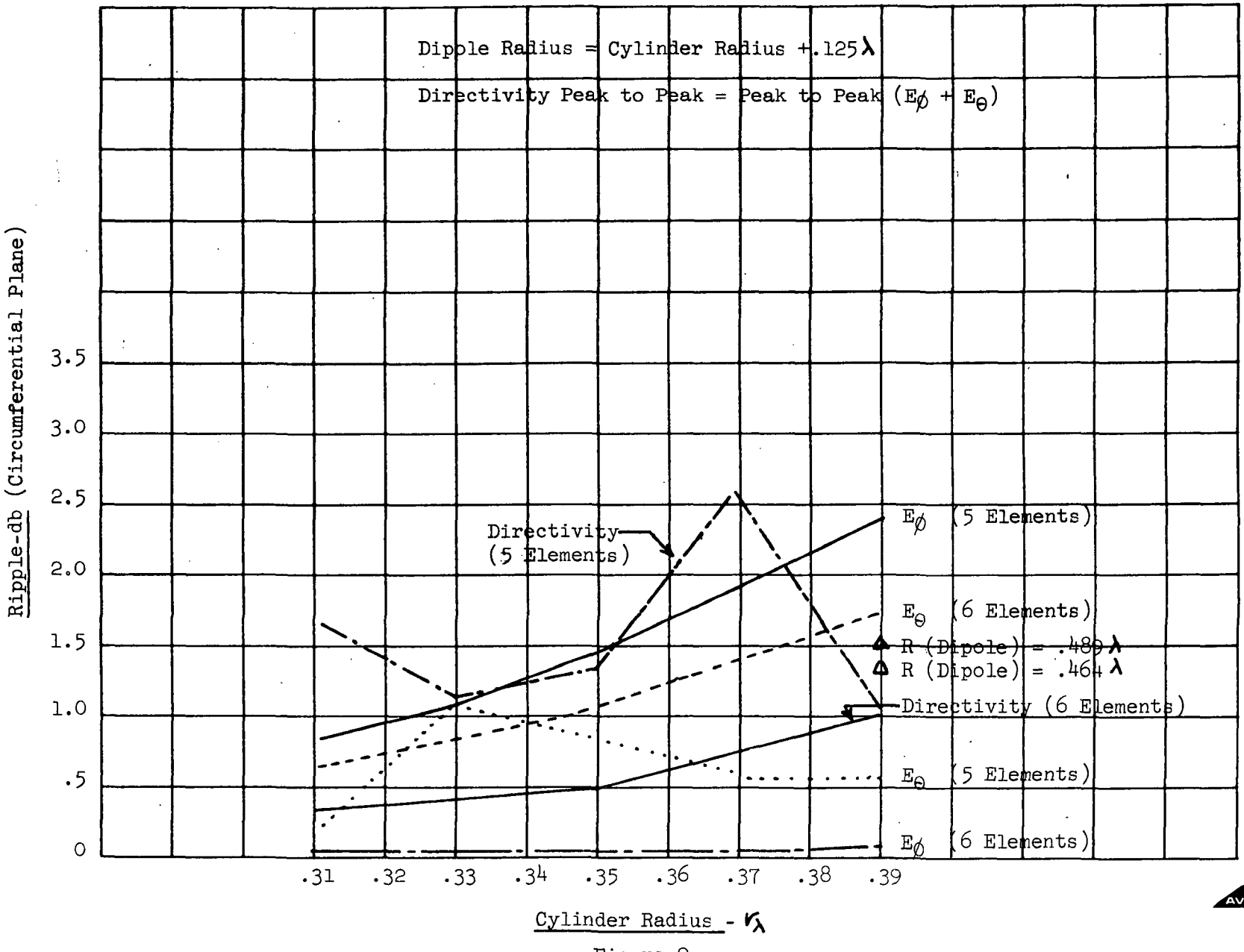

Figure 9

Radiation Pattern Slot/Dipole Typical E (Slot) Response Vs. ϕ

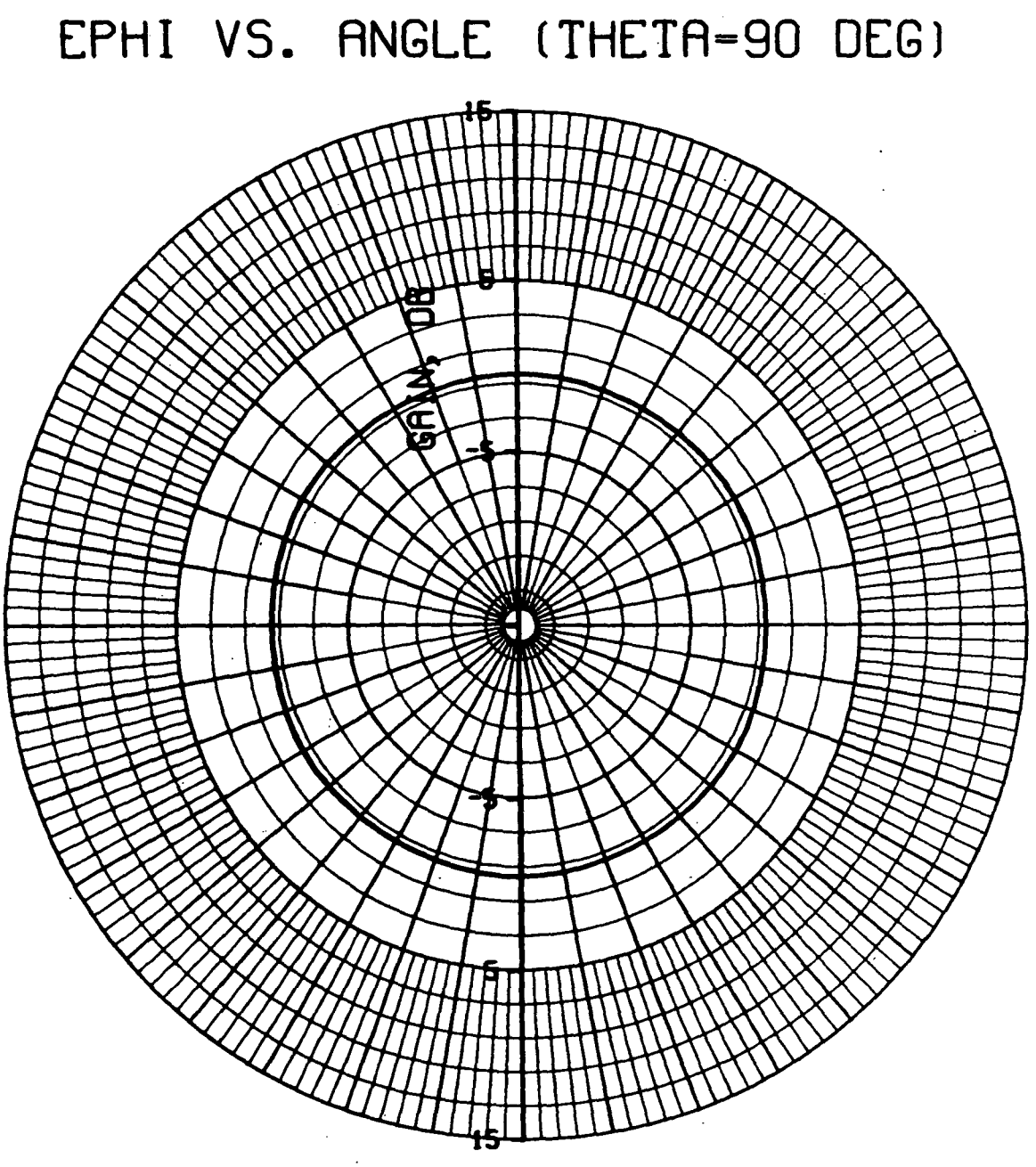

Figure 10

Radiation Pattern Slot/Dipole - Typical E (Dipole) Response Vs. ϕ

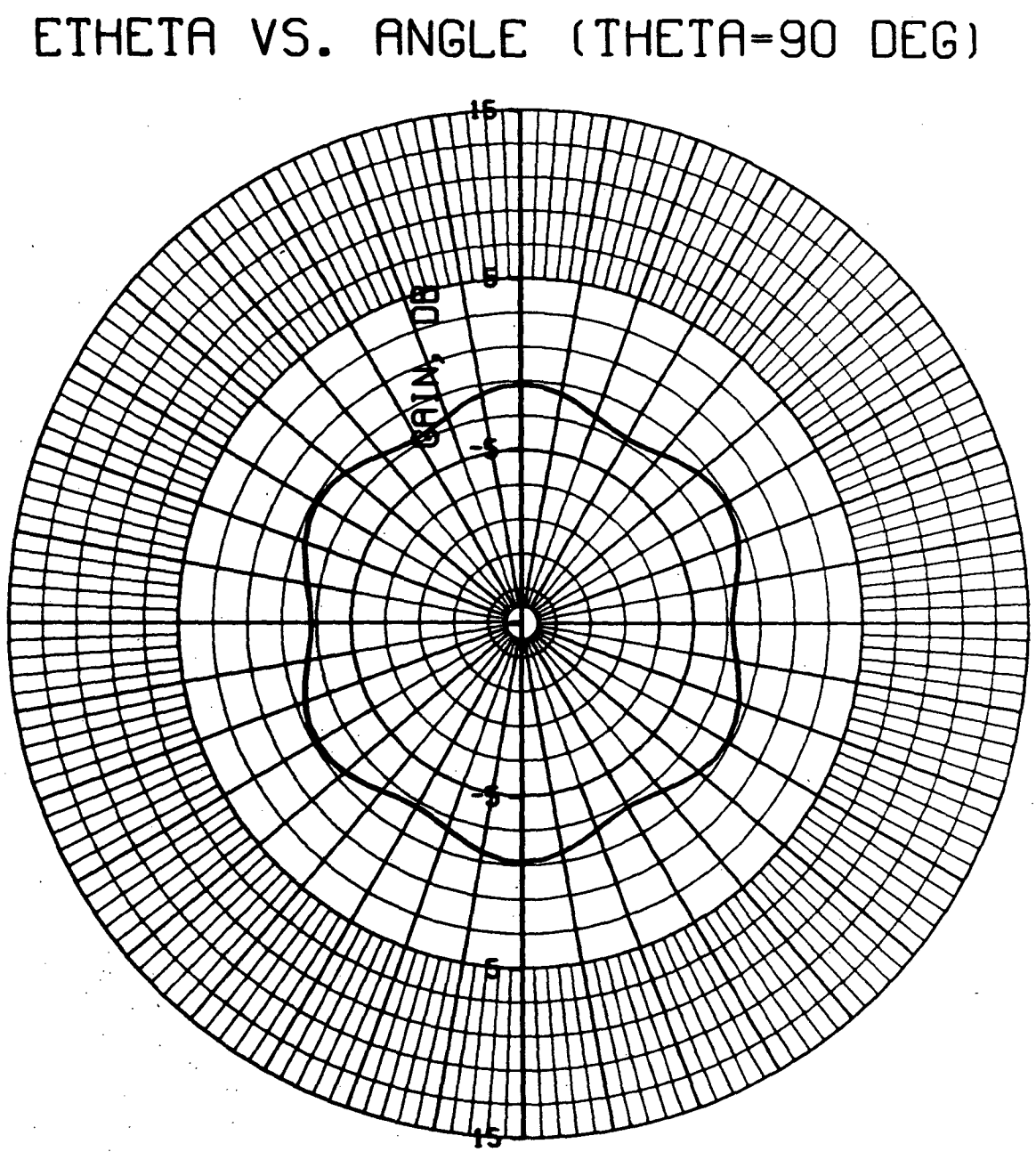

Figure 11

In all cases in Figure 9, the dipole was on a radius $\lambda/8$ larger than the cylinder. The Δ's on the figure show how a decreased height of the dipole above the slot, on a cylinder radius of $.39\lambda$, decreases peak-to-peak field ripple. While there is some improvement, the bandwidth of the dipole is probably decreased due to its proximity to the cylinder ground plane.

At a cylinder radius of $.389\lambda$ (Dia = 10 cm) and a dipole radius d/λ = .514 (Dia = 13.4 cm), the amplitude variation is $\pm$ .45 db about an average field value. This value is considered acceptable and a six-element circumferential array was chosen to proceed with axial array definition studies.

Figure 12 represents the axial pattern of a single circumferential row of 6 elements. As desired, there is a null in the axial direction. One can expect that due to the cardiod pattern shape the directivity of the array at beam position angles of ϕ = 60, 120° will suffer some loss. This is expected to occur noticeably for larger values of steering angles off broadside.

Figures 13 and 14 are typical axial plane patterns at θ = 60°, 90°. Figure 15 is a summary description of the beamwidth and directivity characteristics of a slot dipole array as a function of interelement spacing. The pertinent parameters of the array are listed on the figure. (A complete set of dipole/slot computed patterns are given in Appendix C).

Referring to Figure 15, the directivity of the array for broadside pointing (i.e., θ = 90°) is seen to increase rather uniformally as interelement spacing is increased. At the main beam position of 60° and 120°, however, the directivity reaches a peak at $d/\lambda \sim .68$ and then reverses towards lower values. This downward trend beyond $d/\lambda = .68$ is due to the appearance of grating lobes.[4]

The equivalent array length for 4 rows of elements is also given in Figure 15. For a 4 element dipole/slot array element at an axial spacing of $d/\lambda = .65$, the array physical length is seen to be 34 cm (13.4").

From the beamwidth curves of Figure 15, it becomes clear that the design goal of a 30° beamwidth can be achieved only at a spacing of 0.5λ and a tapered aperture distribution. The reality of the situation, however, is that a practical feed network is lossy. The loss effects of the feed in turn requires an increased directivity to make up for these feed losses.

It is clear from extrapolating the previous discussion that to realize a 6.0 db net gain (Directivity - losses) two things are required:

a) Increased directivity with associated decreased beamwidth
b) Finer incremented beam steering to compensate for narrower beamwidths.

Increased directivity can be achieved in two ways; namely, by increased spacing between elements as shown above, or by adding additional circumferential rows of elements. The decreased beamwidth is a dependent variable (on directivity) and therefore must be accepted and used to define the incre-

SLOT/DIPOLE ARRAY

SINGLE ROW OF

6 ELEMENTS - AXIAL PLANE

LEFT CIRCULAR POLARIZATION (PHI=0 DEG)

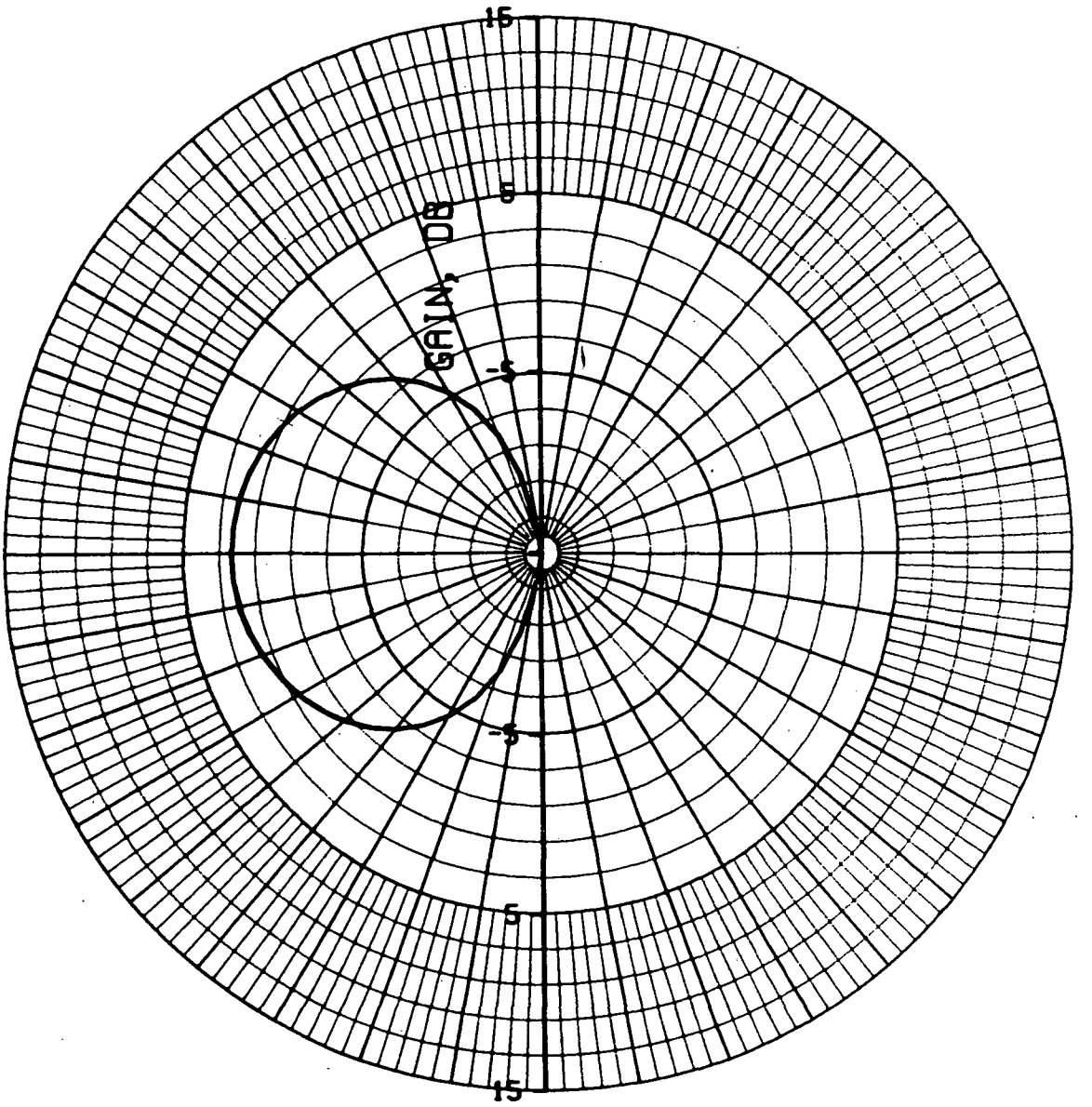

AVCO/SD
30.MAY.74

Figure 12

Slot/Dipole

Computed Radiation Patterns

- Axial Plane
- 6 Element Axial Array (Broadside Pointing)

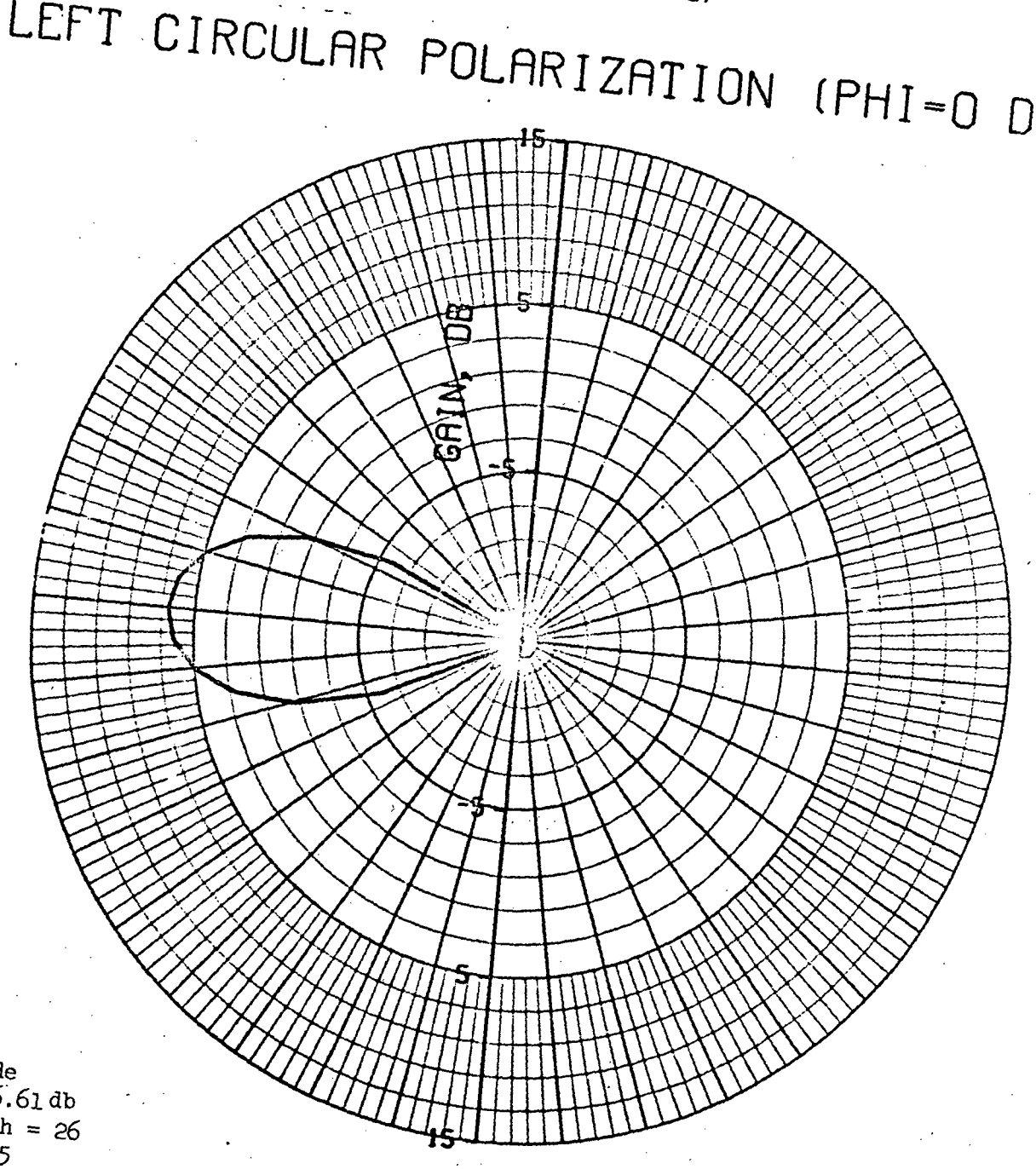

Broadside
Gain = 6.61 db
Beamwidth = 26
d/λ = .5

Figure 13

AVCO/SD
3.JUN.74

Slot/Dipole

Computed Radiation Patterns

- Axial Plane
- 6 Element Axial Array
  (Pointing Angle = 30°
  From Broadside)

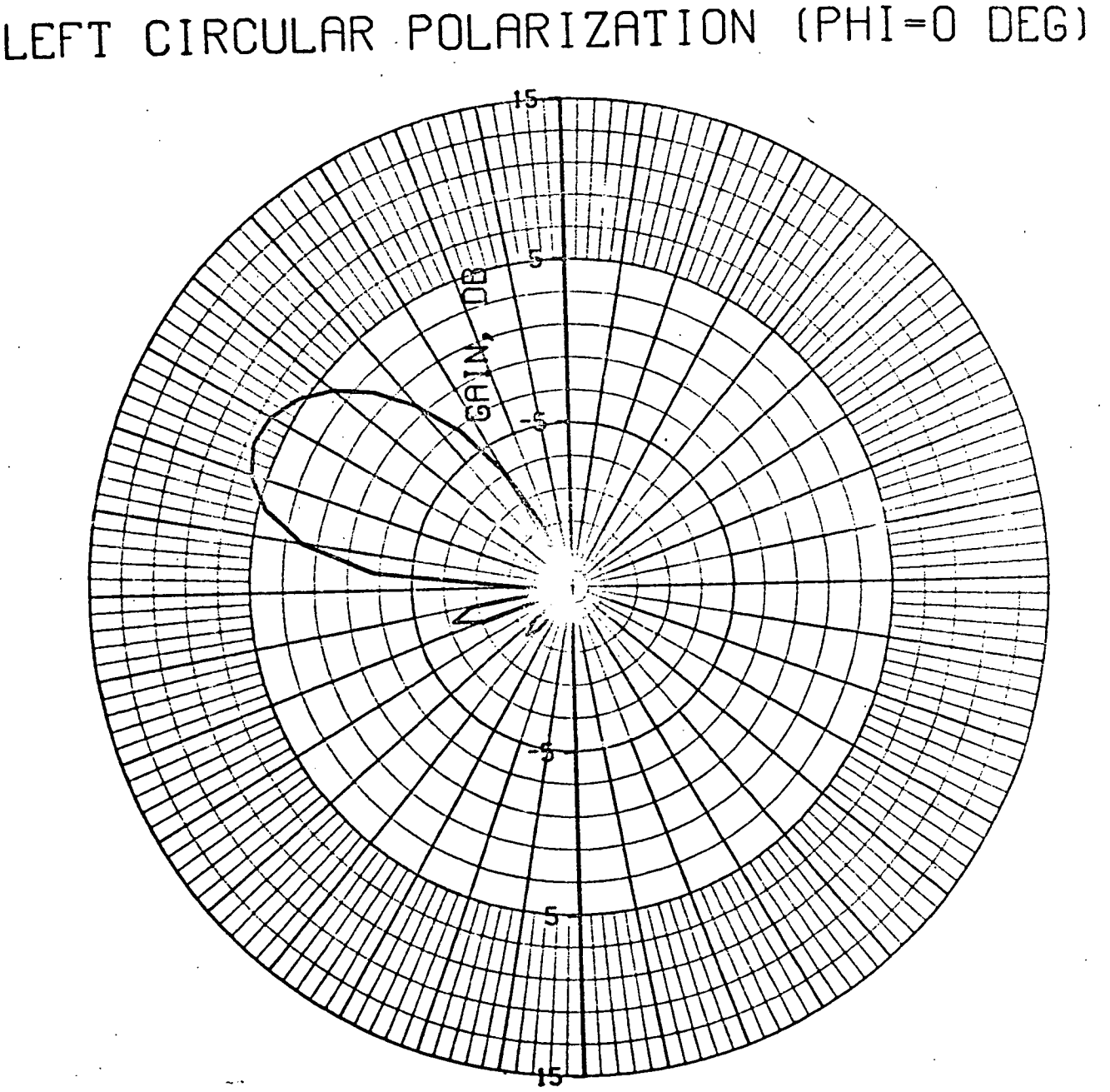

Gain = 6.29 db
Beamwidth = 29°
d/λ = .5

AVCO/SD
3 JUN 74

Figure 14

DIRECTIVITY VS ELEMENT SPACING - SLOT/DIPOLE

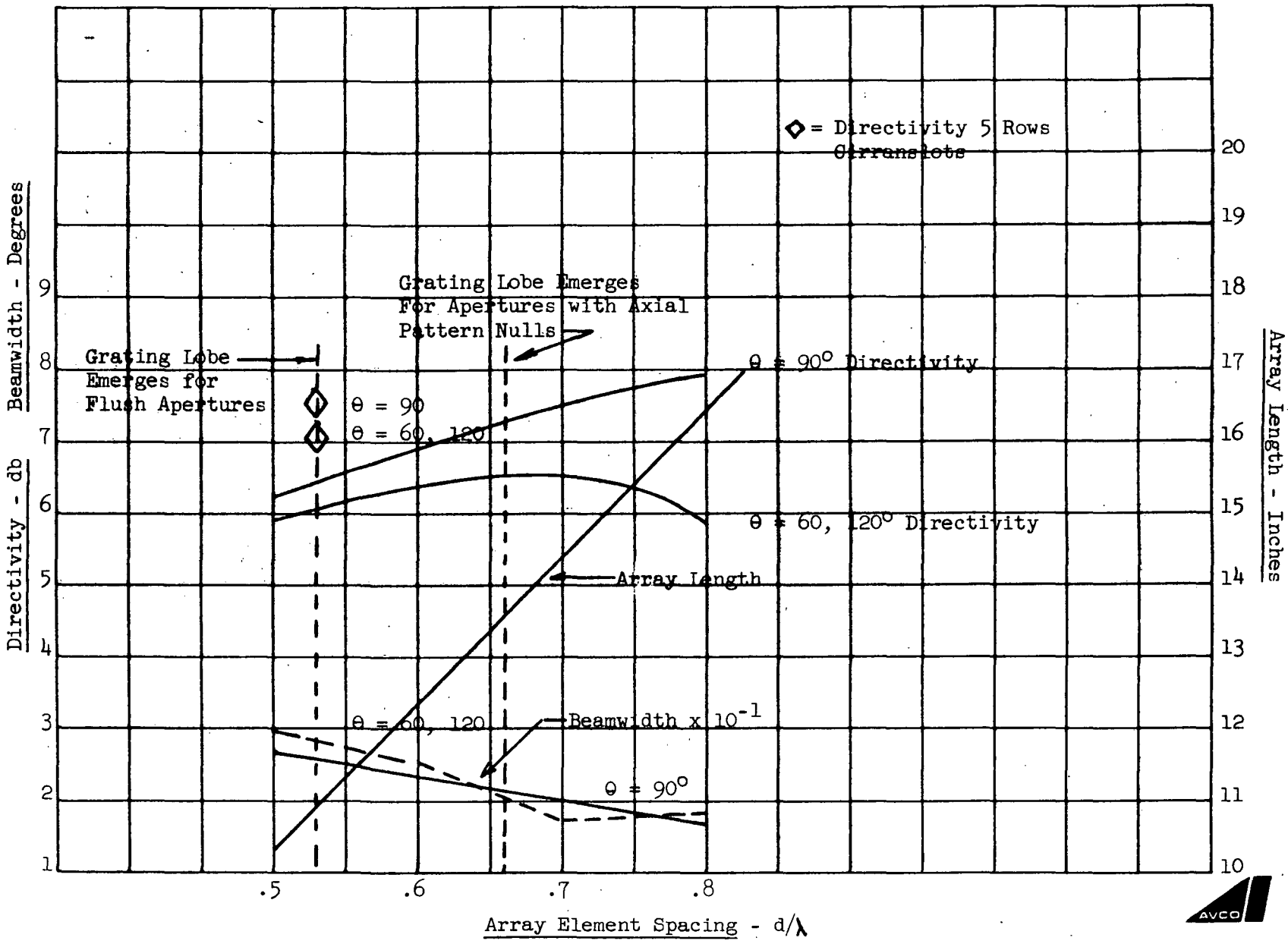

Figure 15

mented beam steering required to provide adequate coverage in the axial plane.

As will be shown later, the estimate of feed losses (2.65 db) requires a directivity of 8.65 db at 90° in order to achieve a gain of 6.0 db at broadside. This feed loss calculation is based on a 5-row axial array with beam steering at 3 discrete locations 60°, 90°, and 120°. (The directivity of the 5-element row is given in Figure 15 at a spacing of $d/\lambda = .53$.)

To illustrate the approximate number of slot/dipole rows required to achieve a specified directivity, the curve of Figure 16 has been plotted. From this figure it is clear that approximately 7 rows of elements spaced $\lambda/2$ apart will yield a directivity of 8.65 db. The corresponding beamwidth is $\sim$ 15 degrees. In order to provide coverage from 60°-120°, the beam would have to be switched 4 times. The additional phase shifting and feed network circuitry would require re-analysis to assess the corresponding network efficiency. A layout of a 7-row feed network was not done during this contract due to lack of available time and resources.

5.0 CONCLUSIONS FOR APERTURE STUDY

The array study conclusions can be stated in summary form as follows:

a) A cylindrical array has a form factor suitable for allowing volume for a low frequency experiment antenna coaxial with the array.
b) The radiating aperture of the array element can take many forms. The circularly polarized annular slot and dipole/slot aperture are two prime candidates for practical implementation.
c) Dual circular polarization capability is available for all apertures studied since there is a practical access to spactially orthogonal R.F. terminals.
d) Wide ranges of directivity and corresponding beamwidths can be obtained by effectively utilizing the row and row spacing parameters.
e) The achievable gain will be a function of the feed system losses and will result in diminishing returns for higher directivities.
f) The bandwidth of the antenna array will be a function of the radiating element and the feed system bandwidth. The system should be tuned to maximum gain at the transmit frequency of 2.3 GHz, allowing some degradation due to bandwidth limitations at the receive frequency of 2.1 GHz.

6.0 FEED DESIGN

The realization of the required gain of the antenna as defined in the previous paragraphs is heavily dependent on the type of feed system utilized to feed the array. Two classes of feed approaches were considered, the traveling mode waveguide feeds and the integral network feed.

In the traveling mode waveguide approach, the array elements would be etched into the wall of the circular waveguide and excited by a circularly

DIRECTIVITY VS ELEMENT DENSITY

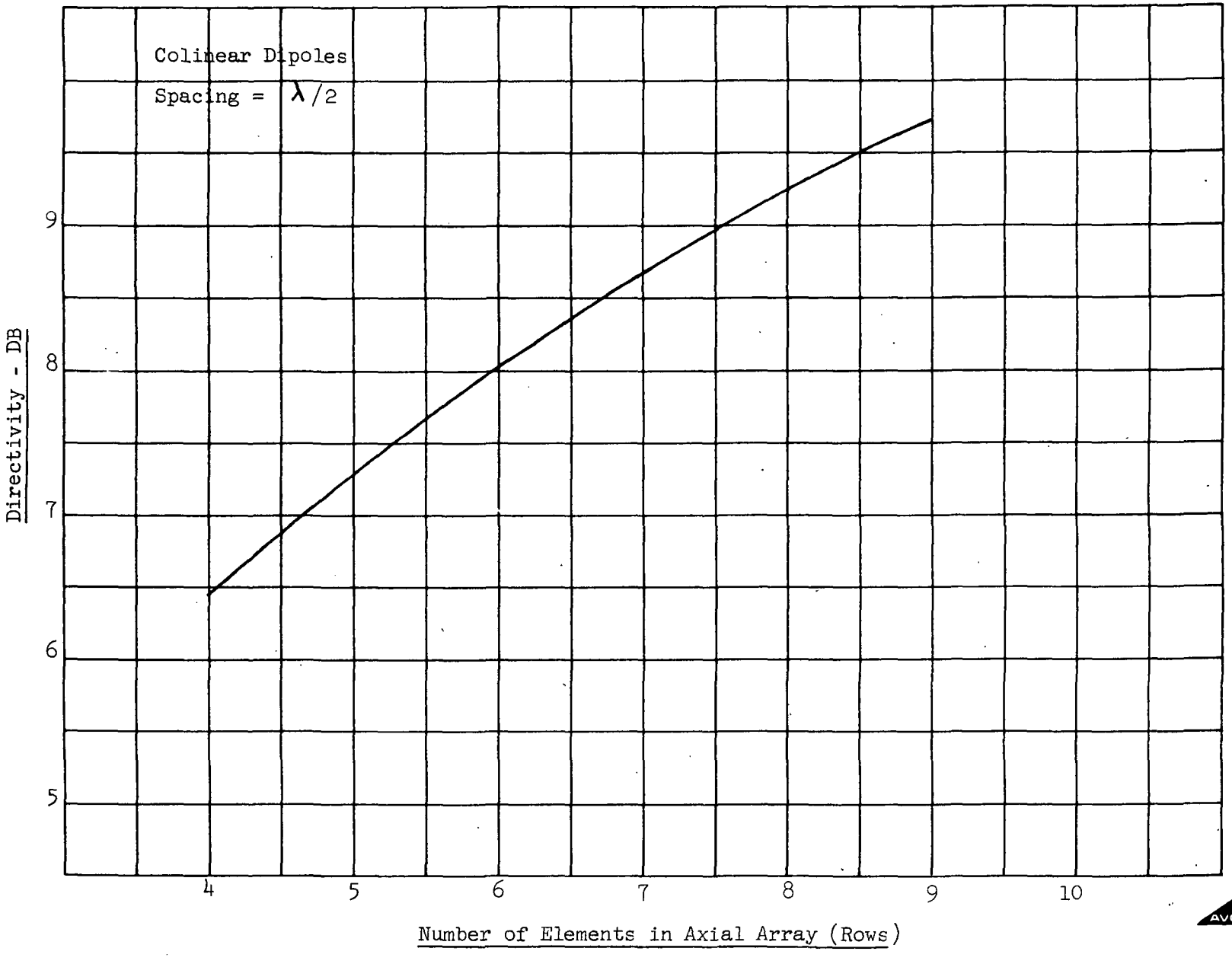

Figure 16

polarized traveling (two orthogonal TE_{11} modes) wave, launched in the cylinder[5]. While this approach offers a most efficient feed, the phase of the field in the circumferential plane rotates 360°. In addition, unless the radiating elements are spaced λg apart (requiring a slow wave structure internally to match the external spacing requirement of $\lambda/2$), the circularly polarized fields will be severely degraded in polarization. Finally, the traveling wave approach does not yield a simple means of positioning a beam at 3 locations. The requirement of 3 beam positions and a constant phase pattern (± 5°) in the roll plane eliminates the circular waveguide traveling wave feed approach from serious consideration.

The other class of feed distribution system, the "integral network feed," can be implemented in a multiplicity of ways. This feed approach utilizes individual transmission lines to each element of the array and can be implemented most easily by stripline or microstrip techniques. The problem in design is how best to utilize the strip transmission technology with its relative ease of manufacture, to result in a minimum loss feed network.

6.1 Feed System Components

Before selecting an approach to the integrated feed network, an understanding of the feed system components required to produce a 3 position beam dual polarized radiation field is required. Refer to Figure 17, and Figure 3a.

Figure 17

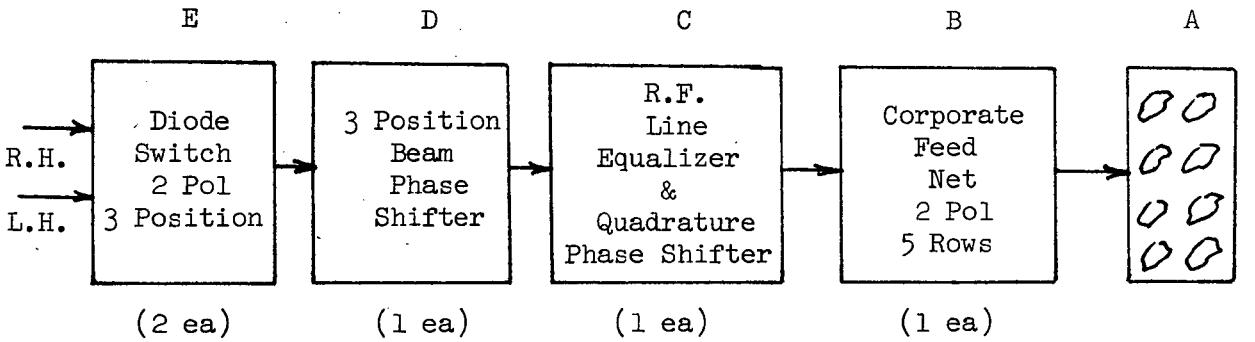

Here the MXN matrix of radiating elements (A) are individually powered via a parallel array of corporate power dividers (B) which supply each row with equi-phase, equi-amplitude signals. In addition to the amplitude and phase characteristics, the corporate divider of each row provides spatially orthogonal feeds for use in generating the orthogonal circularly polarized signals required. The total number of outputs of box B in Figure 17 is 10 representing 5 rows and 2 polarizations (right and left circularly polarized ports). In box C are located R.F. line lengths utilized to compensate for the varying linear distances of each row of the array to the bottom level of the array. In addition, the quadrature hybrids which split the signals with equal time phase quadrature components for circular polarization are included

in box C. Box D contains the phase shifting capability required to steer the beam with its prescribed locations. Finally, in box E, a coaxial or or diode switch is required to select the polarization desired.

In the following discussion, each subsystem block of the integrated feed system will be discussed in terms of options and trade-offs available to providing a baseline or reference design suitable for demonstration in the laboratory.

6.2 MXN Array Element Matrix

In Figures 1, 2 are shown two basically different approaches to aperture element implementation. Figure 2 shows a flush mounted approach. In this approach circular apertures (circularly polarized annular slots, "cirranslot") are etched on the inside surface of an outer cylinder. This cylinder is conceptually a single .16 cm rolled teflon fiberglass substrate copper or aluminum clad on both sides. At the center of each cirranslot is a dual coaxial line (3), (6) which feeds the spatially orthogonal microstrip slot exciters (9) with time quadrature signals for circular polarized excitation. The coaxial lines are brought through to a second cylinder (1) coaxial with the outer cylinder (8). This second coaxial cylinder is also of metal clad teflon quartz rolled into a 7.6 cm diameter cylinder. The coaxial line exits the inside of this cylinder and mates electrically with a dual polarization corporate feed network yet to be discussed. The concentric cylinders are held securely and coaxially by rivets mounted on each side of the coaxial feed lines. Each row of elements is isolated electrically by cavity limit rings (2) as shown in Figure 2. As far as the radiating elements of a row are concerned, the "cavity" behind the slots are coaxial cavities in the circumferential direction and half wave cavities in the vertical dimension. The length of a 5-row aperture proper is 34.3 cm (13.5 inches), with an outer diameter of 10.16 cm (4 inches).

The second alternate configuration is that shown in Figure 1. Here the radiating element consists of a slot/dipole (3), (4) combination yielding two spatially orthogonal linear polarizations. As in the previous case, the region formed by the two concentric cylinders acts as a cavity this time for the radiating axial slots. The cavity length in the circumferential direction is $\lambda/4$ and constitutes the equivalent of a quarter wave cavity fed slot. The dipole is adjacent to the slot and forms the orthogonal polarization required for circular polarization. In the axial direction there is no electrical need for cavity boundaries. This is because the fields of each slot have a zero at the slot end and is confined to the region bounded in the circumferential direction by the copper clad dipole boards (5) and in the axial direction by the virtual walls due to the nature of the field(6).

The slot/dipole apertures are fed from an identical corporate feed network as in the cirranslot case. The interface between this corporate feed and the slot/dipole radiators is different however. In this case, microstrip circuits are used to excite the apertures. In Figure 1 View B item (8) shows the dipole microstrip exciter printed on the side opposite the dipole (View A). The slot exciter is a microstrip tab View B (7), (9) shown intersecting the radiating slot in section cc of Figure 1.

The cylinder diameter at the axial slots location is 10.16 cm (4.0 inches). The diameter of the dipoles is 13.41 cm (5.28 inches).

6.3 Corporate Feed Network

The objective of the corporate feed network is two fold. The first objective is to provide the proper amplitude and phase distribution across the aperture of the array in the circumferential plane. The second objective is to configure the network so as to maintain a volume about the axis of the antenna which is unobstructed, so as to accommodate experimental L.F. antennas. The diameter chosen for this volume was based on estimates of minimum required cavity depth for the array element radiators and the space requirements for the microstrip corporate feed network.

The layout of the corporate feed network was preceded by a tradeoff in which the use of stripline and microstrip was compared. The comparison is summarized in Table 3 below:

Table 3

Stripline/Microstrip Considerations

	Normalized Weight	Estimated Losses	Temperature Sensitivity	Mfgability
Stripline (2.3 GHz)	1.0	.016 db/cm	Thermal gradients can cause gaps between plates	Repeatability fair
Microstrip (2.3 GHz)	1/2	.012 db/cm	No thermal gap problems	Good

From all tradeoff parameters considered, microstrip was selected as the approach for implementing a feed network for IME. The use of microstrip at S-Band in space applications has been documented[7].

The corporate feed network for each circumferential row consists of two subnetworks which are images of each other. These two subnetworks (Figure 3b) carry time phase quadrature signals which feed the orthogonal linear polarized fields for either circular polarization.

Several approaches to this network were examined. These were

a) resonant shunt loaded line (series feed)
b) shunt coupled line and variations (series feed)
c) parallel corporate feed

The resonant shunt feed technique was considered as the potentially most compact design approach. In this feed approach Figure 17b.1, a straight run of transmission line is shunted at $\lambda/2$ intervals by aperture feed lines and terminated in a short circuit. The short circuit termination sets up a standing wave on the line and provides equi-amplitude signals which alternate in phase by 180°. On every other shunt feed line, a $\lambda/2$ addition of length is required to bring all signals to a common phase reference of 0°. While this approach will work over a small bandwidth, it was judged to be inadequate in providing a smooth roll plane pattern over the 2.1-2.3 band of frequencies. An estimate of the degradation at the lower band edge is given in connection with configuration b. The resonant shunt feed approach was eliminated on the basis on frequency sensitivity.

6.3.1 Shunt Coupled Line

This configuration shown in Figure 17b.2 utilizes the single transmission line shunted by directional couplers which couple energy progressively to each radiator feed point. The main transmission line is terminated in a radiator rather than in short circuit as in configuration 1. Calculations were performed on this approach to determine the required tap points and compensation feed lengths in each arm required to produce equi-phase at each element. The phase at each element N is given as:

$$\phi_N = \frac{\pi}{2} + \frac{2\pi}{\lambda_\epsilon} \sum_{n=1}^{N} \alpha_N L_N + \frac{2\pi}{\lambda_\epsilon} \Delta_N$$

where ϕ_N = phase at N^{th} Terminal

α_N = 0 $\quad n = 1$

α_N = 1 $\quad n > 1$

L_N = length of line between shunt couplers

Δ_N = length of compensating line to bring ϕ_N to a multiple of 360°.

Table 4 gives the line lengths as optimized for equi-phase conditions at 2.3 GHz. Leaving the line lengths fixed for operation at 2.3 GHz, the relative phases were computed for the condition at f = 2.1 GHz. The results are shown in the graph of Figure 18. It is clear that the phase pattern in the roll plane has significantly departed from the required ± 5° and at the levels indicated will produce severe nulls and depressions in the roll plane radiation patterns.

The relative phase difference at 2.1 GHz can be decreased by going to a parallel/series combination as shown in Figure 17b.3. Even here, the resulting phase differential (Figure 18) of 30° is too large to obtain smooth roll plane patterns with ± 5° phase deviation.

Corporate Feed Configurations

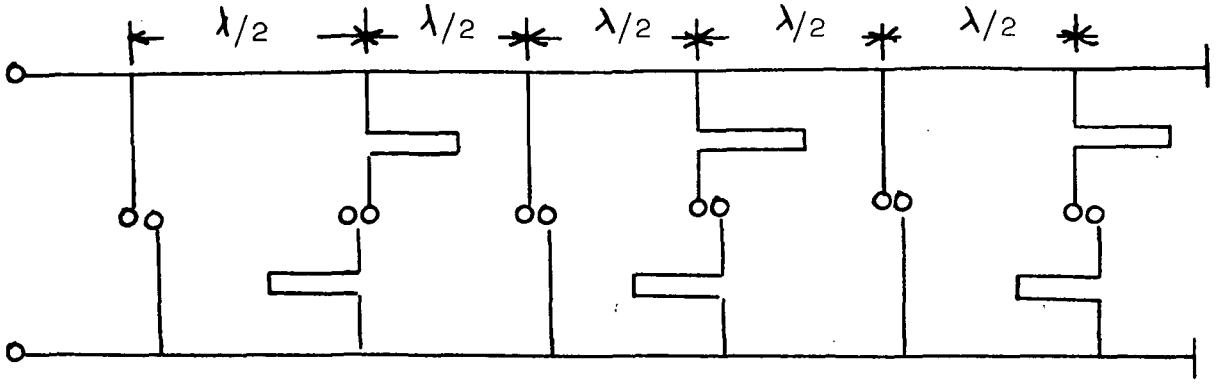

Resonant Shunt Loaded Line - 1

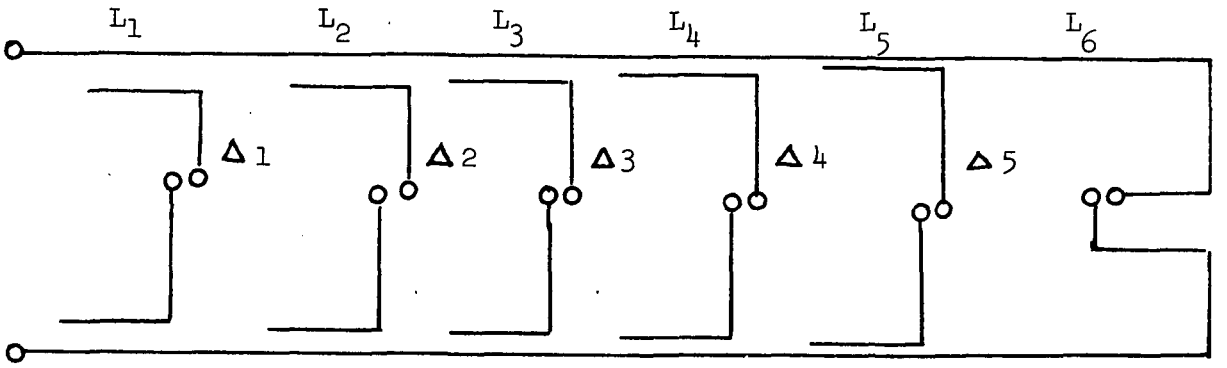

Shunt Coupled Line (Series Feed) - 2

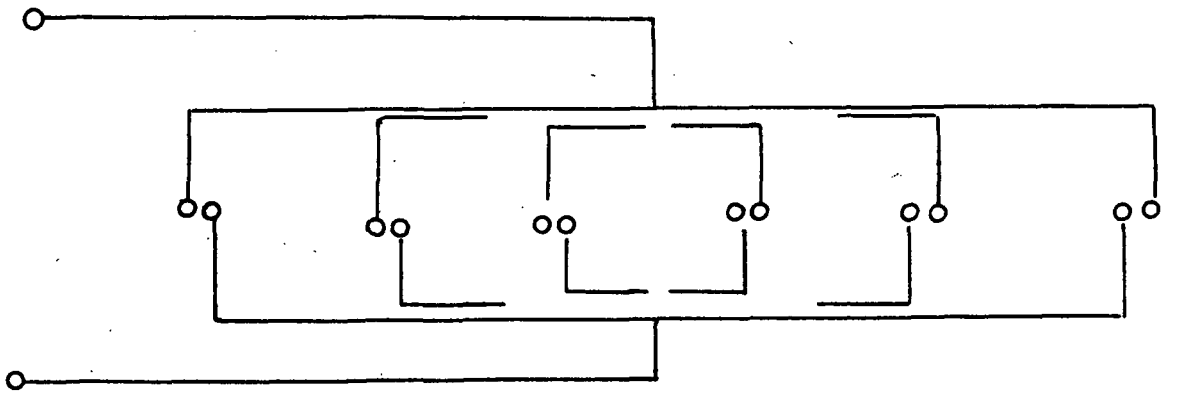

Shunt Coupled Line
(Series/Parallel) - 3

AVCO

Figure 17b

Table 4

Shunt Coupled Feed

Parameter Values for Design Optimized For 2.3 GHz

	cm	cm	∅ (deg) 2.3 GHz	∅ (deg) 2.1 GHz
1	3.0	-	216.31	205.5
2	5.8	5.6	576.31	535.6
3	2.94	2.9	576.31	535.6
4	5.8	5.8	935.31	862.8
5	2.9	2.9	935.31	862.8
6	-	5.1	935.31	865.6

For configuration b - Figure 17

By continuing the procedure, a complete parallel network (Figure 3) will reduce the phase difference to 0 at 2.1 GHz. This occurs because the relative physical path length to each individual element is identical and therefore independent of frequency.

The above analysis leads to the conclusion that only a parallel corporate feed network can meet the roll plane pattern and phase requirements over the frequency band of interest.

Having selected a parallel corporate feed approach as a reference, the next task was to lay out such a network keeping in mind that it must go on the inside surface of a 7.6 cm dia cylinder as a microstrip package. Figure 3 a, b illustrates the circuit derived. The two corporate dividers required for each row (for time phase quadrature signals) is seen to fit in the restricted volume quite easily. The feed lines, however, must ultimately arrive at the bottom of the cylinder to receive the inputs from the row phase shifter boards. As seen from Figure 3a there are 10 of these feed lines.

There are two options in bringing the row feed terminals to the lower part of array. These are the microstrip integrated option and the coaxial line option. Both these options are considered feasible, but require detail mechanical studies to determine the optimum choice. From an electrical and manufacturing point of view, the microstrip approach is attractive.

Corporate Shunt Network

Relative Phase of Elements in Circumferential Plane

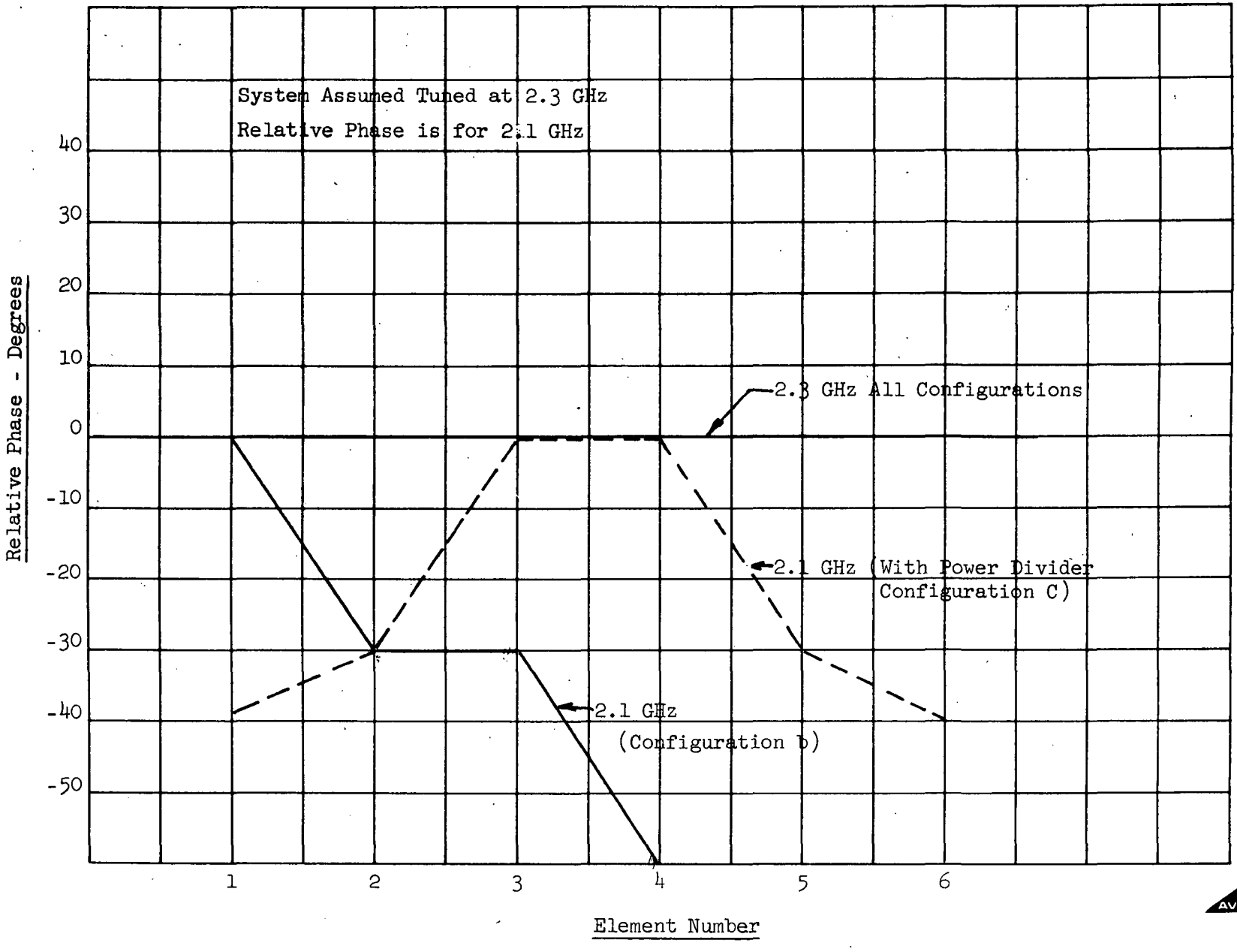

Figure 18

6.3.1.1 Integrated Option

A layout of 10 microstrip feed lines routed between apertures is shown in Figure 3a. The line widths shown (.12 cm) represent 100 Ω impedances. These impedance levels were chosen due to the fact that the requirements of 50 ohms on a .16 cm board is .4 cm which is approximately three times that of a 100-ohm line (.12 cm) and does not allow parallel routing in the initial space available. (i.e. width requirement will not allow the use of 50 ohms without the potential for excessive coupling between strips.) Calculations were performed using microstrip analysis programs developed by Weiss et al[8]. For the configuration shown in Figure 3a, the calculated maximum coupling will be 20 db. The actual coupling is a sinusoidal function of the coupling length, therefore, 20 db is the max. coupling expected. By careful adjustment of line lengths, the coupling can be controlled to insignificant values at the 2.3 GHz frequency. It is anticipated that a prime task of the development phase will be to verify that over the relatively long coupling lengths required, sufficient spacing exists to maintain coupling and phase perturbations at an insignificant level.

6.3.1.2 Coaxial Line Option

A back-up position for the 10 feed lines is to utilize semi-rigid coax line to each row. The coaxial lines would terminate at the end of the array in a microstrip circuit board which would house all phase shifter, line compensation and power divider circuits. Conceptually this board would be miniaturized with a relatively high dielectric constant of about 9.0. Time did not allow a detailed layout of this approach. It should, however, be configured on paper as a back-up design in the electrical development phase.

6.4 Phase Shifter Network

Of prime importance to the multiple beam position capability is the phase shifter design. Examination of the literature suggests that the phase shifter design may provide the largest single contribution to feed system inefficiency. There are a number of options available in providing the aperture phase taper required for steering the beam $\pm$ 30° from broadside (θ = 90°). These are considered below:

Two fundamental phase shifting devices that can be considered are ferrites and diodes. A complete discussion of the tradeoffs available is given in reference 9. It can be shown that ferrite phase shifters have advantages from the point of view of power handling capability, low insertion loss and VSWR. Diodes, however, have faster switching times, are reciprocal devices, and relatively insensitive to changes in temperature.

In this study we have restricted ourselves to the consideration of the reciprocal diode devices which are more amenable to lightweight packaging and strip circuit design approach.

Potential circuit configurations utilizing diodes in phase shifting are given together with advantages and disadvantages in Table 5.

The phase shifter chosen must provide three discrete phase values at each row. With two polarizations each row and 5 rows, there are a total of 10 discrete phase shifts required to provide the steering.

While all the candidates shown in Table 5 have potential as solutions to the beam steering requirement, the circuit of configuration d was chosen to configure a design layout. The result is shown in Figure 19. The R.F. input terminal is J-1. The output terminal is J-2. The three phase states are available by switching the diodes CR1, CR2 to conducting states to provide the delay required. When diode CR1 is forward biased, the R.F. path is through that diode. When diode CR1 is off and CR2 is on, the R.F. path is through diode CR2 producing an additional phase $\Delta \phi$ which is the equivalent path length differential between diodes CR1 and CR2. The third or reference phase state is with diodes CR1 and CR2 in the non-conducting or reverse biased mode, forcing the R.F. current to flow on the outer path of the transmission line.

While detail design has not been a part of this task, the insertion loss expected is typically .5 - 1.0 db depending on the specific diodes chosen, and degree to which they are matched in an R.F. sense. There will be a minimum of 20 diodes for the phase shift package, and reliability must be brought into the design.

6.4.1 Alternate Phase Shifting Approach

An alternate design approach eliminates the diodes and reduces the "switching" to two single pole triple throw (SP3T) switches where each throw position represents a single beam position and polarization. The design approach utilizes the properties of an integrated arrangement of quadrature and 180° hybrids as shown in Figure 20. In this approach the radiating element spacing must be reduced to 0.5λ to produce a progressive 90° phase shift from row to row. In addition, an extra row to the array has been added to increase the directivity such as to compensate for expected total system feed losses. (It is clear that, if required, additional rows can be added by placing rows of similar phase in parallel as shown with rows 1 and 5 of Figure 20.) The resultant "phase shifting" network is completely passive (no diodes) and as will be shown, can be integrated with the corporate feed system of the array in Figure 3a. Table 6 (Figure 20) is given showing the relative phases at the 5 outputs (representing right circular polarization for each of 5 rows) as a function of input (beam position). The losses through this network should be minimal ($\sim$ .5 db) since the circuitry is totally passive.

Figure 3a shows the plan view of the fully integrated corporate feed with the 3 position beam forming matrix. The set of 6 output terminals resulting represents 2 polarizations x 3 beam positions each.

6.5 Switching Matrix

The R.F. circuit component in the array feed network identified as block A in Figure 17 is a single pole triple throw (SP3T) switch required to place a single transmitter or receiver on a single polarization and beam position.

Table 5

Candidate Diode Phase Shifter Approaches

Type	Comment
Hybrid Branch Line Coupler 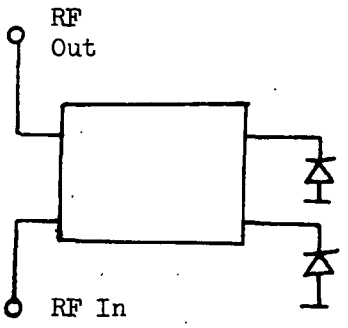 Config. A	a) Utilizes reflective diode terminations b) Utilizes least number of diodes c) Phase shift value arbitrary - by proper termination design d) Bandwidth limit to 5-10%
Rat-Race Coupler with 90^{o} Extension 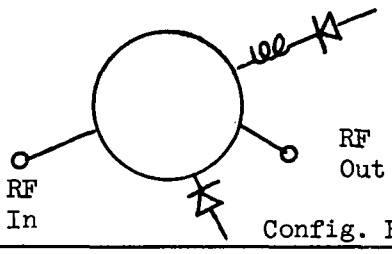 Config. B	a) Broader bandwidth than Hybrid coupler b) Narrower impedance lines than in Hybrid Branch Line Coupler
Backward Wave Coupler 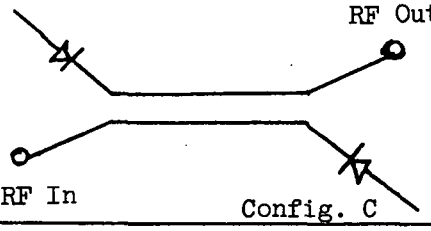 Config. C	a) Broadest bandwidth due to input and directivity being frequency independent b) Octave bandwidth possible
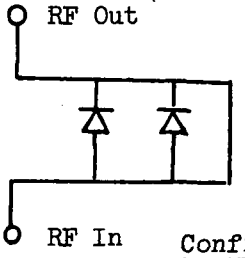 Config. D	a) Loaded line - series or parallel b) Utilize minimum number of diodes

AVCO

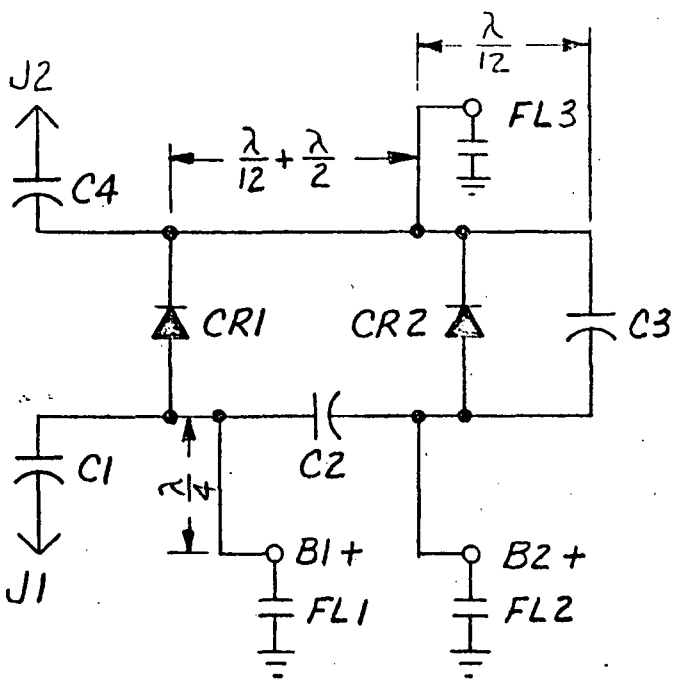

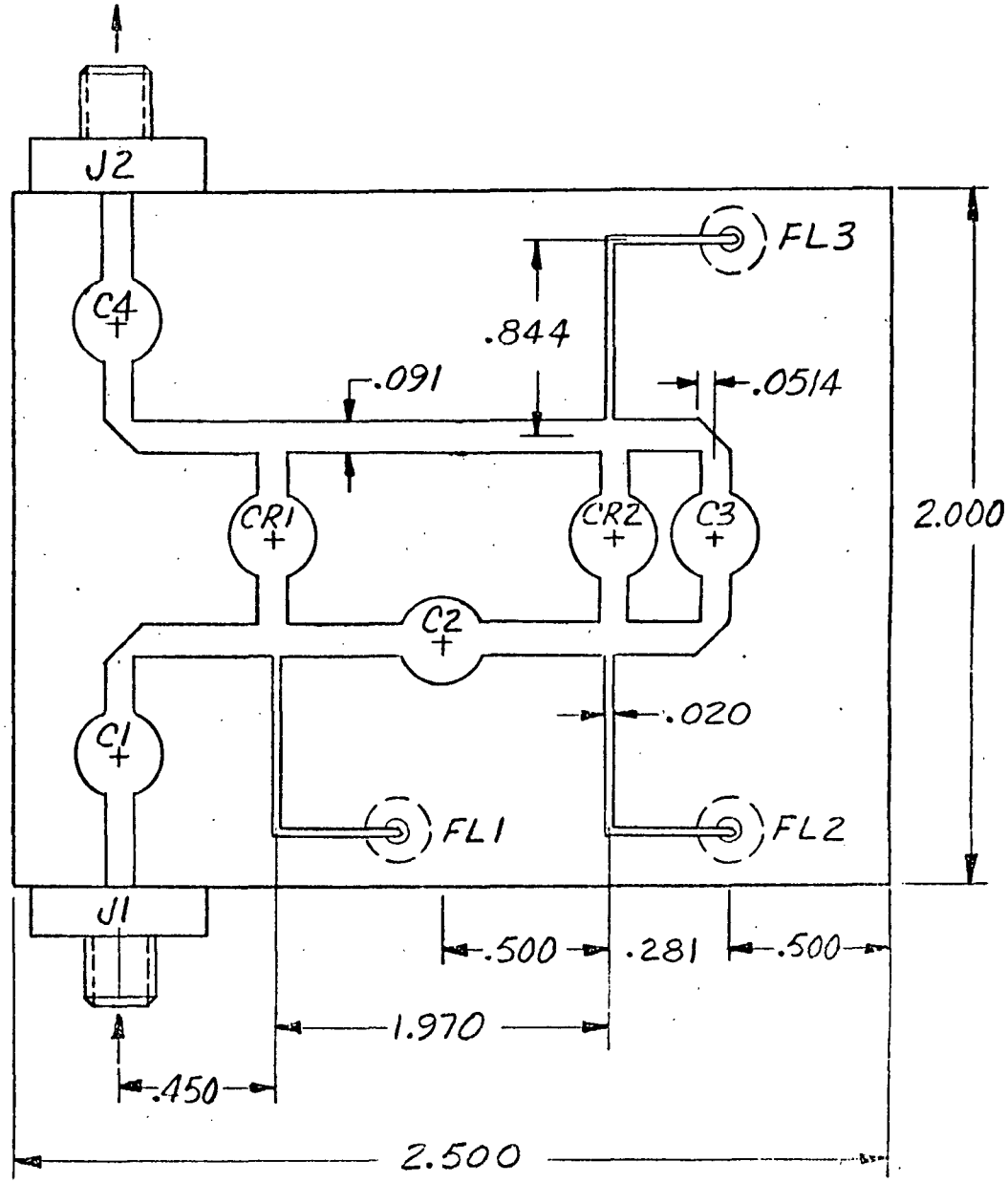

DIELECTRIC MAT'L:
RT/DUROID 5870, .062, 1 OZ
2 SIDES COPPER CLAD

CR1, CR2 — GHZ DEVICES 110A/111A
C1 THRU C4 — EMC 07-125-F
J1, J2 — ESCA 22713
FL1, FL2, FL3 — ERIE 1250-003

Layout Diode Phase Shifter

Figure 19

Relative Phase of Row Vs Beam Position

Table 6

	Row Number					
Feed-In	1	2	3	4	5	Beam Point
A	0	0	0	0	0	$\theta = 90^{\circ}$
B	0	90	180	270	0	$\theta = +60^{\circ}$
C	0	270	180	90	0	$\theta = 120^{\circ}$

Beam Forming Matrix

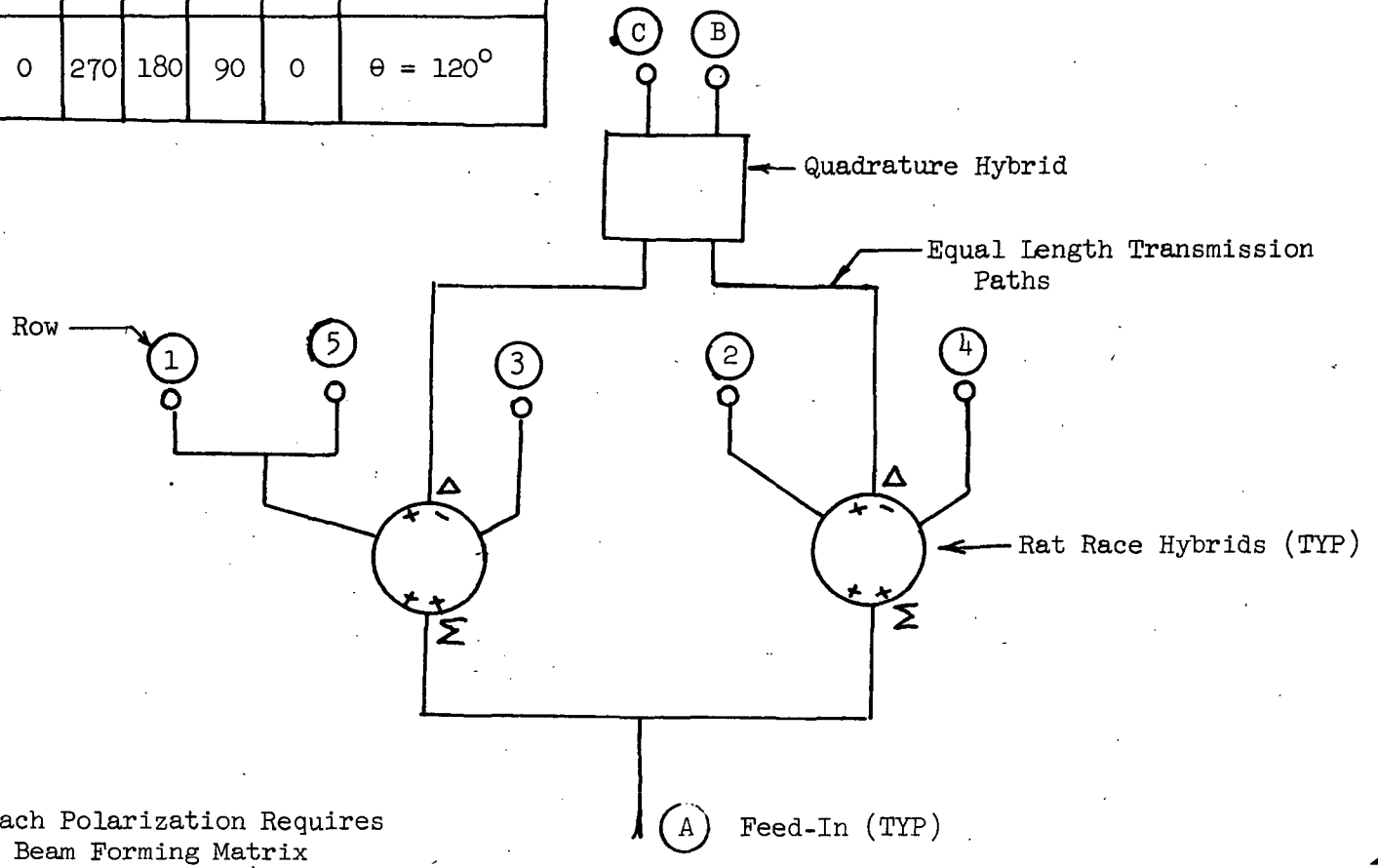

Note: Each Polarization Requires A Beam Forming Matrix (i.e., 2 ea total)

Figure 20

The switch must be reliable, and must be able to handle twenty watts of cw power at S-Band. Insertion loss should be low and independent of switched state. The bandwidth should be adequate to cover the 2.1-2.3 band of frequencies.

The technology of high power, low loss microstrip switches has advanced to where 100 watts cw can be handled in a single pole with insertion loss of 0.25 db at 2.3 GHz.(10)

This high power handling capability which is well above the required 20 watts for the present application, is achieved by use of pin diodes with a microstrip compatibility and a 1000-volt reverse breakdown capability. The switch is reported to be superior to other switching concepts such as circulator designs and the electromechanical types. Superiority is stated in terms of power drain, weight, volume, magnetic cleanliness and reliability.

A layout of an SP3T switch is given in Figure 21. In the layout of Figure 21, the state of each diode at a given time determines the power flow through the switch. Table 7 gives the required logic to channel power for each beam position.

Table 7

Microstrip Diode Logic

Mode of Operation	Diode State		
	D1	D2	D3
Input to 2	F	R	R
Input to 3	R	F	R
Input to 4	R	R	F

F = Forward Bias
R = Reverse Bias

As an example of expected insertion loss and isolation, the insertion loss and switch isolation of an SPDT device is given in Table 8 and was extracted from reference 10.

In its flight configuration, the SP3T switch would be fabricated in a microstrip substrate of alumina for a reduction in size and corresponding light weight. The switches could be located either inside the spacecraft bus, or on support structure near the antenna. Location and placement details must be worked out with vehicle design.

SP3T μ-Strip

R.F. Switch

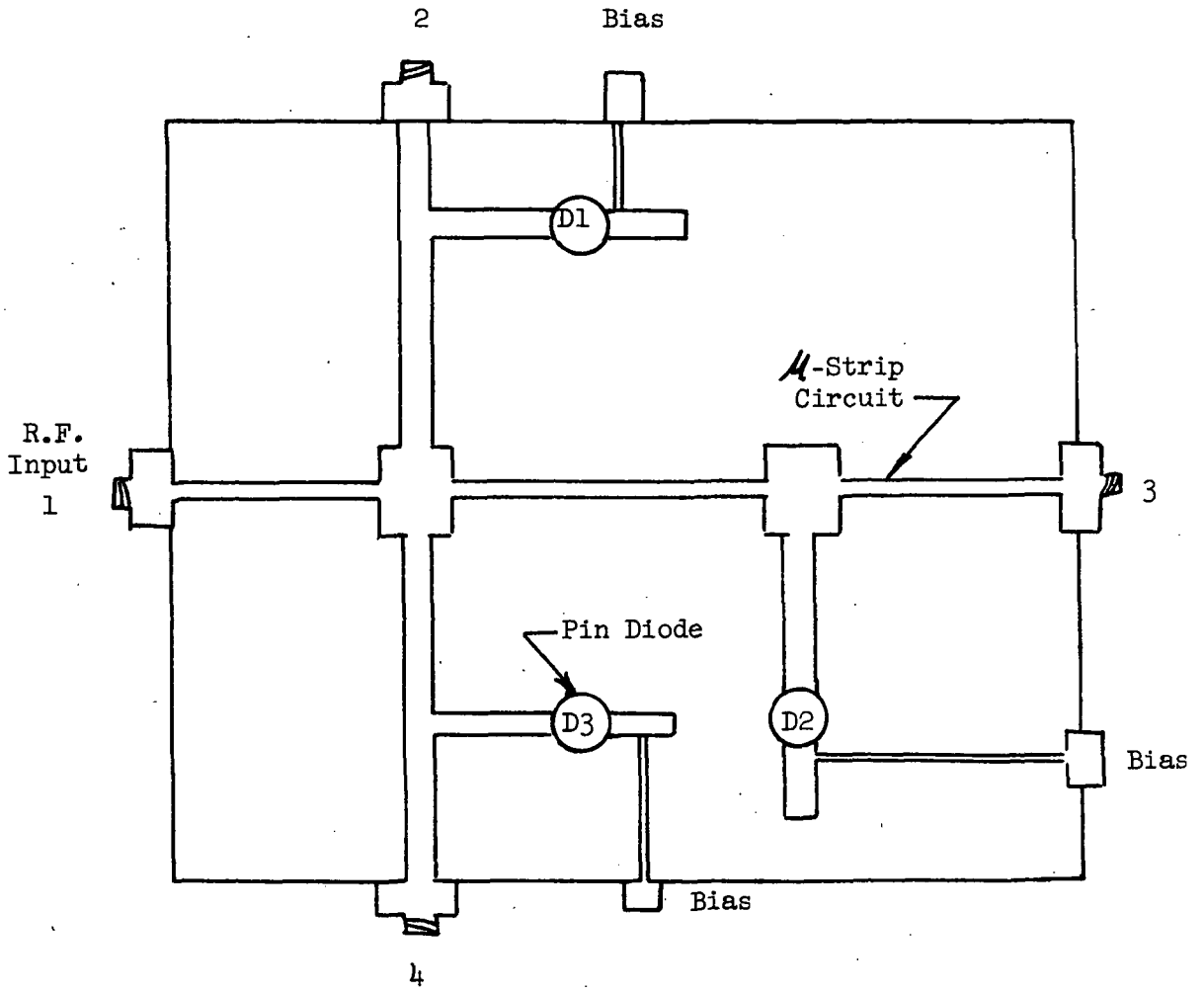

Figure 21

Table 8

R.F. Microstrip Switch

Insertion Loss and Isolation

Characteristics of an SPDT Switch		
	2.3 GHz	2.1 GHz
Insertion Loss	.25 db	.45 db
Isolation	40 db	16 db

7.0 SYSTEM GAIN SUMMARY AND RECOMMENDATIONS

The directivity capabilities of the cylindrical array and the results of the feed network configuration study can be combined to estimate the expected performance of the proposed cylindrical array of radiating apertures. Table 9 lists the expected system losses and the expected directivities when the beam is pointed at broadside (90°) and at 60° or 120°.

From Table 9, it is clear that the 4- and 5-row array while having adequate directivity, result in net gains below the desired 6.0 db due to feed circuit losses. In addition, since a 30° beamwidth represents a directivity of approximately 6.0 db, the best crossover gain (gain at 75°, just prior to switching to e.g. $\theta = 60°$) is 3.0 db corresponding to a lossless network. The higher directivities required to compensate for feed losses result in smaller beamwidths. The narrower beamwidths further reduce crossover gains and require finer phase shift steps to maintain adequate gains over the $\pm$ 30° axial plane sector.

From the above summary of system gains, the question arises as to the feasibility of increasing the rows to say 7 and providing a finer beam steering capability. Seven rows will produce a directivity in the order of 8.6 db with a corresponding beamwidth of approximately 15.5°.

In order to steer the beam $\pm$ 30° from broadside and maintain a minimum loss to gain due to pattern rolloff of 3.0 db, there must be a minimum of 5 discrete beam positions. The switching would occur when the look angles become $\theta = \pm$ 7.5°, 22.5° from the broadside value of $\theta = 90°$.

The feed network requirements to achieve this capability has not been investigated in detail. A preliminary look, however, reveals the need for addition of two rows (total 7) of elements. These two elements appear to provide problems in packaging the four additional feed lines in microstrip form. (See Figure 3a.) Also the new incremental phase requirements do not allow the use of the integrated hybrid beam forming matrix without the addition of phase shift increments to achieve the incremental phase values of

Table 9

System Gain Summary

	Beam Pointing Angle					
	4 Row			5 Row		
Parameter*	90°	60° 120°	** co	90°	60° 120°	co
Directivity -	6.5	6.0	3.5	7.5	7.0	0
Element Efficiency	-.96	→		→		
Corporate Feed	-.85	→		→		
Beam Form Matrix	-.35	→		→		
SP3T -Strip Switch	-.35	→		→		
VSWR	-.03	→		→		
Σ Losses	-2.54	→		→		
Net Gain	3.96	3.46	.96	4.96	4.46	-2.54
System Weight	1.45 kg			1.587 kg		
System Dimensions	61 x 10 cm dia.			68.6 x 10 cm dia.		

*Values in db

** co = crossover just prior to switching

45°. Figure 22 illustrates how addition of a phase shifter in conjunction with the integrated beam forming matrix of Figure 20 might be implemented. The corresponding truth table is given in Table 10.

CONCLUSIONS

The results of this study, indicate that the gains shown in Table 9 represent an achievable design goal.

It is anticipated that the addition of rows to increase directivity reaches diminishing returns. This is primarily due to the requirement to steer the beam more finely which increases losses and makes packaging more impractical.

Should the system gains realized in Table 9 not be adequate for the IME spacecraft, the details of the packaging and associated incremental losses should be studied in the next development phase of the program so as to establish the upper limit of expected gain utilizing this approach.

8.0 ANTENNA CONFIGURATION FOR 9.0 DB GAIN

As part of this study, a preliminary investigation was made to determine the configuration and performance of a 9.0 db gain antenna. The optimum approach to this design has been to make use of the 6.0 db directive design as a sub-array element. An estimate allowing for additional losses due to a three way power divider and associated cabling requires that three such arrays be placed in cascade axially. No beam steering was considered for the 9.0 db antenna.

Avco's computer code 2712 was exercised for the aperture configuration comprising 15 rows of circularly polarized annular slots with 5 slots per row. The broadside pattern response is given in Figures 23a, b. The resultant beamwidth is $\sim 6^{\circ}$ corresponding to 12 db directivity. The 12 db directivity is conservative anticipating a 3 db maximum loss in the feed network.

Feed Network:

The feed arrangement in this cascaded arrangement of 3 ea. 6 db directive gain antennas is identical within each sub-array except that the inputs of the 5 rows is conceived as fed from a 5-way power splitter for each polarization. This splitter replaces the beam forming matrix of Figure 20 which is not required since for this study no steering is required. (Should the additional requirement of steering be added, a diode phase shifter board would be required.) The capability of the phase shifter would be a function of the number of beam positions required to accommodate the narrow beamwidth at 9.0 db gain.

Each 6.0 db sub-array has 2 outputs representing right and left polarizations. These outputs are combined in a 3-way power splitter as shown schematically in Figure 24. The 3-way splitter could fabricated in a microstrip package to perform both a power splitter as shown schematically in

Conceptual

Beam Forming Matrix

For 7 Element Axial

Array

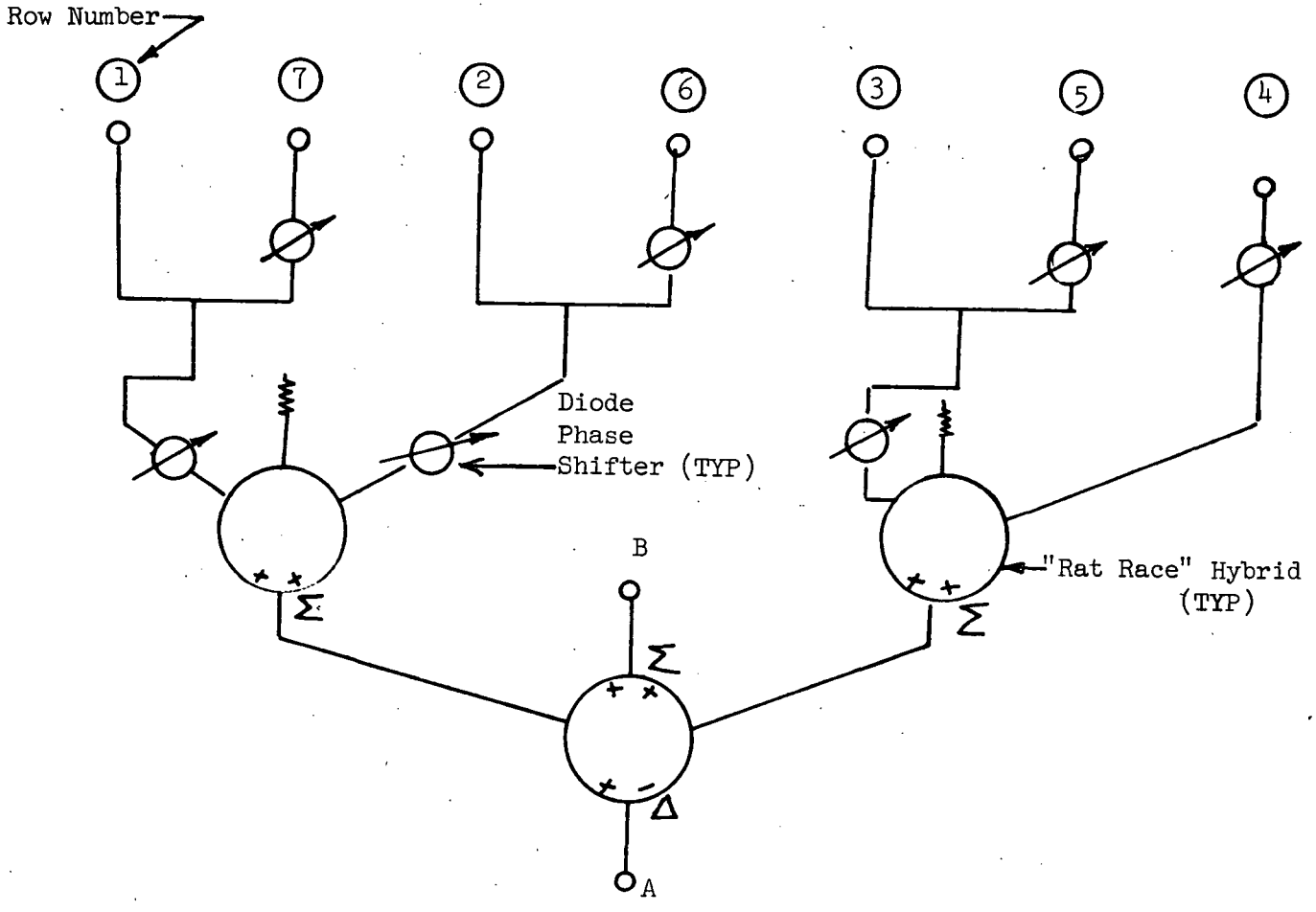

Figure 22

Table 10

Required Phase Shift

Per Row Vs Beam Pointing

For

7 Element Axial Array

Beam Position	Input Port	Phase Element 1	2	3	4	5	6	7	Required Diode Phase Shift A	B	C	D	E	F	G	H
30°	A	0	90	180	270	360	90	180	180	0	180	0	180	270	270	0
15°	B	0	45	90	135	180	225	0	0	180	90	135	180	225	180	180
0	B	0	0	0	0	0	0	0	0	0	0	0	0	0	0	0
-15°	B	0	225	180	135	90	45	0	0	180	90	45	180	45	0	0
-30°	A	180	90	360	270	180	90	0	180	0	180	0	0	270	270	0

Radiation Pattern - 15 Row Design, $\theta = 90^{\circ}$ ϕ Variable

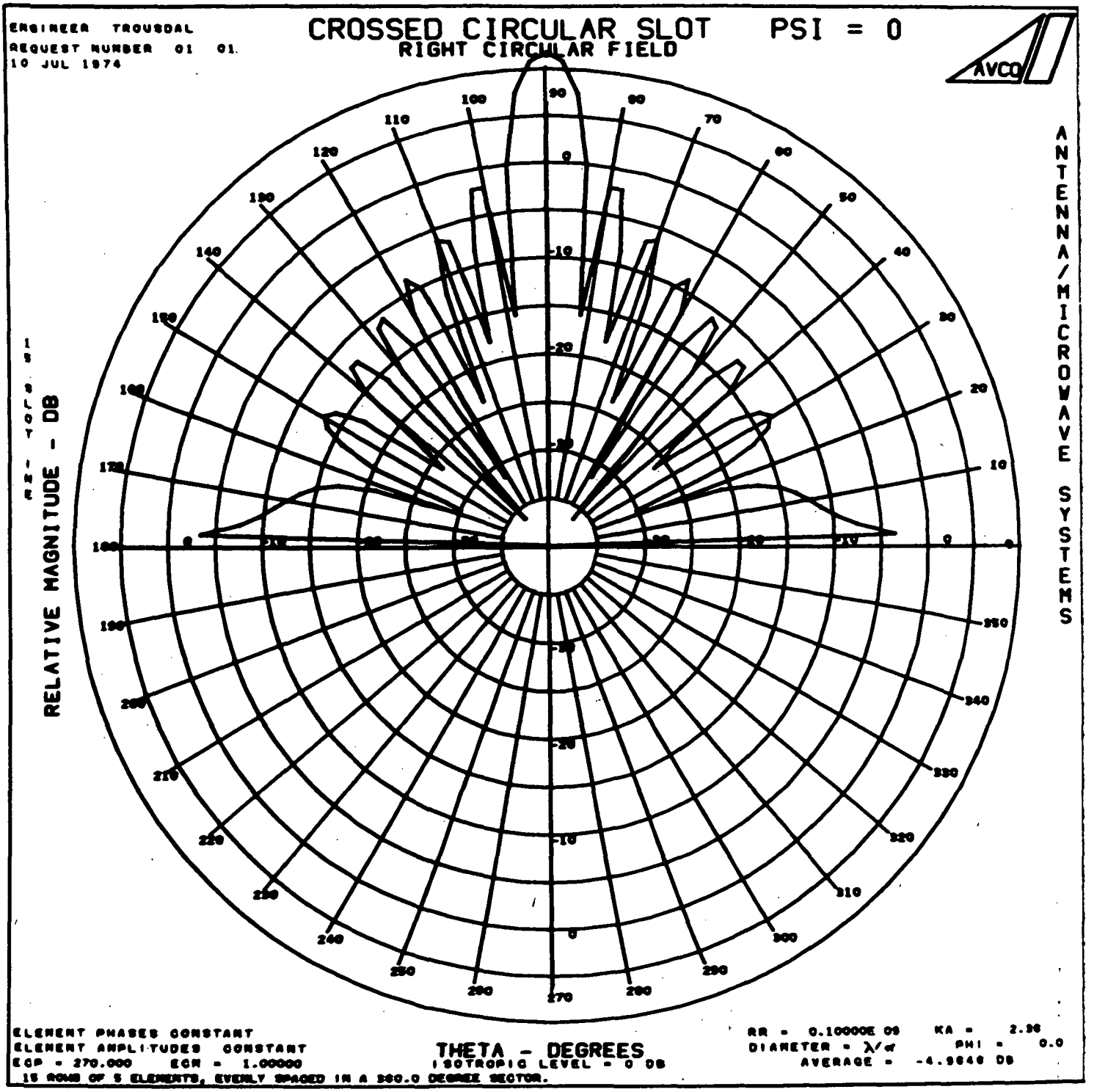

Figure 23a

Radiation Pattern - 15 Row Design, $\phi = 0$ θ Variable

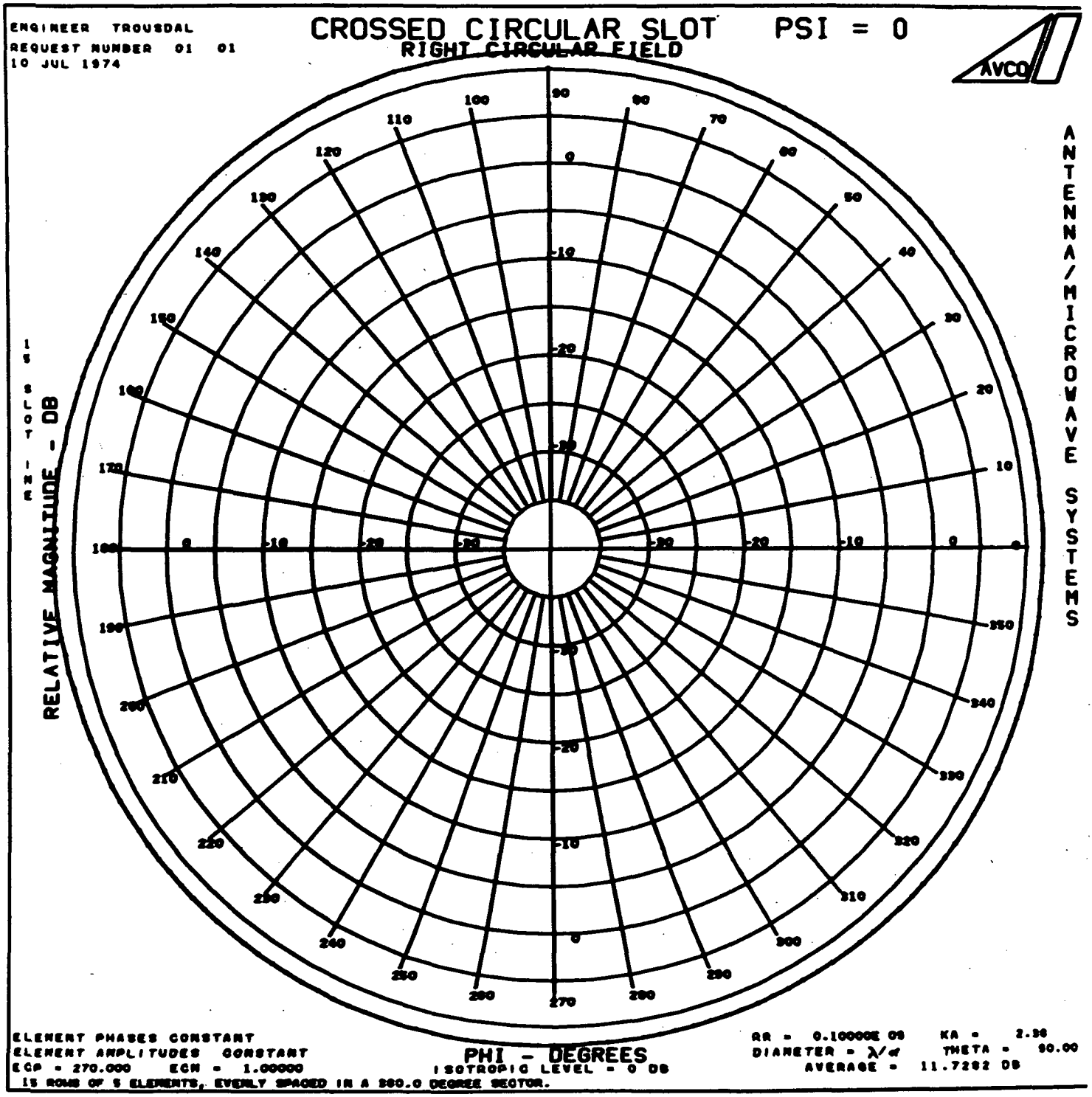

Figure 23b

3-Way Power Division For

3 Element 6.0 db Cascaded Array

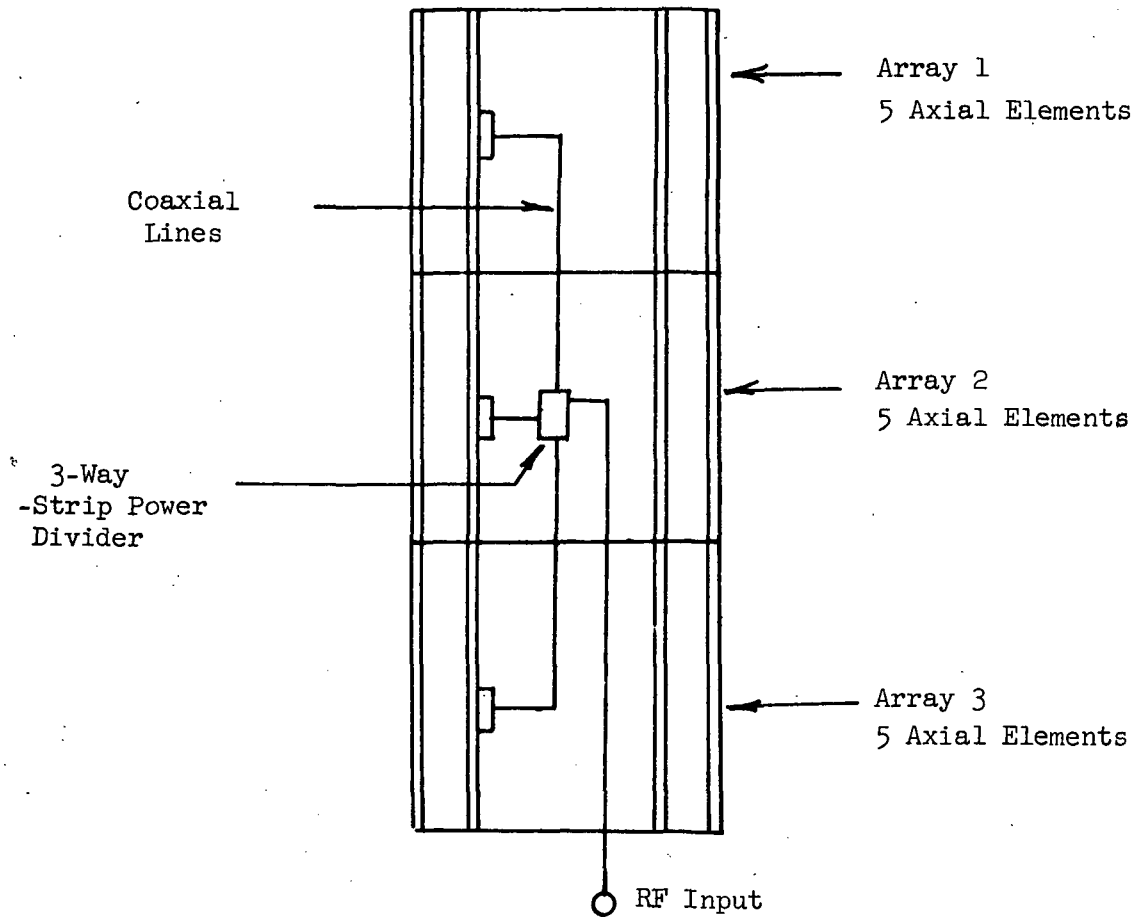

Figure 24

Figure 24. The 3-way splitter could be fabricated in a microstrip package to perform both a power splitting and line compensation function. A use of coaxial lines between the 3-way splitter and each sub-array would also be practical. A gross estimate of the overall array length would be 100 cm with a corresponding weight of 5.4 - 7.2 kg.

9.0 RECOMMENDATIONS FOR DESIGN OF ELECTRICAL PROTOTYPE

The above study has concluded that an omnidirectional communications antenna with a 3-position beam capability can be achieved with peak gains in the order of 4.8 db. It is recommended that the impact of these results on system requirements be reviewed. If system requirements call for the 6.0 db net gain, a detail examination must then be made into the configuration of a seven row array and the added requirements for finer steering to compensate for the associated narrower beamwidths.

The exact performance of the proposed approach must be examined in the laboratory. An electrical design effort is recommended which will allow a detail investigation of the feed system efficiencies which can be expected of a flight unit. Aperture element selection must be firmed up by examining bandwidth potential and basic aperture efficiencies. Finally, the axial array defined herein must be subjected to laboratory evaluation to insure performance in terms of directive gain, beamwidth, and sidelobe response.

References

1. Dion, A. "Non Resonant Slotted Arrays" IRE Transactions on Antenna and Propagation 1958 - October pg. 361.

2. Carter, P. S. "Antenna Arrays Around Cylinder" Proceedings IRE Dec. 1943 pg. 671.

3. Ricardi, L. J. "Directivity of an Array of Slots on the Surface of a Cylinder" TN-1966-52, Lincoln Laboratory, 10 Oct. 1966.

4. Bach, H. "Directivity of Basic Linear Arrays" IEEE Transactions on Antennas and Propagation, Vol. AP-18 Jan. 1970, pg. 107-110.

5. Galindo, V., Green, K. A. "Near Isotropic Circularly Polarized Antenna for Space Vehicles" IEEE Transactions Antennas & Propagation 65 Nov., pg. 872.

6. Schroeder, K. G. "Miniature Slotted Cylinder Antennas" Microwaves, Dec. 1964.

7. Gregorwich, Wis., "An Omnidirectional Telemetry Antenna for Spacecraft" 21st Annual MTC 1971.

8. Weiss, J. A. "Microwave Propagation on Coupled Pairs of Microstrip Transmission Lines" Unpublished Paper and personal communication with author.

9. White, J. F. "Diode Phase Shifters for Array Antennas" IEEE Transactions Microwave Theory & Techniques, June 1974, pg. 658.

10. Boreham, J., Choi, S. D. "High Power Microstrip RF Switches Jet Propulsion Lab - SPS Summary".

Appendix A

Program 2712

Elliptically Polarized Radiation from arrays of apertures on an infinitely long right circular cylinder of arbitrary radius

Program P2712 will compute the electromagnetic field of a linear slot of given length and orientation on a cylinder, two crossed linear slots, a circular slot of diameter λ/π or two crossed circular slots. It will also accept as input the fields as measured at the range or computed by other programs.

Fields may be arrayed circumferentially and/or axially. The program will produce polar plots, rectangular plots, printout, or tapes, of the axial and circumferential fields, the left and right circular fields, the total fields, the total field with maximum and minimum polarization loss, and the ellipticity ratio. The fields may be plotted along phi-cuts or theta-cuts.

The various fields may be integrated over the sphere to obtain coverage factors and the isotropic level.

Parameter studies may be performed on the ripple of the various fields when ka or the number of apertures in a circumferential array is varied. A parameter study of the percentage of a phi-cut with ellipticity below a given level can be done, and each cut can be analyzed for the percentage with ellipticity below various levels.

Drift, phase center shift and random noise can be added to theoretical fields to simulate measured data, or to modify and correct measured data.

APERTURE MATRIX
SAMPLE COMBINATIONS

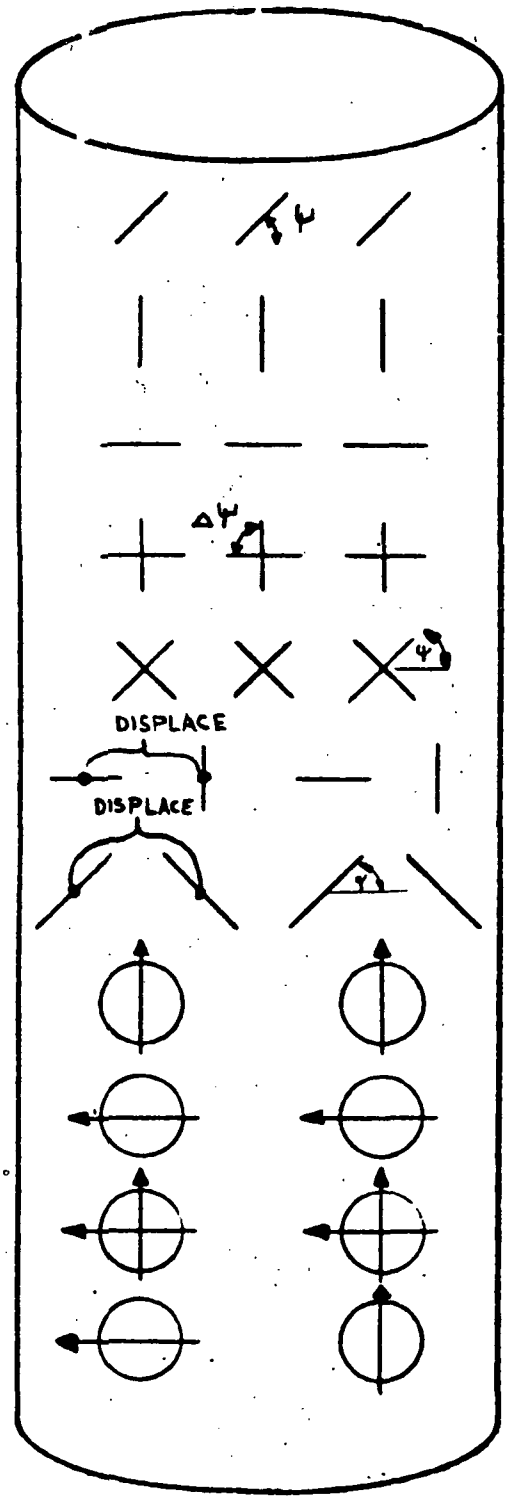

	KIND	PSI	DELTAPSI	DISPLACE
a)	1	45.	N/A	N/A
b)	1	90.	N/A	N/A
c)	1	0.	N/A	N/A
d)	2	0.	90.	0.
e)	2	45.	90.	0.
f)	2	0.	90.	10.
g)	2	45.	90	10.
h)	3	0.	N/A	N/A
i)	3	90.	N/A	N/A
j)	4	0.	90.	0.
k)	4	0.	90.	30.0

Appendix B

Slot/Dipole Antenna

Computer Program Listing

```
FORTRAN IV G LEVEL  21                MAIN              DATE = 74099        16/55/16              PAGE 0001

0001                DIMENSION PHIDEG(721),THEDEG(361),ANGLE(721),TABLE(280),GAMD(21),
                   1 Y1(721),Y2(721),Y3(721),Y4(721),Y5(721)
0002                COMPLEX ETH,EPHI,XI
0003                COMPLEX ER,EL
0004                COMMON/COEFF/BB(21),GAM(21),AD,PSID,BESE
0005                COMMON/INT/A,B,S,XL,XK,NT,NC
0006                COMMON /PLTCAT/GRAFF(10,6),POL(10,4),LTITLE(10,12),LXNAME(10,12),
                   1 LYNAME(10,12),IXTKS(10),IYTKS(10),ILIN(10),IGRID1(10,3),
                   2 IGRID2(10,3),ISYMBL(10),IM(10),XAX(10),YAX(10)
0007                XI=(0.0,1.0)
0008                CALL WHERE(TABLE)
0009                CALL SETUP(8HCYLRAD  ,4,AW)
0010                CALL SETUP(8HRADRAD  ,4,BW)
0011                CALL SETUP(8HNUMEL   ,4,NC)
0012                CALL SETUP(8HNTIERS  ,4,NT)
0013                CALL SETUP(8HSEPTIERS,4,SW)
0014                CALL SETUP(8HVOLT    ,4,BB,21)
0015                CALL SETUP(8HPHASE   ,4,GAMD,21)
0016                CALL SETUP(8HDIPAMP  ,4,AD)
0017                CALL SETUP(8HDIPPHASE,4,PSIDD)
0018                CALL SETUP(8HWAVENUM ,4,XK)
0019                CALL SETUP(8HBESE    ,4,BESE)
0020                CALL SETUP(8HXINTE   ,4,XINTE)
0021                CALL SETUP(8HPHIDEG  ,4,PHIDEG,721)
0022                CALL SETUP(8HTHEDEG  ,4,THEDEG,361)
0023                CALL SETUP(8HNTH     ,4,NTH)
0024                CALL SETUP(8HNPHI    ,4,NPHI)
0025                CALL SETUP(8HXLENGTH ,4,XLW)
0026                CALL SETUP(8HIPLOT   ,4,IPLOT)
0027                CALL SETUP(8HLTITLE  ,4,LTITLE,10,12)
0028                CALL SETUP(8HLXNAME  ,4,LXNAME,10,12)
0029                CALL SETUP(8HLYNAME  ,4,LYNAME,10,12)
0030                CALL SETUP(8HIXTICKS ,4,IXTKS,10)
0031                CALL SETUP(8HIYTICKS ,4,IYTKS,10)
0032                CALL SETUP(8HILINEAR ,4,ILIN,10)
0033                CALL SETUP(8HGRAF    ,4,GRAFF,10,6)
0034                CALL SETUP(8HPOLAR   ,4,POL,10,4)
0035                CALL SETUP(8HIGRID1  ,4,IGRID1,10,3)
0036                CALL SETUP(8HIGRID2  ,4,IGRID2,10,3)
0037                CALL SETUP(8HISYMBOL ,4,ISYMBL,10)
0038                CALL SETUP(8HIMARK   ,4,IM,10)
0039                CALL SETUP(8HXAXIS   ,4,XAX,10)
0040                CALL SETUP(8HYAXIS   ,4,YAX,10)
0041                IPLCT=0
0042                IPS=0
0043                PI=3.1415927
0044              901 CALL READIN(INCOL1,6998)
0045                IF (IPLOT.EQ.0.OR.IPS.EQ.1) GO TO 5
```

```
0046            CALL IDFRM8('OTAZO   ','44',5,'TITLE',12)
0047            CALL CALCMP(0.,0.,0,2)
0048            IPS=1
0049          5 DO 7 K=1,NC
0050          7 GAM(K)=GAMD(K)*PI/180.
0051            PSID=PSIDD*PI/180.
0052            XLAM=2.0*PI/XK
0053            A=AN*XLAM
0054            B=BW*XLAM
0055            S=SW*XLAM
0056            XL=XLAM*XLW
0057            CALL TRAPZ(XITH,XIPH,XINTE)
0058            DEN=XITH*NC*NC*AD*AD*PI+XIPH*NC*NC*PI
0059            DEN=DEN/(4.0*PI)
0060            DO 1 K=1,NPHI
0061            PHID=PHIDEG(K)
0062            PHI=PHID*PI/180.
0063            DO 2 J=1,NTH
0064            THD=THEDEG(J)
0065            TH=THD*PI/180.
0066            IF(THD  .NE. 0.0  .AND.  THD  .NE. 180.) GO TO 90
0067            ETH=(0.0,0.0)
0068            EPHI=(0.0,0.0)
0069            GO TO 91
0070         90 CALL FIELD(TH,PHI,ETH,EPHI)
0071         91 DIR=(CABS(ETH)**2+CABS(EPHI)**2)/DEN
0072            ER=.5*(EPHI+XI*ETH)
0073            EL=.5*(EPHI-XI*ETH)
0074            ERA=CABS(ER)
0075            ELA=CABS(EL)
0076            TEST=CABS(ER-EL)
0077            IF(ERA .NE. 0.0 .OR. ELA  .NE. 0.0) GO TO 92
0078            AR=0.0
0079            GO TO 81
0080         92 IF(ERA .NE. ELA) GO TO 80
0081            AR=.1E90
0082            GO TO 81
0083         80 AR=ABS((ERA+ELA)/(ERA-ELA))
0084         81 ETHR=ETH
0085            EPHR=ETH
0086            ETHI=-XI*ETH
0087            EPHR=EPHI
0088            EPHI=-EPHI*XI
0089            ATH=CABS(ETH)
0090            APH=CABS(EPHI)
0091            IF(ETHR .NE. 0.0 .OR. ETHI .NE. 0.) GO TO 70
0092            PTH=0.0
0093            GO TO 71
```

```
0094          70 PTH=ATAN2(ETHI,ETHR)
0095          71 IF(EPHR .NE. 0.0 .OR. EPHII .NE. 0.0) GO TO 72
0096             PPHI=0.0
0097             GO TO 73
0098          72 PPHI=ATAN2(EPHII,EPHR)
0099          73 PTHD=PTH*180./PI
0100             PPHID=PPHI*180./PI
0101             WRITE(6,200) PHID,THD,ATH,PTHD,APH,PPHID,DIR
0102             WRITE(6,201) ERA,ELA,AR
0103             IF(ERA .EQ. 0.0) GO TO 150
0104             ERDB=10.*ALOG10(ERA**2/DEN)
0105             GO TO 151
0106         150 ERDB=-40.0
0107         151 IF(ELA .EQ. 0.0) GO TO 152
0108             ELDB=10.*ALOG10(ELA**2/DEN)
0109             GO TO 153
0110         152 ELDB=-40.0
0111         153 IF(AR .EQ. 0.0) GO TO 154
0112             AXDB=20.*ALOG10(AR)
0113             GO TO 155
0114         154 AXDB=-40.0
0115         155 IF(ATH .EQ. 0.0) GO TO 156
0116             ETHDB=10.*ALOG10(ATH**2/DEN)
0117             GO TO 157
0118         156 ETHDB=-40.0
0119         157 IF(APH .EQ. 0.0) GO TO 158
0120             EPHIDB=10.*ALOG10(APH**2/DEN)
0121             GO TO 159
0122         158 EPHIDB =-40.
0123         159 CONTINUE
0124         201 FORMAT(1H ,'ER=',E11.4,5X,'EL=',E11.4,5X,' AR=',E11.4,/)
0125             IF(NPHI .EQ. 1) ANGLE(J)=THD
0126             IF(NTH .EQ. 1) ANGLE(K)=PHID
0127             IF (NPHI.EQ.1) INDEX=J
0128             IF (NTH.EQ.1) INDEX=K
0129             Y1(INDEX)=ERDB
0130             Y2(INDEX)=ELDB
0131             Y3(INDEX)=AXDB
0132             Y4(INDEX)=ETHDB
0133             Y5(INDEX)=EPHIDB
0134           2 CONTINUE
0135           1 CONTINUE
0136         200 FORMAT(1H ,'PHI=',F6.2,5X,'THE.=',F6.2,5X,'/ETH/=',E11.4,5X,
                1'PHASETH=',F7.2,/,1H ,'/EPHI/=',E11.4,5X,'PHASEPHI=',F7.2,5X,
                1'DIR.=',E11.4)
0137             IF (IPLOT.EQ.0) GO TO 901
0138             IF (NTH.GT.NPHI) NPTS=NTH
0139             IF (NPHI.GT.NTH) NPTS=NPHI
```

```
0140            CALL DPLOT(1,ANGLE,Y1,NPTS)
0141            CALL DPLOT(2,ANGLE,Y2,NPTS)
0142            CALL DPLOT(3,ANGLE,Y3,NPTS)
0143            CALL DPLOT(4,ANGLE,Y4,NPTS)
0144            CALL DPLOT(5,ANGLE,Y5,NPTS)
0145            GO TO 901
0146        998 IF (IPLOT.EQ.0) GO TO 999
0147            CALL ENDJ88
0148        999 STOP
0149            END
```

COMMON BLOCK /COEFF / MAP SIZE 84

SYMBOL	LOCATION	SYMBOL	LOCATION	SYMBOL	LOCATION	SYMBOL	LOCATION	SYMBOL	LOCATION
BB	0	GAM	54	AD	A8	PSID	AC	BESE	B0

COMMON BLOCK /INT / MAP SIZE 1C

SYMBOL	LOCATION	SYMBOL	LOCATION	SYMBOL	LOCATION	SYMBOL	LOCATION	SYMBOL	LOCATION
A	0	B	4	S	8	XL	C	XX	10
NT	14	NC	18						

COMMON BLOCK /PLTDAT / MAP SIZE 938

SYMBOL	LOCATION	SYMBOL	LOCATION	SYMBOL	LOCATION	SYMBOL	LOCATION	SYMBOL	LOCATION
GRAFF	0	POL	F0	LTITLE	190	LXNAME	370	LYNAME	550
IXTKS	730	IYTKS	758	ILIN	780	IGRID1	7A8	IGRID2	820
ISYMBL	898	IM	8C0	XAX	8E8	YAX	910		

SUBPROGRAMS CALLED

SYMBOL	LOCATION	SYMBOL	LOCATION	SYMBOL	LOCATION	SYMBOL	LOCATION	SYMBOL	LOCATION
WHERE	1C0	SETUP	1C4	READIN	1C8	IDFRMB	1CC	CALCMP	1D0
TRAPZ	1D4	FIELD	1D8	CMPY=	1DC	IBCOM=	1E0	DPLOT	1E4
ENDJBB	1E8	CABS	1EC	ATAN2	1F0	ALOG10	1F4		

SCALAR MAP

SYMBOL	LOCATION	SYMBOL	LOCATION	SYMBOL	LOCATION	SYMBOL	LOCATION	SYMBOL	LOCATION
XI	4E8	ETH	4F0	EPHI	4F8	ER	500	EL	508
AW	510	BW	514	SW	518	PSIDD	51C	XINTE	520
NTH	524	NPHI	528	XLW	52C	IPLOT	530	IPS	534
PI	538	INCCLI	53C	K	540	XLAM	544	XITH	548
XIPH	54C	DEN	550	PHID	554	PHI	558	J	55C
THD	560	TH	564	DIR	568	ERA	56C	ELA	570
TEST	574	AR	578	ETHR	57C	ETHI	580	EPHR	584
EPHII	588	ATH	58C	APH	590	PTH	594	PPHI	598
PTHD	59C	PPHID	5A0	ERDB	5A4	ELDB	5A8	AXDB	5AC
ETHDB	5B0	EPHIDB	5B4	INDEX	5B8	NPTS	5BC		

ARRAY MAP

SYMBOL	LOCATION	SYMBOL	LOCATION	SYMBOL	LOCATION	SYMBOL	LOCATION	SYMBOL	LOCATION
PHIDEG	5C0	THEDEG	1104	ANGLE	16A8	TABLE	21EC	GAMD	264C
Y1	26A0	Y2	31E4	Y3	3D28	Y4	486C	Y5	53B0

FORMAT STATEMENT MAP

SYMBOL	LOCATION	SYMBOL	LOCATION	SYMBOL	LOCATION	SYMBOL	LOCATION	SYMBOL	LOCATION

```
  201       6000          200       6030

  *OPTIONS IN EFFECT*   ID,EBCDIC,SOURCE,NOLIST,NODECK,LOAD,MAP
  *OPTIONS IN EFFECT*   NAME = MAIN     , LINECNT =      50
  *STATISTICS*     SOURCE STATEMENTS =      149,PROGRAM SIZE =    27686
  *STATISTICS*  NO DIAGNOSTICS GENERATED
```

```
FORTRAN IV G LEVEL  21                TRAPZ            DATE = 74099        16/55/16            PAGE 0001

0001                  SUBROUTINE TRAPZ(XITH,XIPH,ERROR)
0002                  PI=3.1415927
0003                  DTH=SQRT(ERROR)
0004                  NTH=PI/DTH
0005                  L=0
0006               10 SUM1=0.
0007                  SUM2=0.
0008                  NTHM1=NTH-1
0009                  DO 1 K=2,NTHM1
0010                  DTH=PI/(NTH-1)
0011                  TH=(K-1)*DTH
0012                  CALL INTEG(TH,FTH,FPHI)
0013                  SUM1=SUM1+FTH*SIN(TH)
0014                1 SUM2=SUM2+FPHI*SIN(TH)
0015                  XITH=DTH*SUM1
0016                  XIPH=DTH*SUM2
0017                  L=L+1
0018                  NTH=2*NTH
0019                  NTHM1=NTH-1
0020                  IF(L .EQ. 1) GO TO 7
0021                  A1=ABS((XITH-XITHP)/XITH)
0022                  A2=ABS((XIPH-XIPHP)/XIPH)
0023                  IF(A1 .LE. ERROR .AND. A2 .LE. ERROR) GO TO 15
0024                  XITHP=XITH
0025                  XIPHP=XIPH
0026                  GO TO 10
0027               7  XITHP=XITH
0028                  XIPHP=XIPH
0029                  GO TO 10
0030              15  RETURN
0031                  END
```

SUBPROGRAMS CALLED

SYMBOL	LOCATION	SYMBOL	LOCATION	SYMBOL	LOCATION	SYMBOL	LOCATION	SYMBOL	LOCATION
INTEG	B4	SQRT	B8	SIN	BC				

SCALAR MAP

SYMBOL	LOCATION	SYMBOL	LOCATION	SYMBOL	LOCATION	SYMBOL	LOCATION	SYMBOL	LOCATION
PI	E0	DTH	E4	ERROR	E8	NTH	EC	L	F0
SUM1	F4	SUM2	F8	NTHM1	FC	K	100	TH	104
FTH	108	FPHI	10C	XITH	110	XIPH	114	A1	118
XITHP	11C	A2	120	XIPHP	124				

OPTIONS IN EFFECT ID,EBCDIC,SOURCE,NOLIST,NODECK,LOAD,MAP
OPTIONS IN EFFECT NAME = TRAPZ , LINECNT = 50
STATISTICS SOURCE STATEMENTS = 31,PROGRAM SIZE = 952
STATISTICS NO DIAGNOSTICS GENERATED

```
0001          SUBROUTINE NUMAX(XMIN,ARG,NMAX)
0002          INTEGER XNUP
0003          PI=3.1415927
0004          E=2.718282
0005          XNUP=3
0006          XNUP=1
0007      100 F=1./SQRT(2.*PI*XNUP)
0008          F=F*(E*ARG/(2.*XNUP))**XNUP
0009          IF(F .LE. XMIN) GO TO 5
0010          XNUP=XNUP+1
0011          GO TO 100
0012        5 NMAX=XNUP
0013          RETURN
0014          END
```

SUBPROGRAMS CALLED

SYMBOL	LOCATION	SYMBOL	LOCATION	SYMBOL	LOCATION	SYMBOL	LOCATION	SYMBOL	LOCATION
FRXPI=	A4	SQRT	A8						

SCALAR MAP

SYMBOL	LOCATION	SYMBOL	LOCATION	SYMBOL	LOCATION	SYMBOL	LOCATION	SYMBOL	LOCATION
PI	88	E	8C	XNUP	C0	F	C4	ARG	C8
XMIN	CC	XMAX	D0						

```
    *OPTIONS IN EFFECT*   ID,EBCDIC,SOURCE,NOLIST,NODECK,LOAD,MAP
    *OPTIONS IN EFFECT*   NAME = NUMAX    , LINECNT =      50
    *STATISTICS*     SOURCE STATEMENTS =       14,PROGRAM SIZE =      614
    *STATISTICS*   NO DIAGNOSTICS GENERATED
```

```
0001            SUBROUTINE FIELD(TH,PH,ETH,EPHI)
0002            DIMENSION XJA(101),XJB(101),XYA(101),XYB(101)
0003            COMPLEX UA(101),UB(101),UPA(101),TERM1,TERM2,XI,DI,ACC,ETH,EPHI
0004            COMMON/COEFF/BB(21),GAM(21),AD,PSID,BESE
0005            COMMON/INT/A,B,S,XL,XK,NT,NC
0006            XI=(0.0,1.0)
0007            PI=3.1415927
0008            STH=SIN(TH)
0009            CTH=COS(TH)
0010            ARGA=XK*A*STH
0011            ARGB=XK*B*STH
0012            CALL NUMAX(BESE,ARGB,NMAX)
0013            NR=NMAX/NC+1
0014            NR1=NR+1
0015            NP=NC*NR
0016            NP1=NP+1
0017            CALL BESJ(ARGA,NP1,XJA,.1E-5,IER)
0018            CALL BESY(ARGA,NP1,XYA,IER)
0019            CALL BESJ(ARGB,NP1,XJB,.1E-5,IER)
0020            CALL BESY(ARGB,NP1,XYB,IER)
0021            DO 1 K=1,NP1
0022            UA(K)=CMPLX(XJA(K),-XYA(K))
0023            UB(K)=CMPLX(XJB(K),-XYB(K))
0024            IF( K .EQ. 1) GO TO 1
0025            UPA(K-1)=(K-2)*UA(K-1)/ARGA-UA(K)
0026          1 CONTINUE
0027            UA(NP1+1)=CMPLX(XJA(NP1+1),-XYA(NP1+1))
0028            UPA(NP1)=NP*UA(NP1)/ARGA-UA(NP1+1)
0029            TERM1=XJB(1)-XJA(1)*(UB(1)/UA(1))
0030            TERM2=1.0/UPA(1)
0031            DO 2 K=2,NR1
0032            KK=(K-1)*NC
0033            KP=KK+1
0034            DI=2.0*XI**KK
0035            CRTH=COS(KK*PH)
0036            TERM1=DI*(XJB(KP)-XJA(KP)*(UB(KP)/UA(KP)))*CRTH+TERM1
0037          2 TERM2=TERM2+DI*CRTH/UPA(KP)
0038            ACC=(0.0,0.0)
0039            DO 3 KJ=1,NT
0040          3 ACC=ACC+BB(KJ)*CEXP(XI*((KJ-1)*XK*S*CTH+GAM(KJ)))
0041            ETH=ACC*TERM1*NC*AD*CEXP(XI*PSID)*STH
0042            ARG1=.5*XK*XL*CTH
0043            ARG2=ARG1*2./PI
0044            F1=COS(ARG1)/(1.-ARG2**2)
0045            XM1=XL/(A*PI**3)
0046            EPHI=ACC*TERM2*NC*F1*XM1
0047            RETURN
0048            END
```

COMMON BLOCK /COEFF / MAP SIZE 84

SYMBOL	LOCATION	SYMBOL	LOCATION	SYMBOL	LOCATION	SYMBOL	LOCATION	SYMBOL	LOCATION
BB	0	GAM	54	AD	A8	PSID	AC	BESE	80

COMMON BLOCK /INT / MAP SIZE 1C

SYMBOL	LOCATION	SYMBOL	LOCATION	SYMBOL	LOCATION	SYMBOL	LOCATION	SYMBOL	LOCATION
A	0	B	4	S	8	XL	C	XK	10
NT	14	NC	18						

SUBPROGRAMS CALLED

SYMBOL	LOCATION	SYMBOL	LOCATION	SYMBOL	LOCATION	SYMBOL	LOCATION	SYMBOL	LOCATION
NUMAX	84	BESJ	88	BESY	8C	CMPY=	C0	CDVD=	C4
FCXPI=	C8	SIN	CC	COS	D0	CEXP	D4		

SCALAR MAP

SYMBOL	LOCATION	SYMBOL	LOCATION	SYMBOL	LOCATION	SYMBOL	LOCATION	SYMBOL	LOCATION
XI	238	TERM1	240	TERM2	248	DI	250	ACC	258
ETH	260	EPHI	268	PI	270	STH	274	TH	278
CTH	27C	ARGA	280	ARGB	284	NMAX	288	NR	28C
NR1	290	NP	294	NP1	298	IER	29C	K	2A0
KK	2A4	KP	2A8	CRTH	2AC	PH	2B0	KJ	2B4
ARG1	2B8	ARG2	2BC	F1	2C0	XM1	2C4		

ARRAY MAP

SYMBOL	LOCATION	SYMBOL	LOCATION	SYMBOL	LOCATION	SYMBOL	LOCATION	SYMBOL	LOCATION
XJA	2C8	XJB	45C	XYA	5F0	XYB	784	UA	918
UB	C40	UPA	F68						

```
*OPTIONS IN EFFECT*   ID,EBCDIC,SOURCE,NOLIST,NODECK,LOAD,MAP
*OPTIONS IN EFFECT*   NAME = FIELD    , LINECNT =     50
*STATISTICS*    SOURCE STATEMENTS =       48,PROGRAM SIZE =     6960
*STATISTICS*  NO DIAGNOSTICS GENERATED
```

```
0001            SUBROUTINE INTEG(TH,FTH,FPHI)
0002            DIMENSION XJA(101),XJB(101),XYA(101),XYB(101)
0003            COMPLEX UA(101),UB(101),UPA(101)
0004            COMMON/CCEFF/BB(21),GAM(21),AD,PSID,BESE
0005            COMMON/IN1/A,B,S,XL,XK,NT,NC
0006            PI=3.1415927
0007            STH=SIN(TH)
0008            CTH=COS(TH)
0009            ARGA=XK*A*STH
0010            ARGB=XK*B*STH
0011            CALL NUMAX(BESE,ARGB,NMAX)
0012            NR=NMAX/NC+1
0013            NR1=NR+1
0014            NP=NC*NR
0015            NP1=NP+1
0016            CALL BESJ(ARGA,NP1,XJA,.1E-5,IER)
0017            CALL BESY(ARGA,NP1,XYA,IER)
0018            CALL BESJ(ARGB,NP1,XJB,.1E-5,IER)
0019            CALL BESY(ARGB,NP1,XYB,IER)
0020            DO 1 K=1,NP1
0021            UA(K)=CMPLX(XJA(K),-XYA(K))
0022            UB(K)=CMPLX(XJB(K),-XYB(K))
0023            IF( K .EQ. 1) GO TO 1
0024            UPA(K-1)=(K-2)*UA(K-1)/ARGA-UA(K)
0025          1 CONTINUE
0026            UA(NP1+1)=CMPLX(XJA(NP1+1),-XYA(NP1+1))
0027            UPA(NP1)=NP*UA(NP1)/ARGA-UA(NP1+1)
0028            TERM1=CABS(XJB(1)-XJA(1)*(UB(1)/UA(1)))**2
0029            TERM1=2.*TERM1
0030            TERM2=CABS(1.0/UPA(1))**2
0031            TERM2=2.*TERM2
0032            DO 2 K=2,NR1
0033            KK=(K-1)*NC
0034            KP=KK+1
0035            TERM1=TERM1+4.0*CABS(XJB(KP)-XJA(KP)*(UB(KP)/UA(KP)))**2
0036          2 TERM2=TERM2+CABS(2.0/UPA(KP))**2
0037            P=2.
0038            ACC=(0.0,0.0)
0039            DO 10 K=1,NT
0040            DO 10 J=1,K
0041            IF (K .EQ.J) P=1.
0042            ACC=ACC+P*BB(J)*BB(K)*COS(GAM(J)-GAM(K)+XK*S*CTH*(J-K))
0043            P=2.
0044         10 CONTINUE
0045            FTH=STH*STH*TERM1*ACC
0046            ARG=.5*XL*XK*CTH
0047            ARG1=2.*ARG/PI
0048            F1=COS(ARG)/(1.-ARG1*ARG1)
```

```
0049              F1=F1*F1
0050              XM1=XL/(A*PI**3)
0051              XM1=XM1*XM1
0052              FPHI=F1*XM1*TERM2*ACC
0053              RETURN
0054              END
```

COMMON BLOCK /COEFF / MAP SIZE 84

SYMBOL	LOCATION	SYMBOL	LOCATION	SYMBOL	LOCATION	SYMBOL	LOCATION	SYMBOL	LOCATION
BB	0	GAM	54	AD	A8	PSIO	AC	BESE	80

COMMON BLOCK /INT / MAP SIZE 1C

SYMBOL	LOCATION	SYMBOL	LOCATION	SYMBOL	LOCATION	SYMBOL	LOCATION	SYMBOL	LOCATION
A	0	B	4	S	8	XL	C	XK	10
NT	14	NC	18						

SUBPROGRAMS CALLED

SYMBOL	LOCATION	SYMBOL	LOCATION	SYMBOL	LOCATION	SYMBOL	LOCATION	SYMBOL	LOCATION
NUMAX	BC	BESJ	C0	BESY	C4	CMPY=	C8	CDVD=	CC
SIN	D0	COS	D4	CABS	D8				

SCALAR MAP

SYMBOL	LOCATION	SYMBOL	LOCATION	SYMBOL	LOCATION	SYMBOL	LOCATION	SYMBOL	LOCATION
PI	188	STH	18C	TH	1C0	CTH	1C4	ARGA	1C8
ARGB	1CC	NMAX	1D0	NR	1D4	NR1	1D8	NP	1DC
NP1	1E0	IER	1E4	K	1E8	TERM1	1EC	TERM2	1F0
KK	1F4	KP	1F8	P	1FC	ACC	200	J	204
FTH	2C8	ARG	20C	ARG1	210	F1	214	XM1	218
FPH1	21C								

ARRAY MAP

SYMBOL	LOCATION	SYMBOL	LOCATION	SYMBOL	LOCATION	SYMBOL	LOCATION	SYMBOL	LOCATION
XJA	220	XJB	384	XYA	548	XYB	60C	UA	870
UB	898	UPA	EC0						

OPTIONS IN EFFECT ID,EBCDIC,SOURCE,NOLIST,NODECK,LOAD,MAP
OPTIONS IN EFFECT NAME = INTEG , LINECNT = 50
STATISTICS SOURCE STATEMENTS = 54,PROGRAM SIZE = 6308
STATISTICS NO DIAGNOSTICS GENERATED

```
0001            SUBROUTINE BESY(X,N,BY,IER)
0002            DIMENSION BY(200)
0003            IF(N)180,10,10
0004         10 IER=0
0005            IF(X)190,190,20
0006         20 IF(X-4.0)40,40,30
0007         30 T1=4.0/X
0008            T2=T1*T1
0009            P0=((((-.0000037043*T2+.00017356 5)*T2-.0000487613)*T2
               1  +.00017343)*T2-.001753062)*T2+.3989423
0010            Q0=((((.00000032312*T2-.0000142078)*T2+.0000342468)*T2
               1  -.0000869791)*T2+.0004564324)*T2-.0124669
0011            P1=((((.00000042414*T2-.0000200 2)*T2+.0000580759)*T2
               1  -.000223203)*T2+.002921826)*T2+.3989423
0012            Q1=((((-.0000036594*T2+.00001622)*T2-.0000398708)*T2
               1  +.0001064741)*T2-.00063904)*T2+.03740084
0013            A=2.0/SQRT(X)
0014            B=A*T1
0015            C=X-.7853982
0016            Y0=A*P0*SIN(C)+B*Q0*COS(C)
0017            Y1=-A*P1*COS(C)+B*Q1*SIN(C)
0018            GO TO 90
0019         40 XX=.5*X
0020            X2=XX*XX
0021            T=ALOG(XX)+.5772157
0022            SUM=0.
0023            TERM=T
0024            Y0=T
0025            DO 70 L=1,15
0026            IF(L-1)50,60,50
0027         50 SUM=SUM+1./FLOAT(L-1)
0028         60 FL=L
0029            TS=T-SUM
0030            TERM=(TERM*(-X2)/FL**2)*(1.-1./(FL*TS))
0031         70 Y0=Y0+TERM
0032            TERM=XX*(T-.5)
0033            SUM=0.
0034            Y1=TERM
0035            DO 80 L=2,16
0036            SUM=SUM+1./FLOAT(L-1)
0037            FL=L
0038            FL1=FL-1.
0039            TS=T-SUM
0040            TERM=(TERM*(-X2)/(FL1*FL))*((TS-.5/FL)/(TS+.5/FL1))
0041         80 Y1=Y1+TERM
0042            PI2=.6366198
0043            Y0=PI2*Y0
0044            Y1=-PI2/X+PI2*Y1
```

```
0045            90 BY(1)=Y0
0046               BY(2)=Y1
0047               YA=Y0
0048               YB=Y1
0049               K=1
0050           140 T=FLOAT(2*K)/X
0051               YC=T*YB-YA
0052               IF(ABS(YC)-1.0E70)145,145,141
0053           141 IER=3
0054               RETURN
0055           145 K=K+1
0056               IF(K .EQ. N) GO TO 160
0057               YA=YB
0058               YB=YC
0059               BY(K+1)=YC
0060               GO TO 140
0061           160 BY(K+1)=YC
0062           170 RETURN
0063           180 IER=1
0064               RETURN
0065           190 IER=2
0066               RETURN
0067               END
```

SUBPROGRAMS CALLED

SYMBOL	LOCATION	SYMBOL	LOCATION	SYMBOL	LOCATION	SYMBOL	LOCATION	SYMBOL	LOCATION
SQRT	104	SIN	108	COS	10C	ALOG	110		

SCALAR MAP

SYMBOL	LOCATION	SYMBOL	LOCATION	SYMBOL	LOCATION	SYMBOL	LOCATION	SYMBOL	LOCATION
N	13C	IER	140	X	144	T1	148	T2	14C
P0	150	Q0	154	P1	158	Q1	15C	A	160
B	164	C	168	Y0	16C	Y1	170	XX	174
X2	178	T	17C	SUM	180	TERM	184	L	188
FL	18C	TS	190	FL1	194	PI2	198	YA	19C
YB	1A0	K	1A4	YC	1A8				

ARRAY MAP

SYMBOL	LOCATION	SYMBOL	LOCATION	SYMBOL	LOCATION	SYMBOL	LOCATION	SYMBOL	LOCATION
BY	1AC								

OPTIONS IN EFFECT ID,EBCDIC,SOURCE,NOLIST,NODECK,LOAD,MAP
OPTIONS IN EFFECT NAME = BESY , LINECNT = 50
STATISTICS SOURCE STATEMENTS = 67,PROGRAM SIZE = 1998
STATISTICS NO DIAGNOSTICS GENERATED

```
0001            SUBROUTINE BESJ(X,N,BJ,D,IER)
0002            DIMENSION BJ(200)
0003            N1=N+1
0004            IF(N) 10,20,20
0005         10 IER=1
0006            RETURN
0007         20 IF(X)30,30,31
0008         30 DO 21 K=2,N1
0009         21 BJ(K)=0.0
0010            BJ(1)=1.0
0011            IER=0
0012            RETURN
0013         31 IF(X-15.)32,32,34
0014         32 NTEST=20.0+10.*X-X**2/3
0015            GO TO 36
0016         34 NTEST=90.+.5*X
0017         36 IF(N-NTEST)40,38,38
0018         38 IER=4
0019            RETURN
0020         40 IER=0
0021            BPREV=0.0
0022            IF(X-5.)50,60,60
0023         50 MA=X+6.
0024            GO TO 70
0025         60 MA=1.4*X+60./X
0026         70 MB=N+IFIX(X)/4+2
0027            MZERO=MAXO(MA,MB)
0028            MMAX=NTEST
0029        100 DO 190 M=MZERO,MMAX,3
0030            FM1=1.E-28
0031            FM=0.0
0032            ALPHA=0.0
0033            IF(M-(M/2)*2)120,110,120
0034        110 JT=-1
0035            GO TO 130
0036        120 JT=1
0037        130 M2=M-2
0038            DO 160 K=1,M2
0039            MK=M-K
0040            BMK=2.*FLOAT(MK)*FM1/X-FM
0041            FM=FM1
0042            FM1=BMK
0043            IF(MK-N-1)140,140,150
0044        140 BJ(MK)=BMK
0045        150 JT=-JT
0046            S=1+JT
0047        160 ALPHA=ALPHA+BMK*S
0048            BJ(1)=2.*FM1/X-FM
```

```
0049              ALPHA=ALPHA+BJ(1)
0050              BJ(N1)=BJ(N1)/ALPHA
0051              A=BJ(N1)
0052              IF(ABS(A-BPREV)-ABS(D*A))200,200,190
0053          190 BPREV=A
0054          200 DO 1 K=1,N
0055            1 BJ(K)=BJ(K)/ALPHA
0056              RETURN
0057              END
```

SUBPROGRAMS CALLED

SYMBOL	LOCATION	SYMBOL	LOCATION	SYMBOL	LOCATION	SYMBOL	LOCATION	SYMBOL	LOCATION
MAXO	138								

SCALAR MAP

SYMBOL	LOCATION	SYMBOL	LOCATION	SYMBOL	LOCATION	SYMBOL	LOCATION	SYMBOL	LOCATION
N1	154	N	158	IER	15C	X	160	K	164
NTEST	168	BPREV	16C	MA	170	MB	174	MZERO	178
MMAX	17C	M	180	FM1	184	FM	188	ALPHA	18C
JT	190	M2	194	MK	198	BMK	19C	S	1A0
A	1A4	D	1A8						

ARRAY MAP

SYMBOL	LOCATION	SYMBOL	LOCATION	SYMBOL	LOCATION	SYMBOL	LOCATION	SYMBOL	LOCATION
BJ	1AC								

```
   *OPTIONS IN EFFECT*   ID,EBCDIC,SOURCE,NOLIST,NODECK,LOAD,MAP
   *OPTIONS IN EFFECT*   NAME = BESJ     , LINECNT =      50
   *STATISTICS*     SOURCE STATEMENTS =      57,PROGRAM SIZE =     1670
   *STATISTICS*  NO DIAGNOSTICS GENERATED
```

```
0001          SUBROUTINE DPLOT(N,XIN,YIN,NPTS)
0002          DIMENSION XIN(1),YIN(1)
0003          DUMMY=0.
0004          RETURN
0005          END
```

SCALAR MAP

SYMBOL	LOCATION	SYMBOL	LOCATION	SYMBOL	LOCATION	SYMBOL	LOCATION	SYMBOL	LOCATION
DUMMY	90	N	94	NPTS	98				

ARRAY MAP

SYMBOL	LOCATION	SYMBOL	LOCATION	SYMBOL	LOCATION	SYMBOL	LOCATION	SYMBOL	LOCATION
XIN	9C	YIN	A0						

```
*OPTIONS IN EFFECT*  ID,EBCDIC,SOURCE,NOLIST,NODECK,LOAD,MAP
*OPTIONS IN EFFECT*  NAME = DPLOT    , LINECNT =      50
*STATISTICS*   SOURCE STATEMENTS =        5,PROGRAM SIZE =     342
*STATISTICS*  NO DIAGNOSTICS GENERATED

*STATISTICS*  NO DIAGNOSTICS THIS STEP 2
```

```
F88-LEVEL LINKAGE EDITOR OPTIONS SPECIFIED MAP,LET,LIST
        DEFAULT OPTION(S) USED - SIZE=(98304,8192)

                                MODULE MAP

CONTROL SECTION                          ENTRY
  NAME    ORIGIN  LENGTH                   NAME   LOCATION    NAME   LOCATION    NAME   LOCATION    NAME   LOCATION
MAIN         00    6C26
TRAPZ      6C28     308
NUMAX      6FE0     266
FIELD      7248    1B30
INTFG      8D78    13A4
BESY       A620     7CE
BESJ       ADF0     686
OPLOT      B478     156
IHCSATN2*  B5D0     1CB                  ATAN2    B5D0    ATAN     B5E4
IHCCCABS*  B7A0      94                  CABS     B7A0
CALCMP  *  B858    17AC
IHCCSAS *  D008      C4                  CMPY=    D008    CDVD=    D022
ENDJOB  *  D0D0     734                  DISPFR   D100
IHCECOMH*  D808     F61                  IBCOM=   D808    FDIOCS=  D8C4    INTSWTCH E74E
IHCCOMH2*  E770     65D                  SEQDASD  EAE8
IDFRMB  *  EDD0    14CA                  ACCPLT   EE00
LAOCCOOO*  102A0    150D                 READIN   102A0   HEDING   111A6   WHERE    111E2   SETUP    11288
                                         ZEROIN   1138C
IHCSLOG *  11780     186                 ALOG10   11780   ALOG     117C8
IHCCSEXP*  11968     21D                 CEXP     11968
IHCSSCN *  11888     109                 COS      11888   SIN      118A0
IHCFCXPI*  11D68     1E5                 FCXPI=   11D68
IHCFRXPI*  11F50     141                 FRXPI=   11F50
IHCERRM *  12098     504                 ERRMON   12098   IHCERRE  12080
IHCFMAXI*  12670      C9                 MAXO     12670   MINO     12686   AMAXO    1269C   AMINO    12682
IHCSSORT*  12740     145                 SQRT     12740
IHCFCVTH*  12888     119D                ADCON=   12888   FCVAJUTP 12932   FCVLOUTP 129C2   FCVZOUTP 12B12
```

NAME	ORIGIN	LENGTH
IHCEFNTH*	13A28	542
CALCOP *	13F70	A64
DATE *	149D8	134
IHCEFIOS*	14B10	FBC
IHCFIOS2*	159D0	52E
IHCFIXPI*	15F00	14F
FLAGS8 *	16050	1AA
JBNAMB *	16200	D0
KSLT *	16200	168
SYMBOL *	16438	5DC
SBLOGAND*	16A18	B4
CLCK *	16AD0	84
CORE= *	16B58	A8
IHCFEXIT*	16C00	1C
IHCFDXPI*	16C20	14D
FLWRD8 *	16D70	88
IHCUOPT *	16DF8	3C8
EMPTY *	171C0	210
DCBS *	173D0	140
DCBDUMP *	17510	F4
OUT2 *	17608	81E
BINHEX *	17E28	D0
WTO *	17EF8	C0
MIBCOM *	17FB8	334
LOADPT *	182F0	F8
SBLOGOR *	183E8	B4
SMFWTM *	184A0	F0
IHCFOPT *	18590	304
IHCSEXP *	18898	192
IHCETRCH*	18A30	28E
IHCUATBL*	18CC0	638
SNAP *	192F8	2D0
COEFF	195C8	B4

NAME	LOCATION	NAME	LOCATION	NAME	LOCATION	NAME	LOCATION
FCVIOUTP	12EC0	FCVEOUTP	133C2	FCVCOUTP	135DC	INT6SWCH	138C3
ARITH=	13A28	ADJSWTCH	13DC4				
FIOCS=	14B10	FIOCSBEP	14B16				
FIXPI=	15F00						
AND	16A18						
CLOCK	16AD0						
CORE	16B58						
EXIT	16C00						
FDXPI=	16C20						
MYSTAE	17204	CLSPLT	17246	FIXUP	1728A		
DCBADD	173D0	MIBUNI	17478				
DUMPDD	17510						
OUTDD	17DAC						
FULOMP	18220	IHCOMP	18264	IHCERR	182A8		
OR	183E8						
ERRSET	18590	ERRSAV	1878A	ERRSTR	187B0		
EXP	18898						
IHCTRCH	18A30	ERRTRA	18A38				
SNAPIT	192F8	ABEND	19494				

```
   NAME     ORIGIN  LENGTH                NAME   LOCATION     NAME   LOCATION     NAME   LOCATION     NAME   LOCATION

  INT         19680      1C
  PLTOAT      196A0     938

  ENTRY ADDRESS       00
  TOTAL LENGTH      19FD8

 ****FGXXMAIN  DOES NOT EXIST BUT HAS BEEN ADDED TO DATA SET
```

APPENDIX C

"SLOT/DIPOLE COMPUTED RADIATION PATTERNS"

Cylinder Radius = 5.0 cm

Frequency = 2.3 GHz

Dipole Length = 0.5 λ

Slot Length = 0.5 λ

Slot/Dipole

Computed Radiation Patterns

- Axial Plane
- 6 Element Axial Array
  (Broadside Pointing)

LEFT CIRCULAR POLARIZATION (PHI=0 DEG)

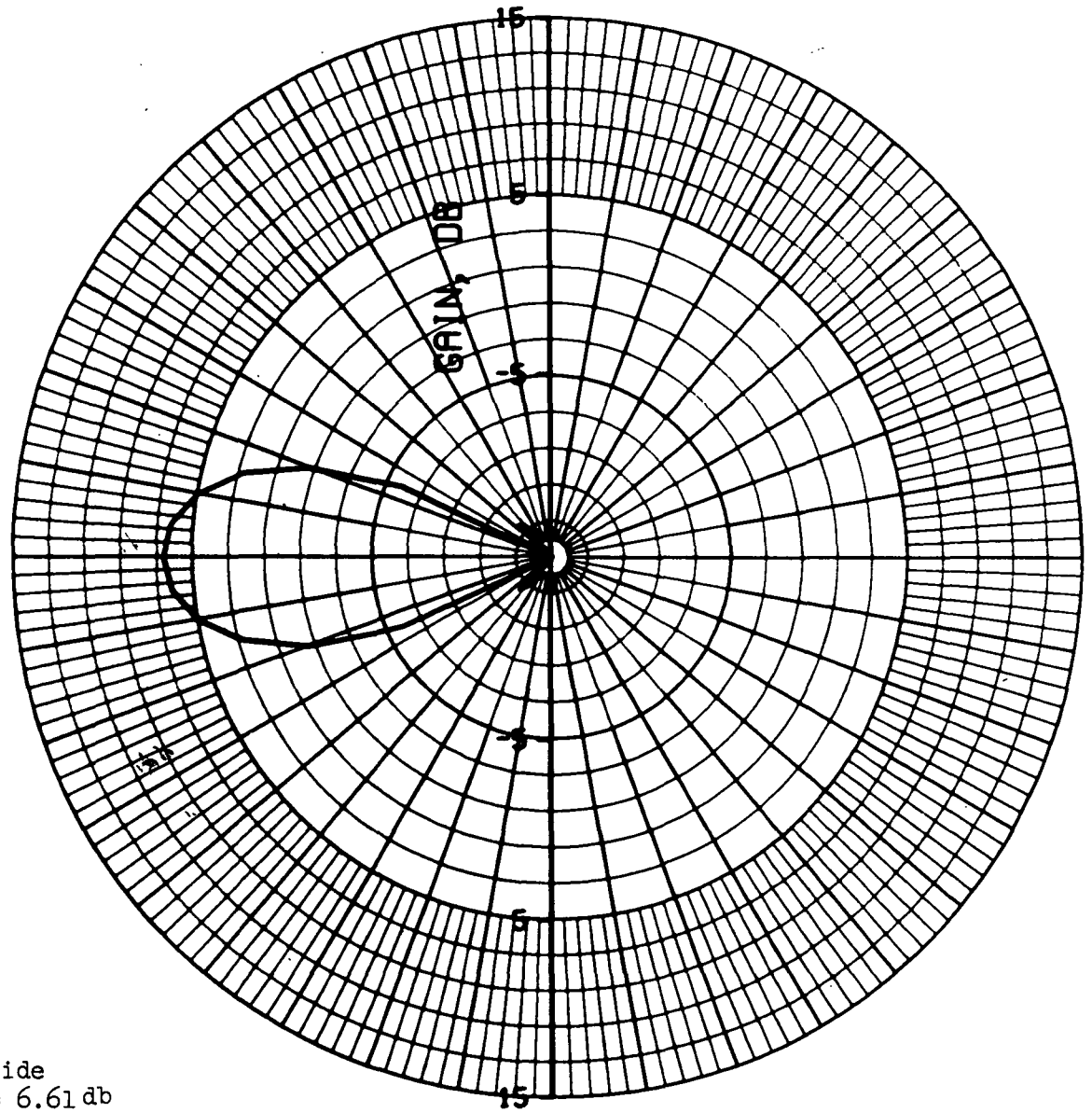

Broadside
Gain = 6.61 db
Beamwidth = 26
d/λ = .5

AVCO/SD
3.JUN.74

AXIAL RATIO VS. ANGLE (PHI=0 DEG)

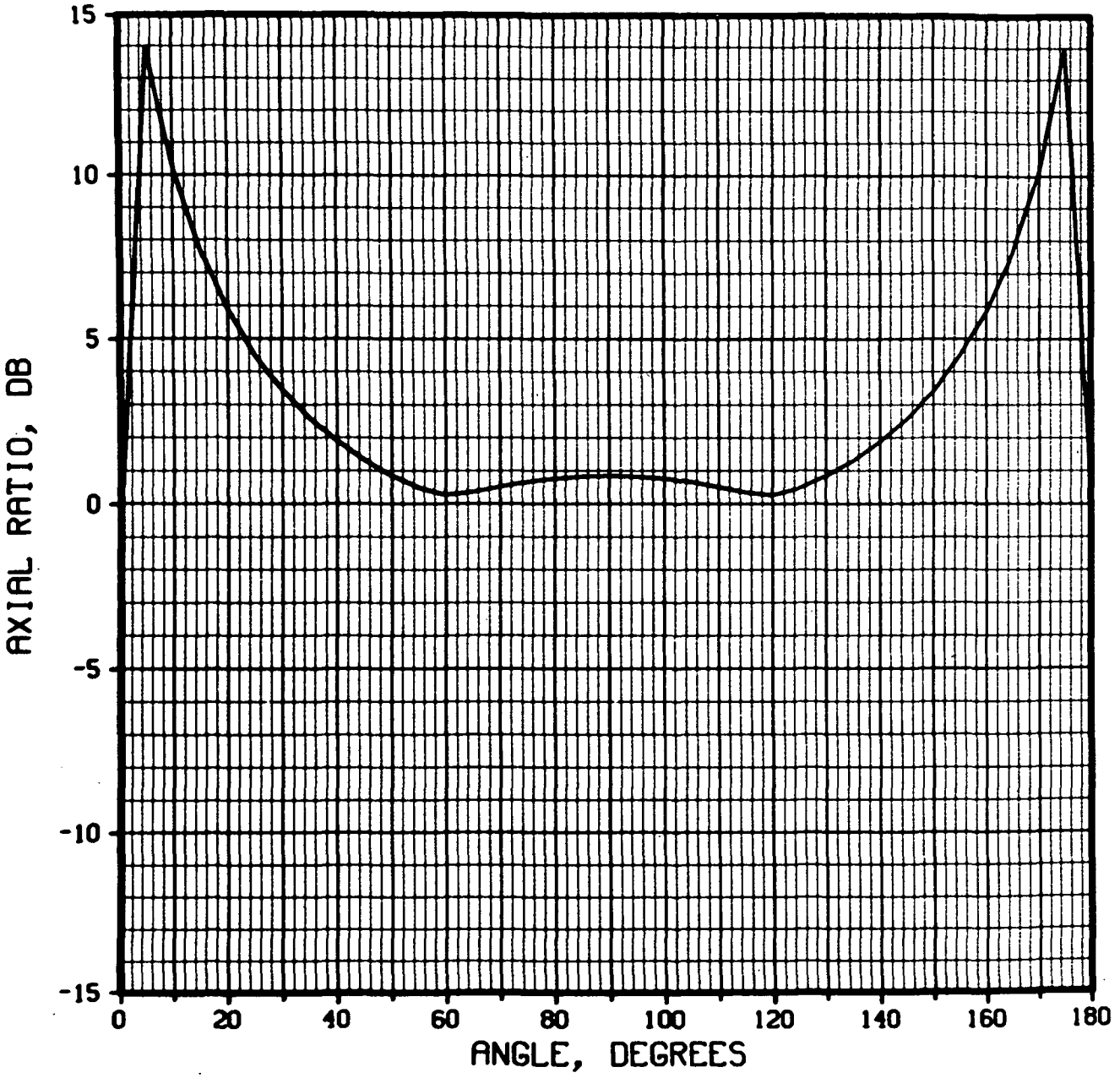

AVCO/SD
3.JUN.74

ETHETA VS. ANGLE (PHI=0 DEG)

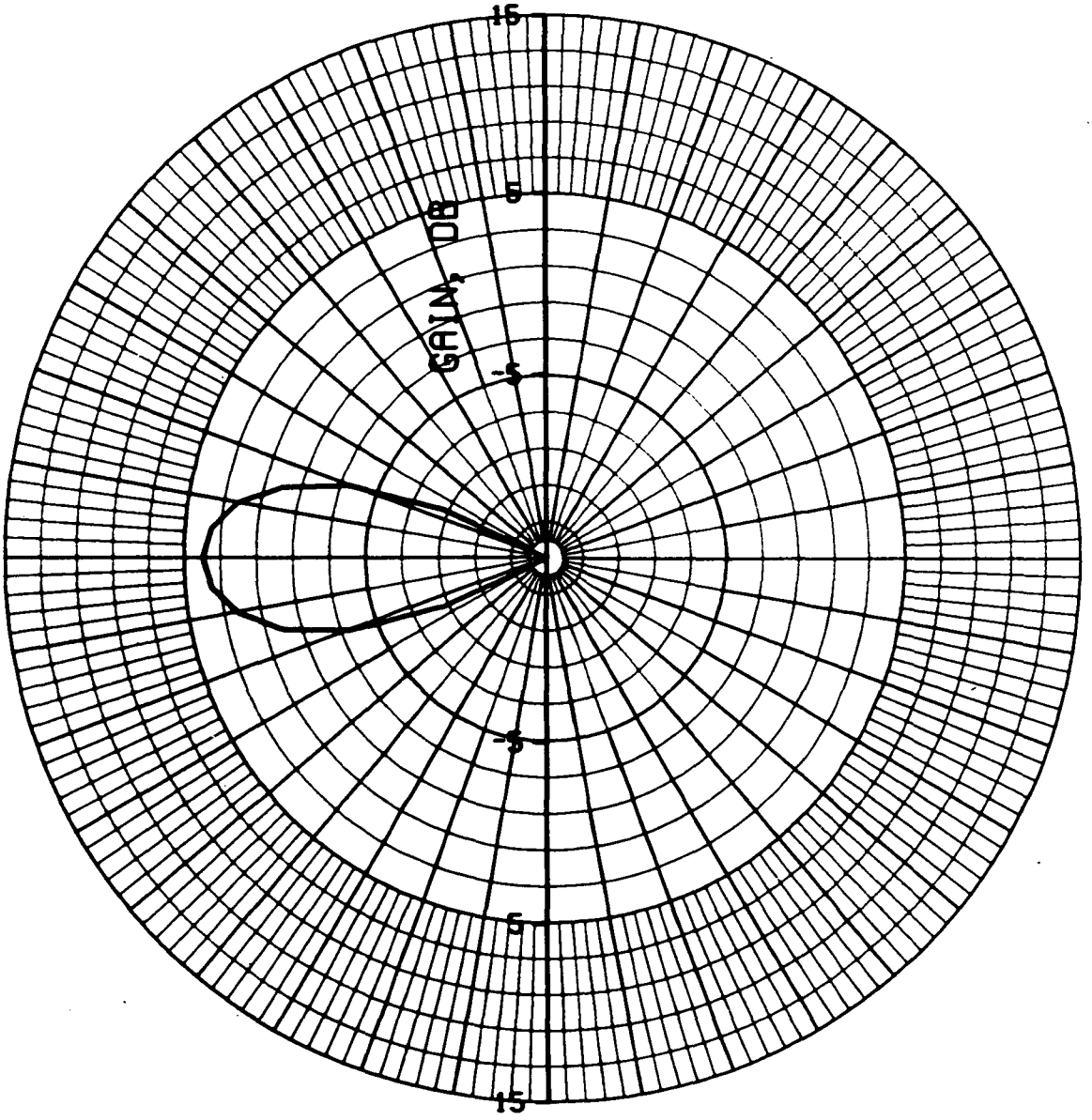

AVCO/SD
3.JUN.74

EPHI VS. ANGLE (PHI=0 DEG)

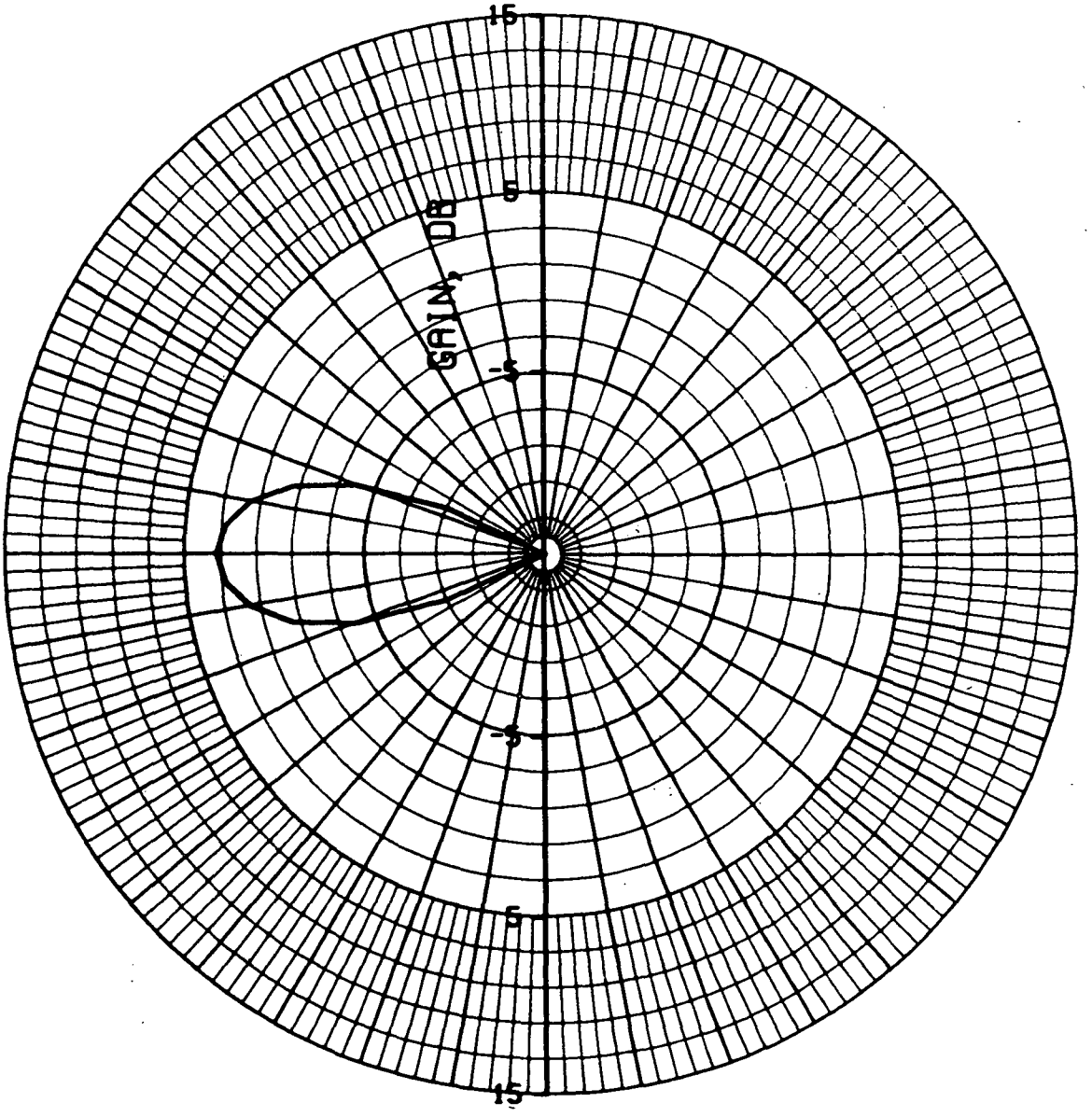

AVCO/SD
3.JUN.74

LEFT CIRCULAR POLARIZATION (PHI=0 DEG)

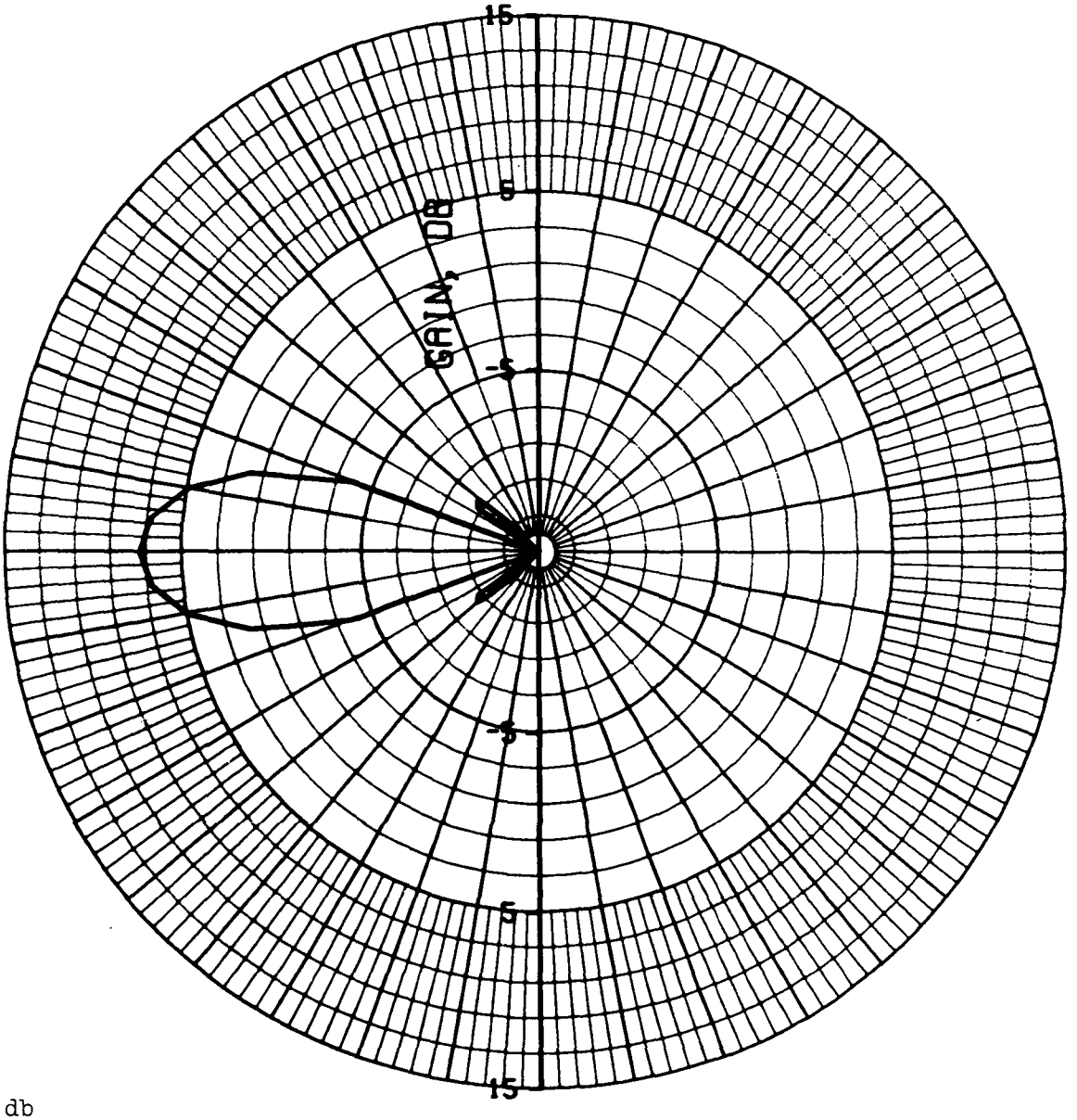

Gain = 7.32 db
Beamwidth = 22°
d/λ = .6

AVCO/SD
3.JUN.74

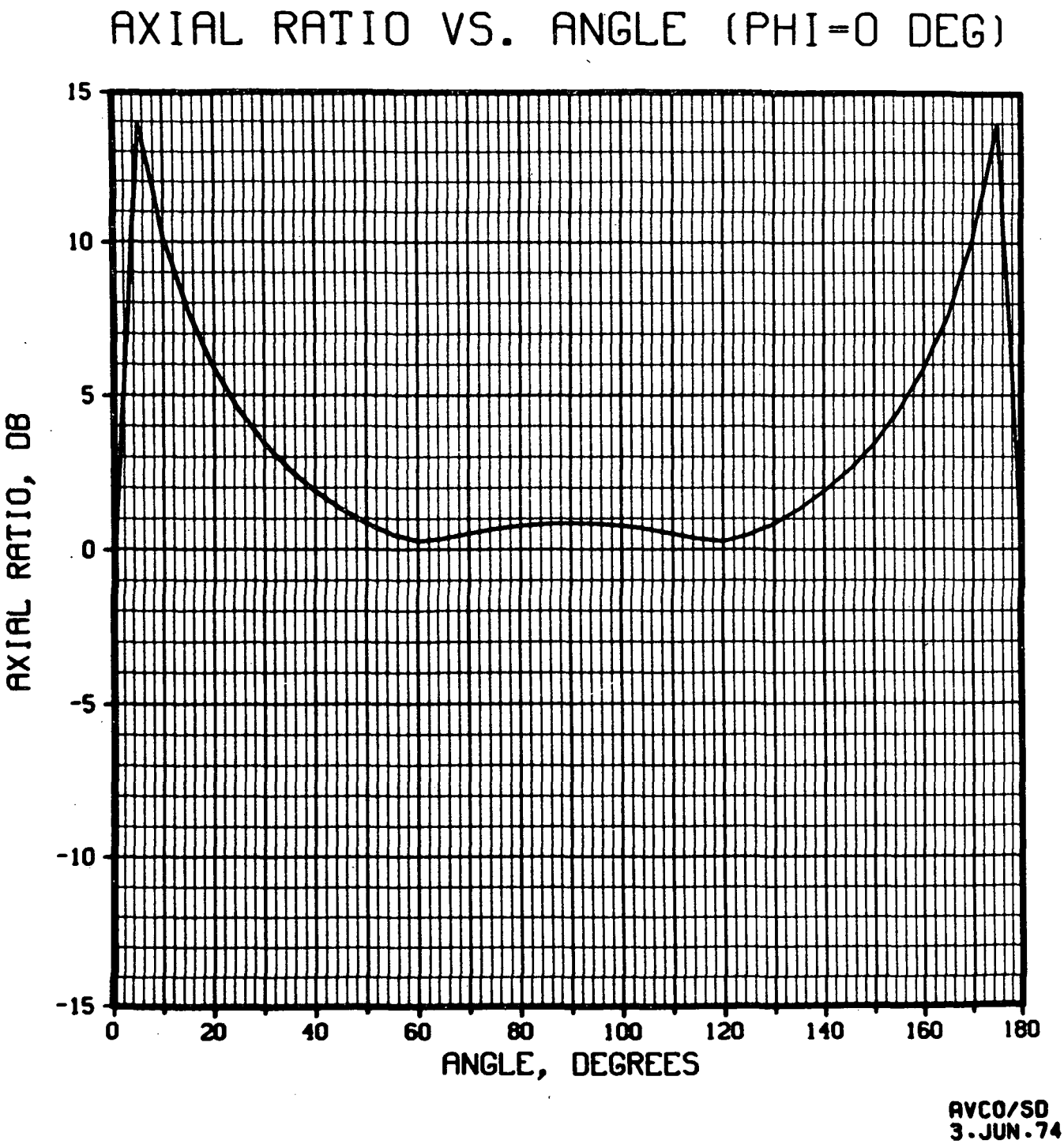
AXIAL RATIO VS. ANGLE (PHI=0 DEG)
AXIAL RATIO, DB
15
10
5
0
-5
-10
-15
0
20
40
60
80
100
120
140
160
180
ANGLE, DEGREES
AVCO/SD
3.JUN.74

ETHETA VS. ANGLE (PHI=0 DEG)

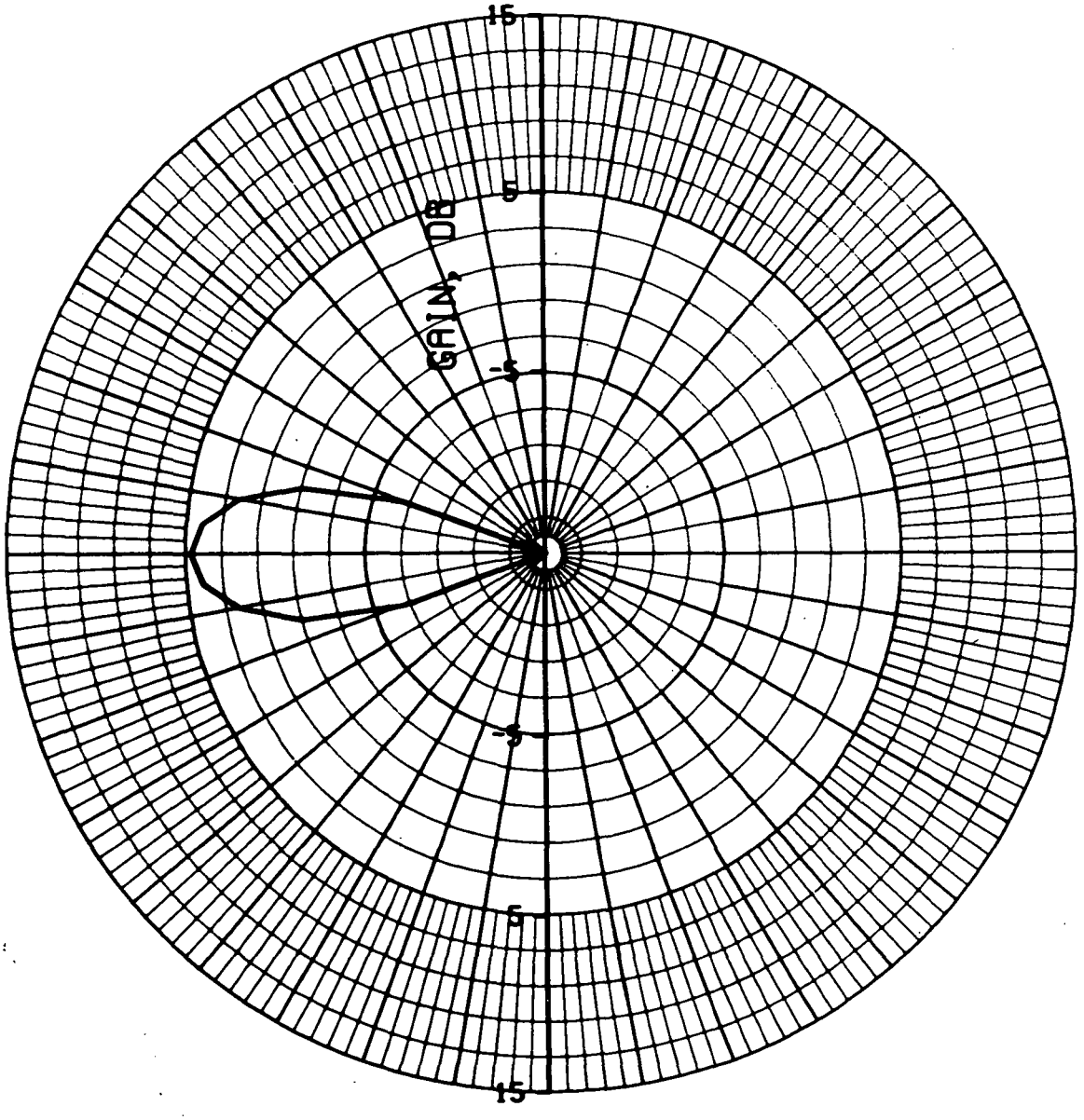

AVCO/SD
3.JUN.74

EPHI VS. ANGLE (PHI=0 DEG)

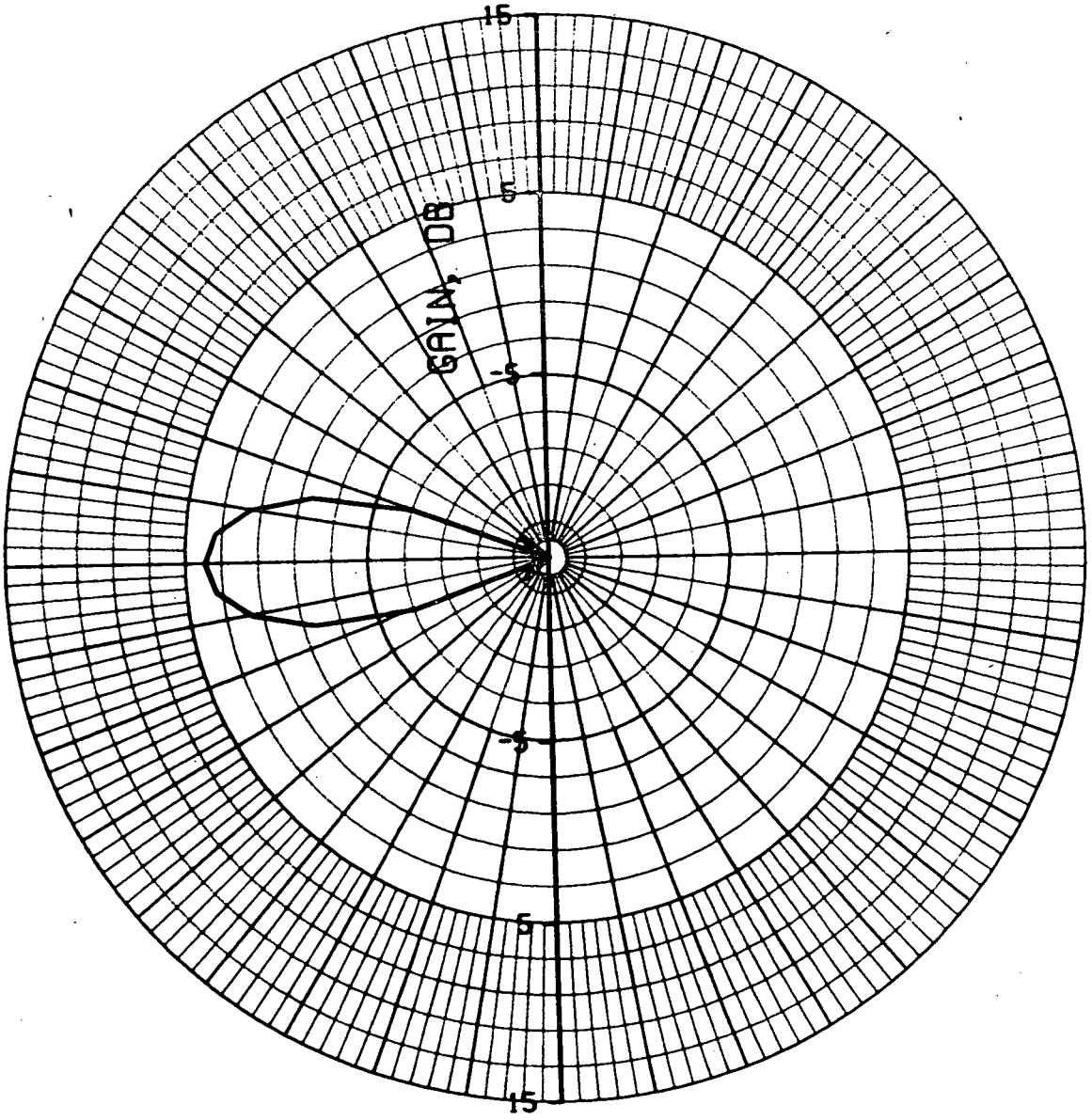

AVCO/SD
3.JUN.74

LEFT CIRCULAR POLARIZATION (PHI=0 DEG)

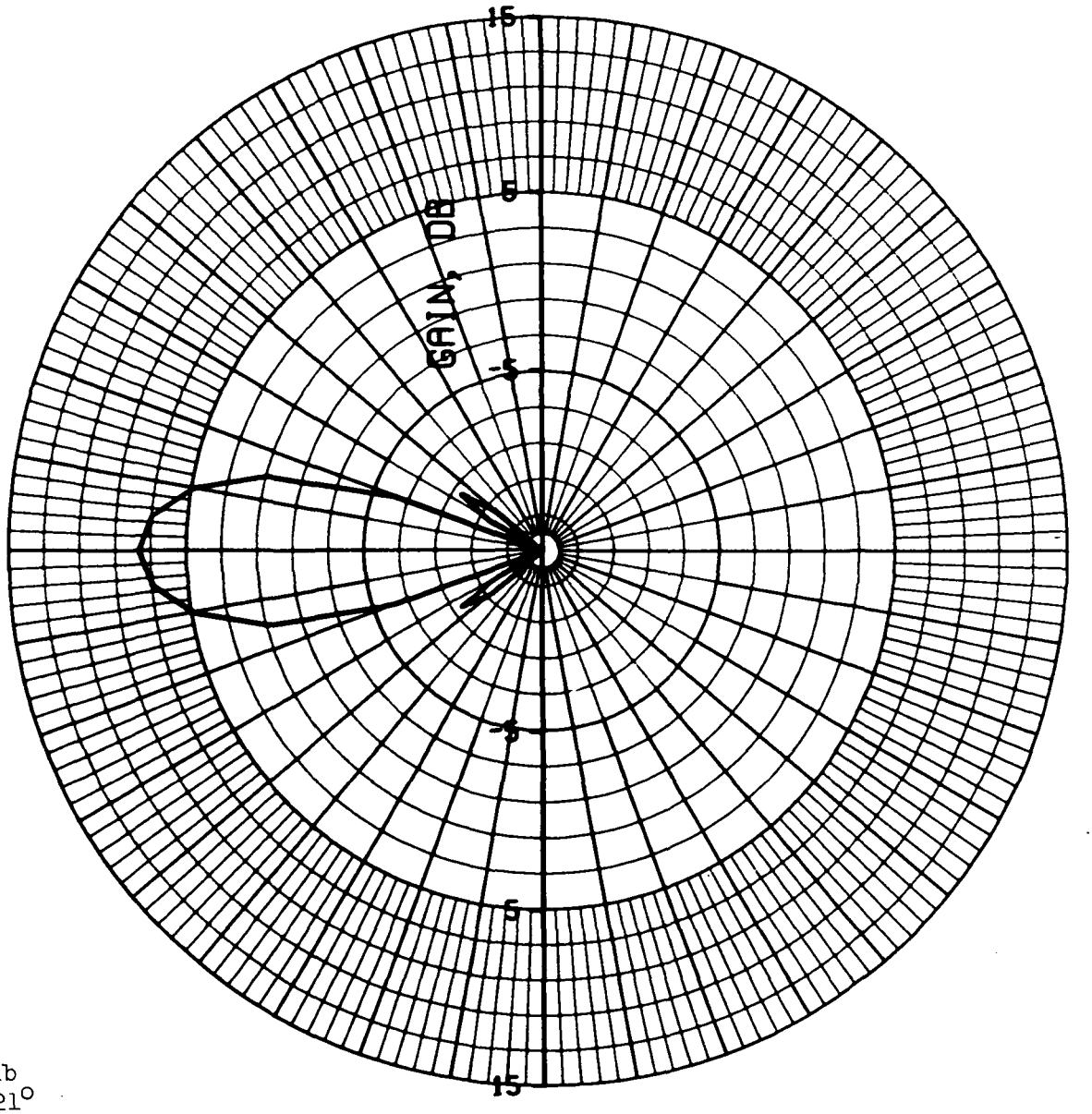

Gain = 7.63 db
Beamwidth = 21°
d/λ = .65

AVCO/SD
3.JUN.74

AXIAL RATIO VS. ANGLE (PHI=0 DEG)

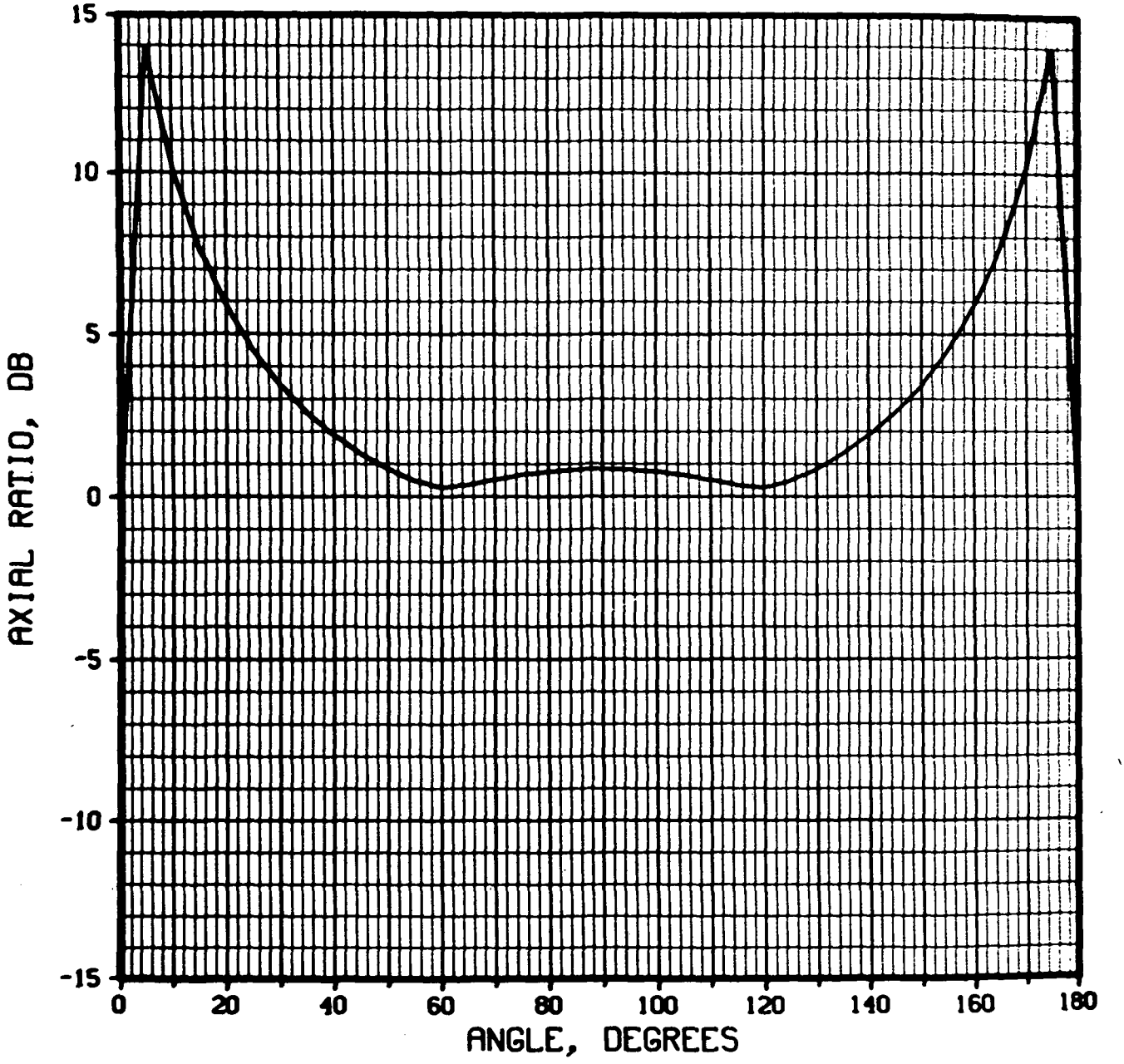

AVCO/SD
3.JUN.74

ETHETA VS. ANGLE (PHI=0 DEG)

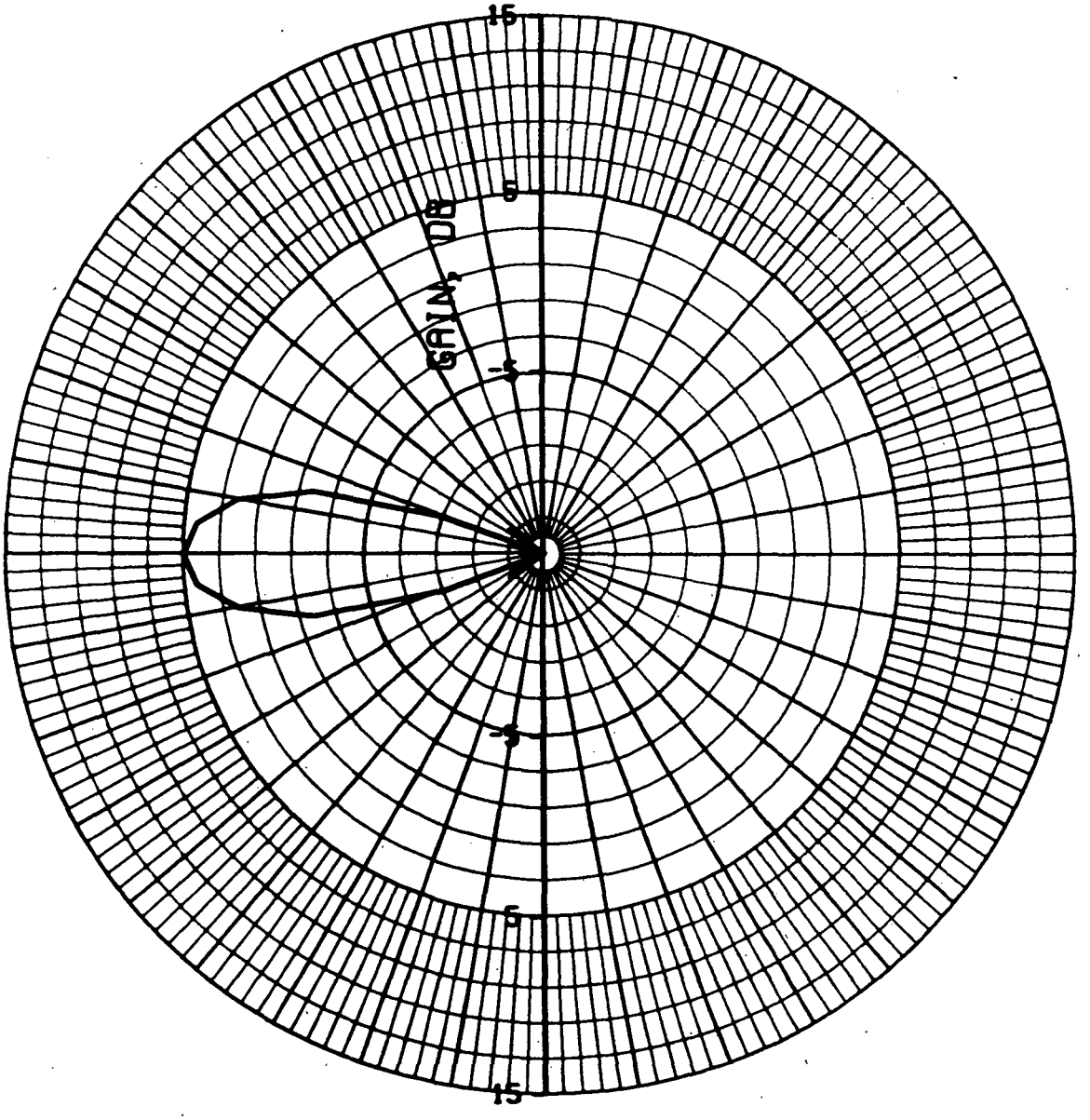

AVCO/SD
3.JUN.74

EPHI VS. ANGLE (PHI=0 DEG)

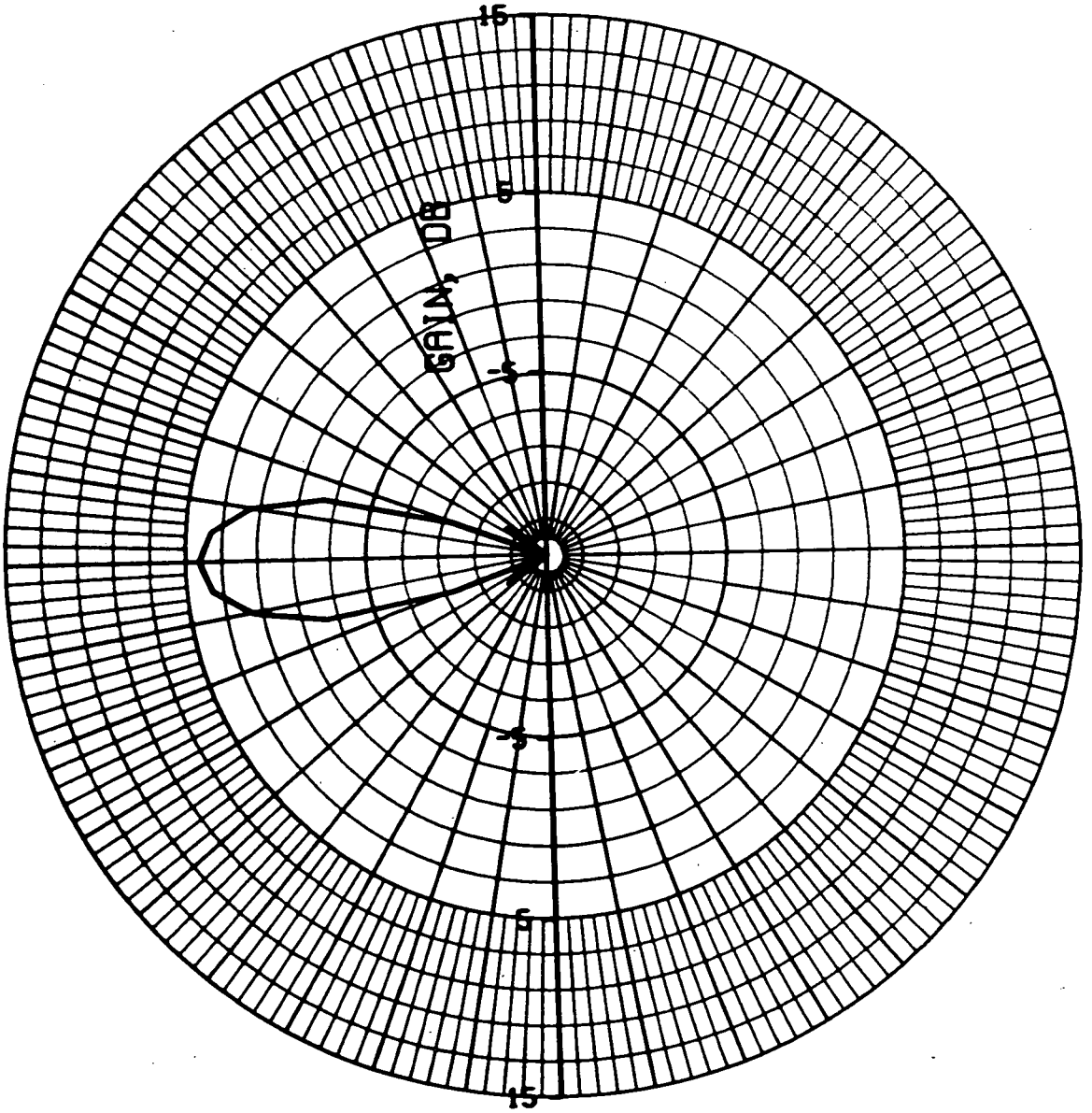

AVCO/SD
3.JUN.74

LEFT CIRCULAR POLARIZATION (PHI=0 DEG

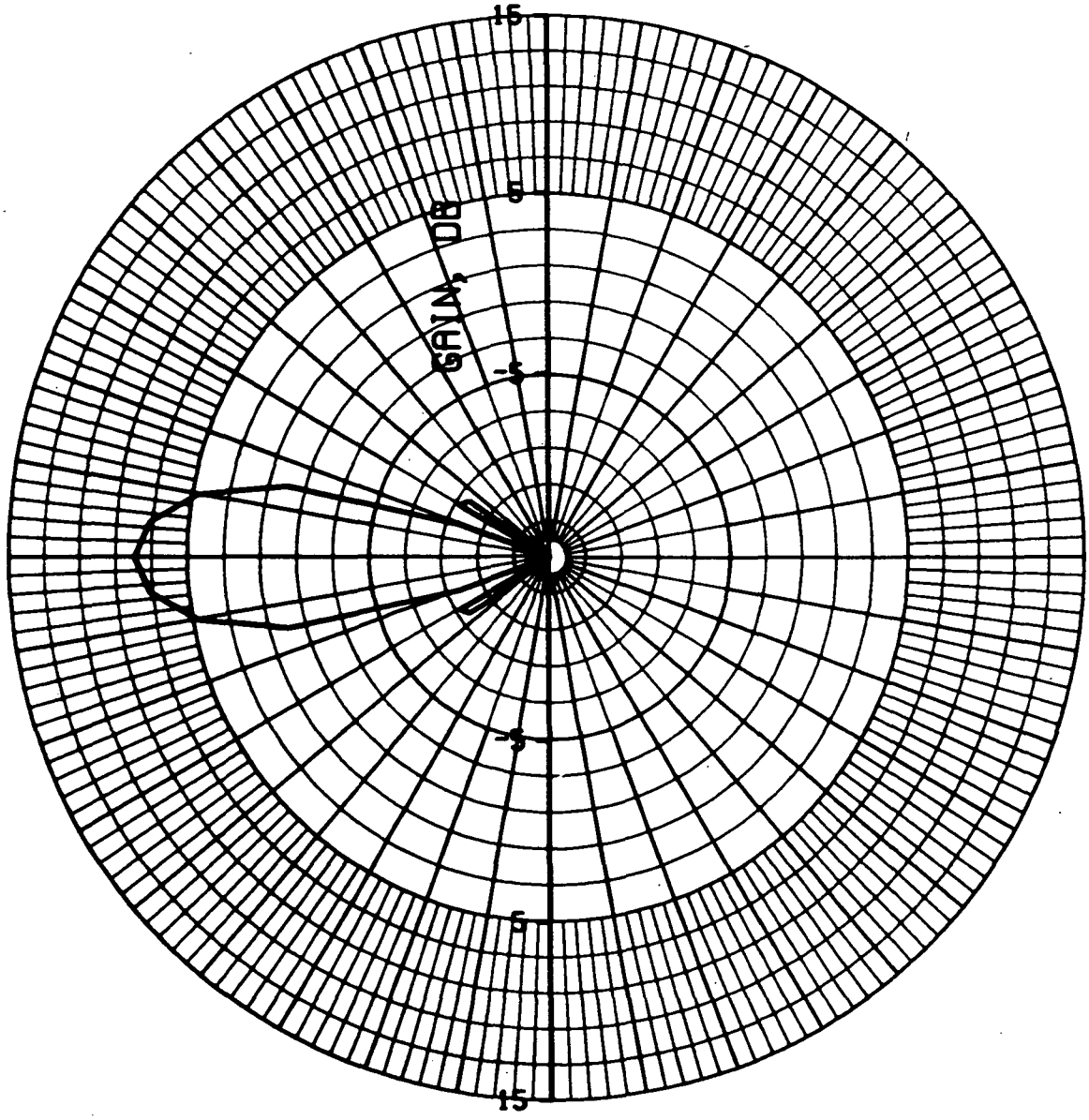

Gain = 7.9 db
Beamwidth = 20°
d/λ = .7

AVCO/SE
5 JUN.

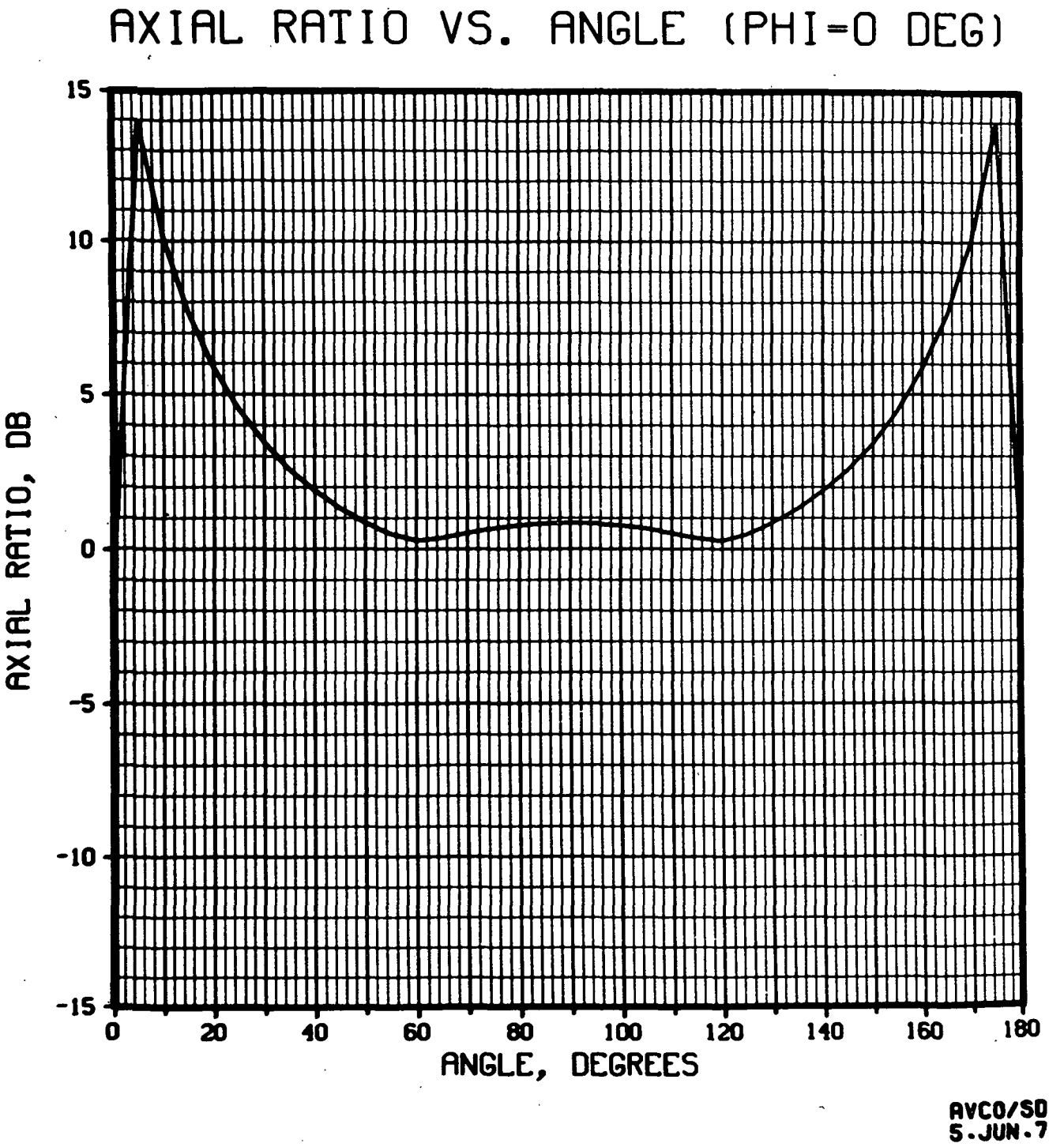
AXIAL RATIO VS. ANGLE (PHI=0 DEG)
AXIAL RATIO, DB
15
10
5
0
-5
-10
-15
0
20
40
60
80
100
120
140
160
180
ANGLE, DEGREES
AVCO/SD
5.JUN.7

ETHETA VS. ANGLE (PHI=0 DEG)

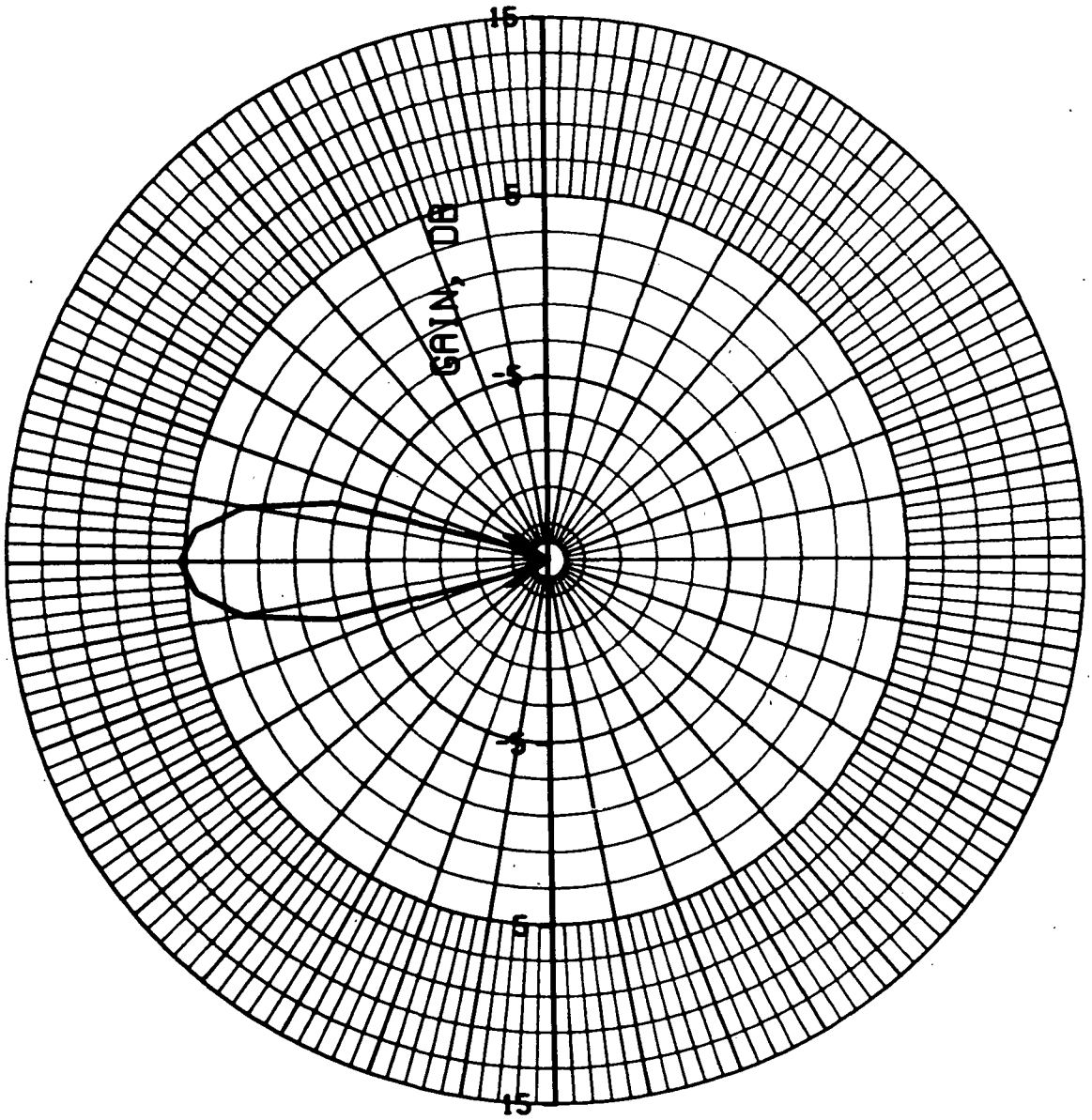

AVCO/SD
5.JUN.7

EPHI VS. ANGLE (PHI=0 DEG)

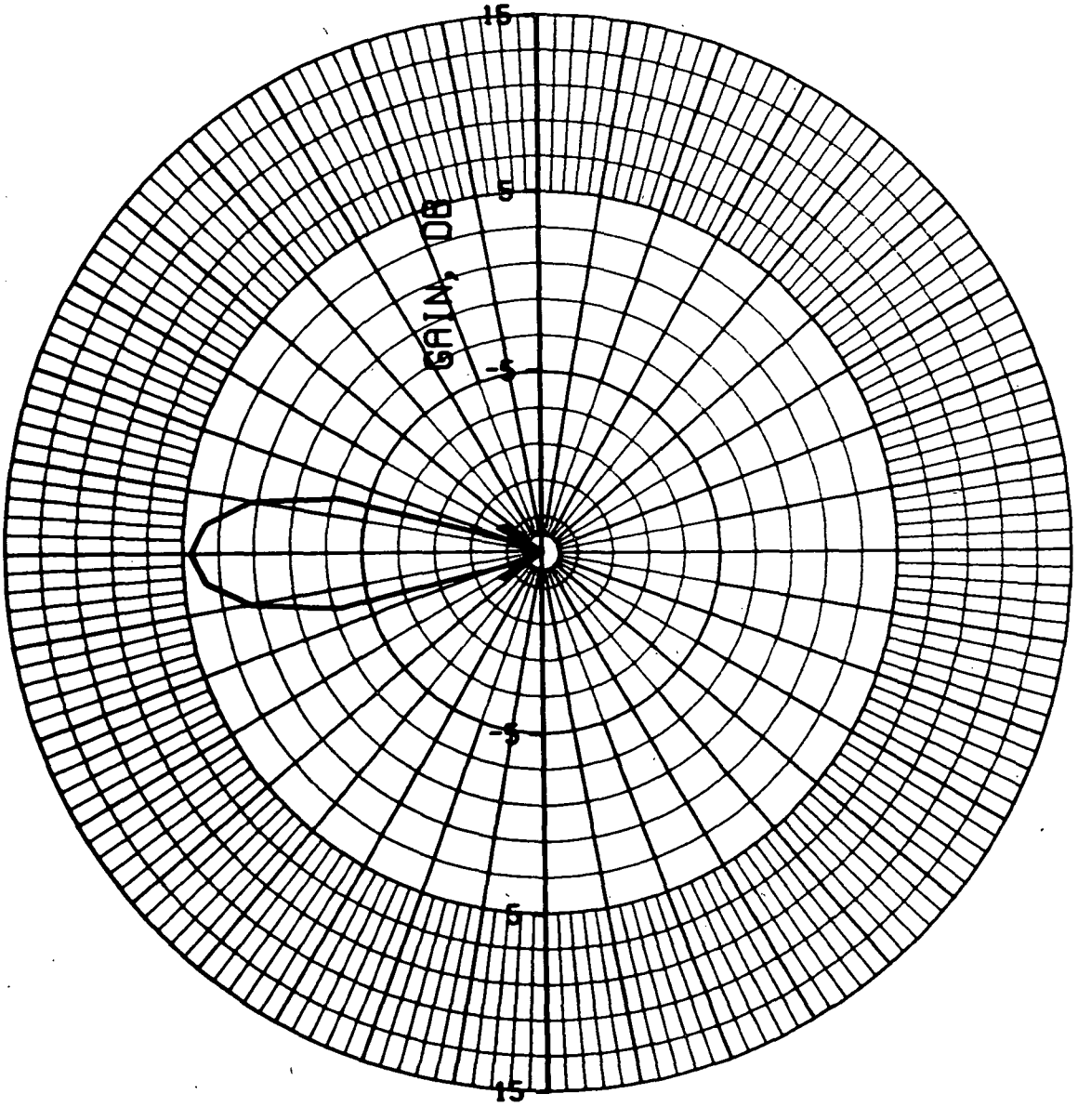

AVCO/SE
5.JUN.

LEFT CIRCULAR POLARIZATION (PHI=0 DEG)

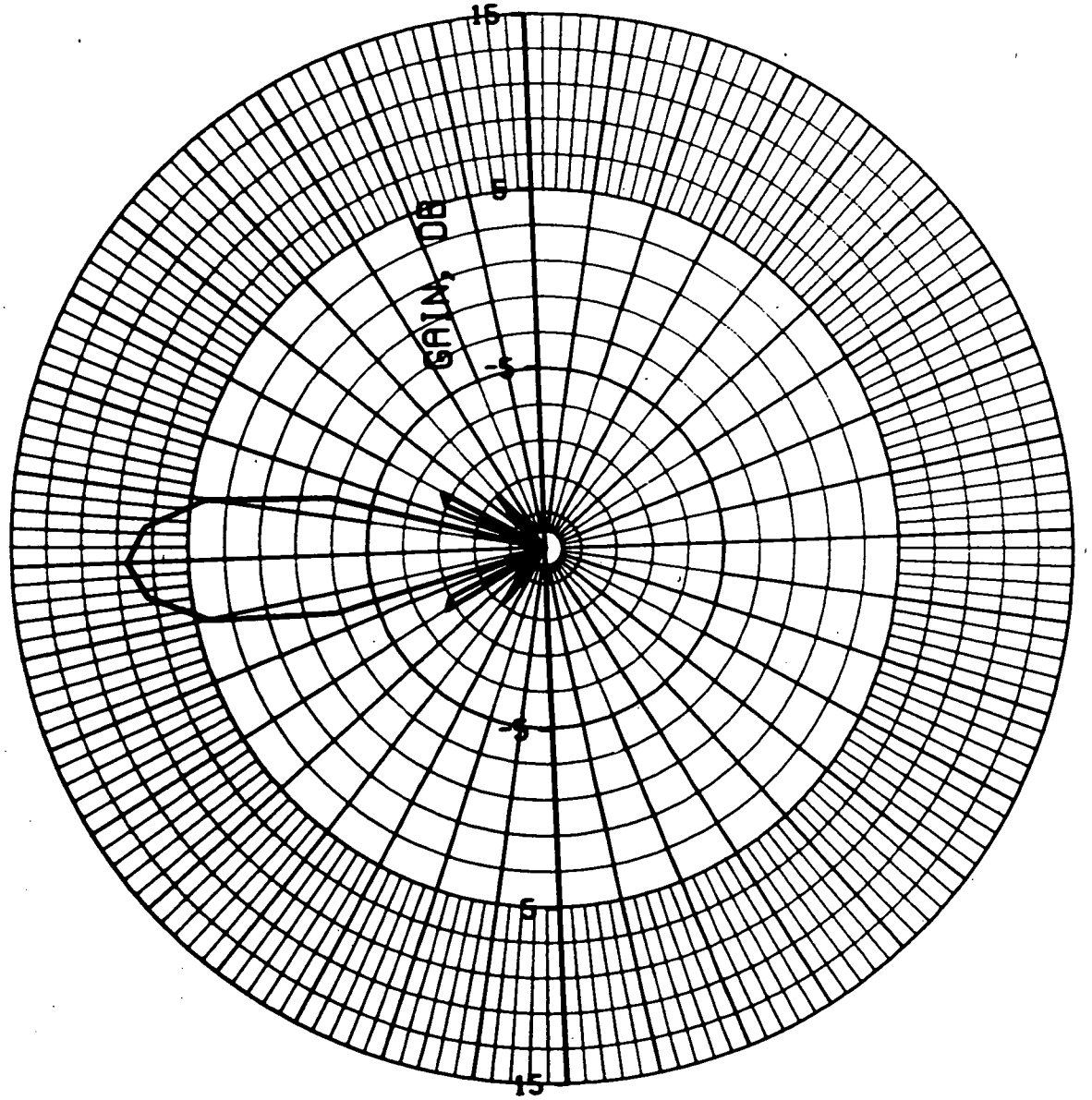

Gain = 8.44db
Beamwidth = 16
d/λ = .8

AVCO/SD
3.JUN.71

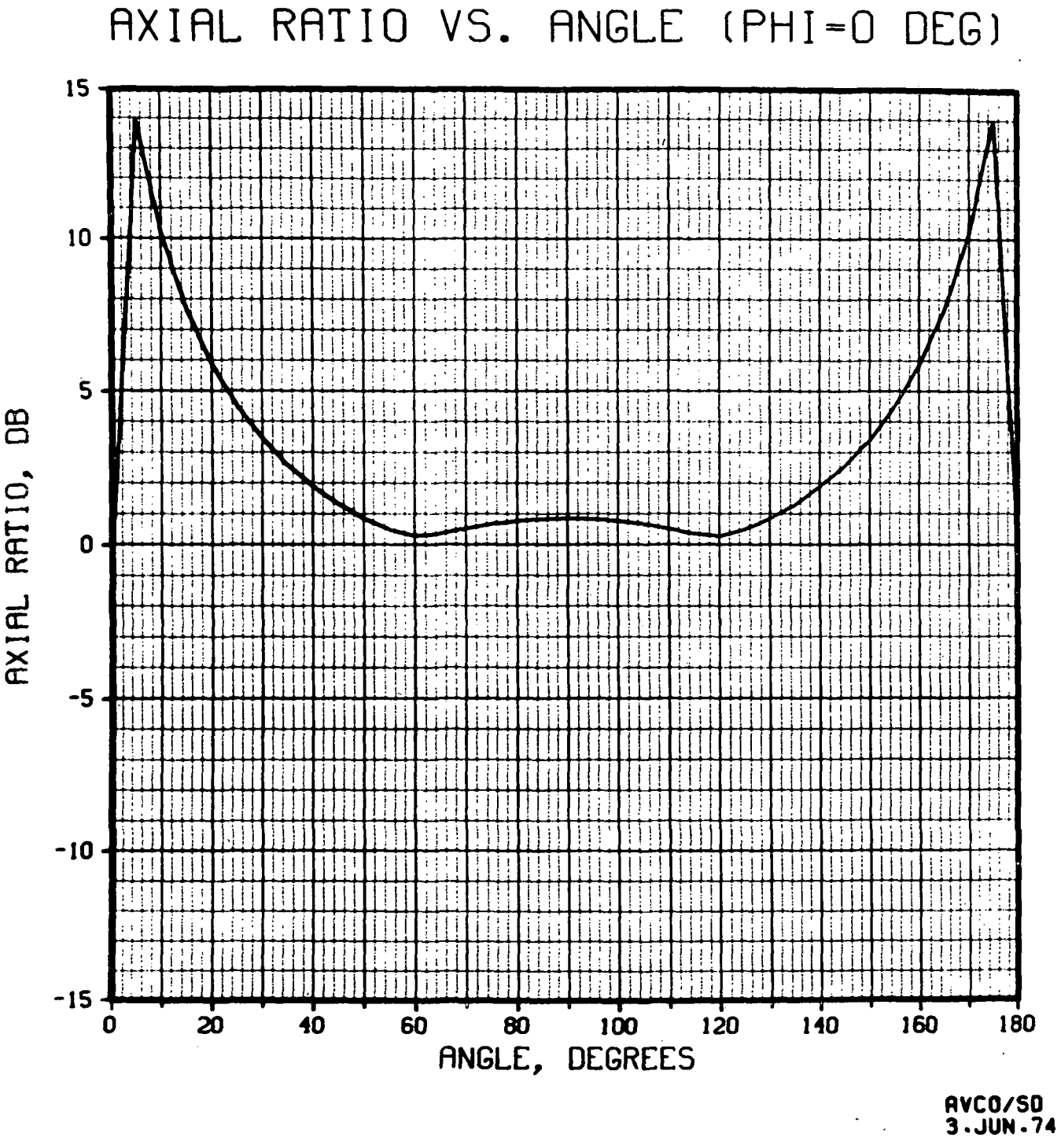
AXIAL RATIO VS. ANGLE (PHI=0 DEG)
AXIAL RATIO, DB
15
10
5
0
-5
-10
-15
0
20
40
60
80
100
120
140
160
180
ANGLE, DEGREES
AVCO/SD
3.JUN.74

ETHETA VS. ANGLE (PHI=0 DEG)

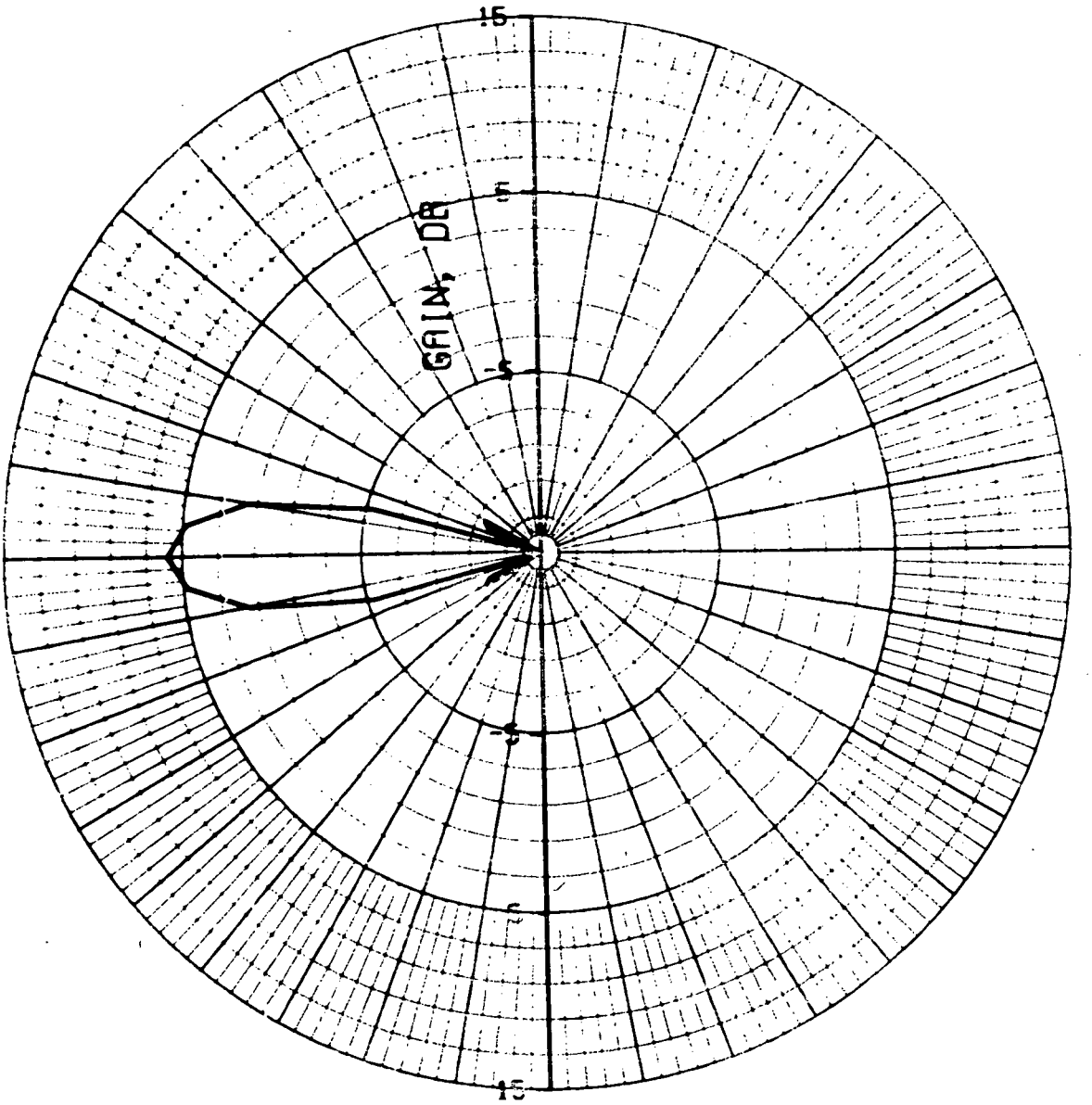

AVCO/SD
3.JUN.74

EPHI VS. ANGLE (PHI=0 DEG)

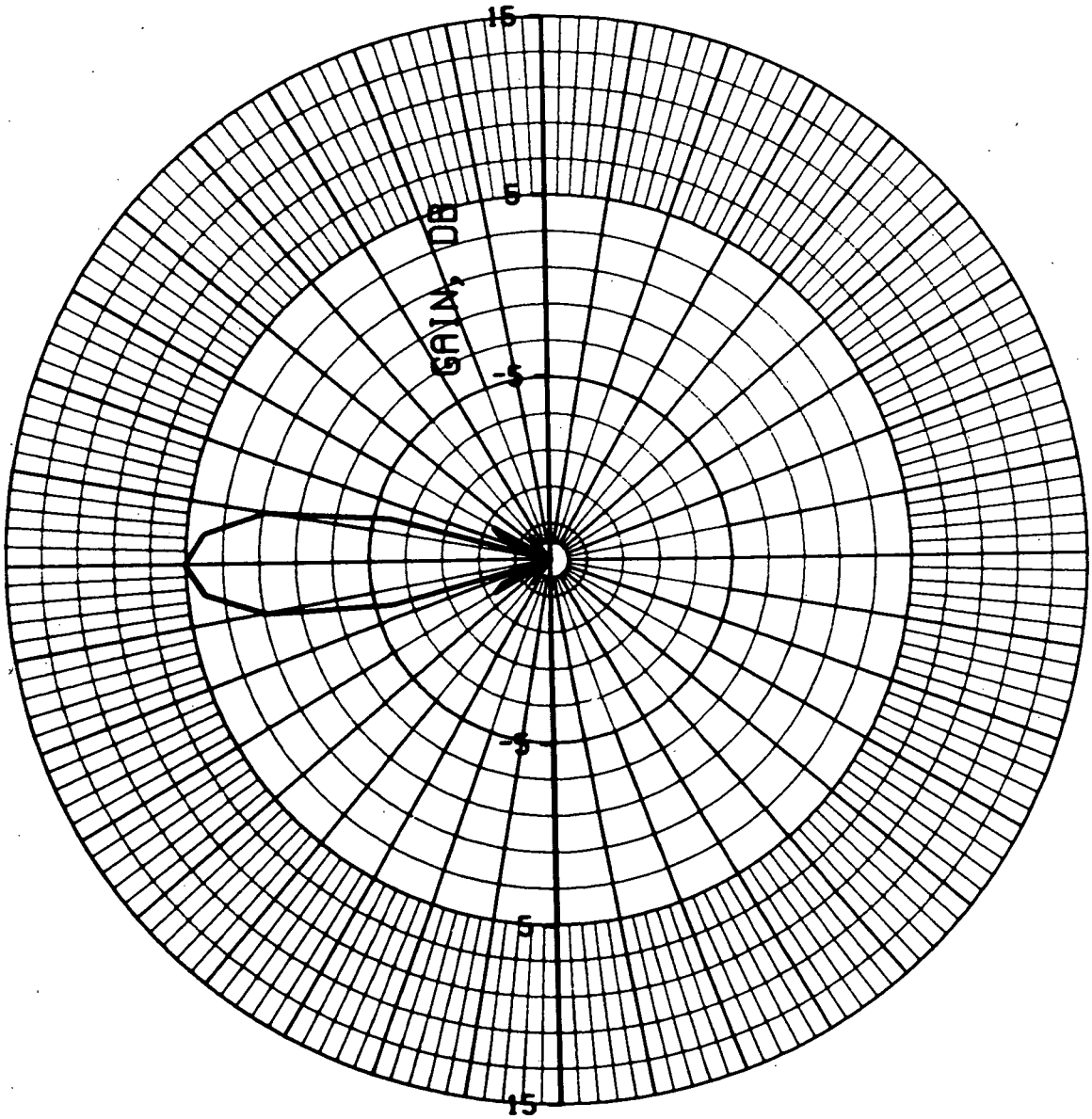

AVCO/SD
3.JUN.74

Slot/Dipole

Computed Radiation Patterns

- Axial Plane
- 6 Element Axial Array
  (Pointing Angle = 30°
  From Broadside)

LEFT CIRCULAR POLARIZATION (PHI=0 DEG)

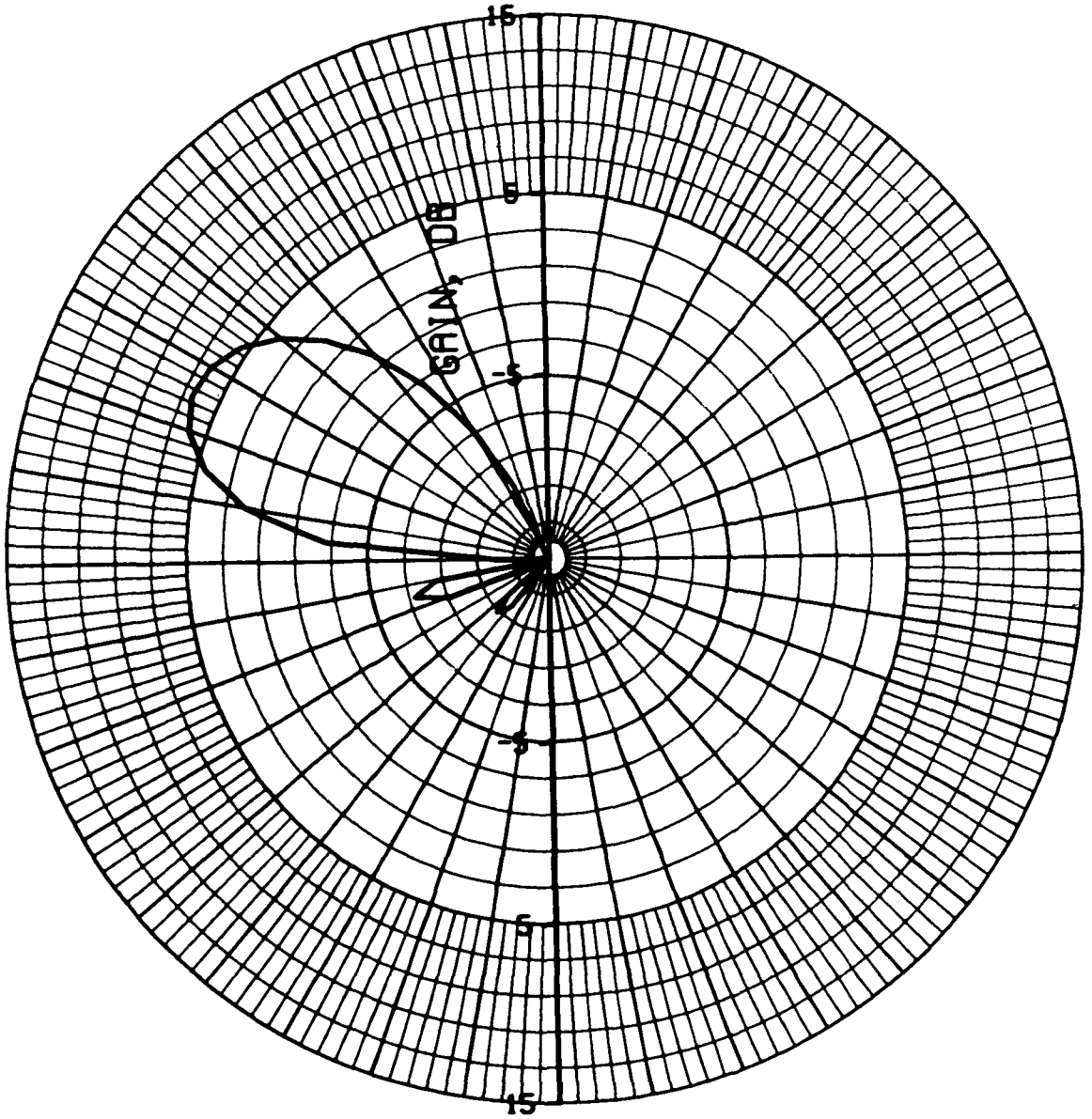

Gain = 6.29 db
Beamwidth = 29°
d/λ = .5

AVCO/SD
3.JUN.74

AXIAL RATIO VS. ANGLE (PHI=0 DEG)

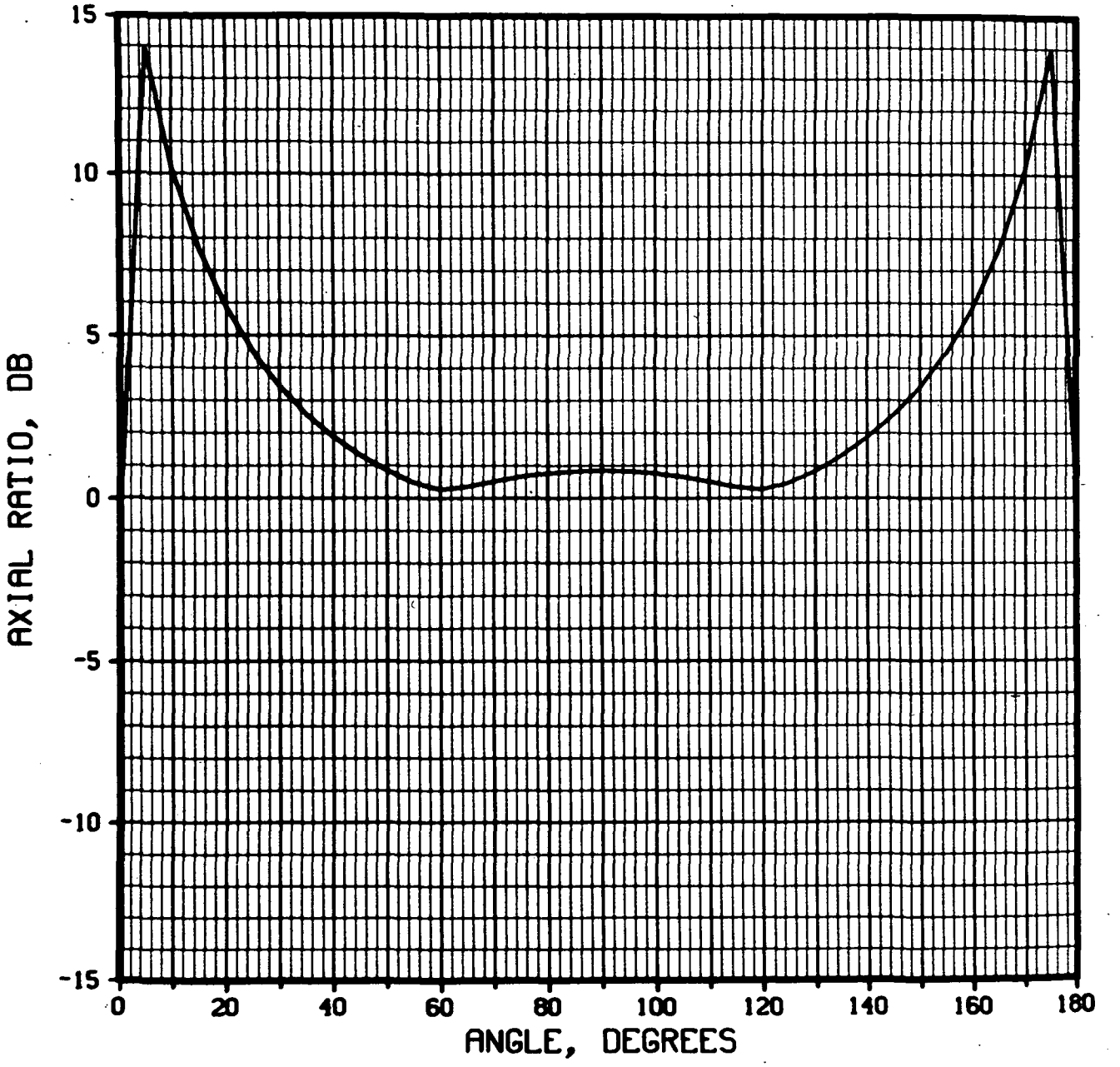

AVCO/SD
3.JUN.74

ETHETA VS. ANGLE (PHI=0 DEG)

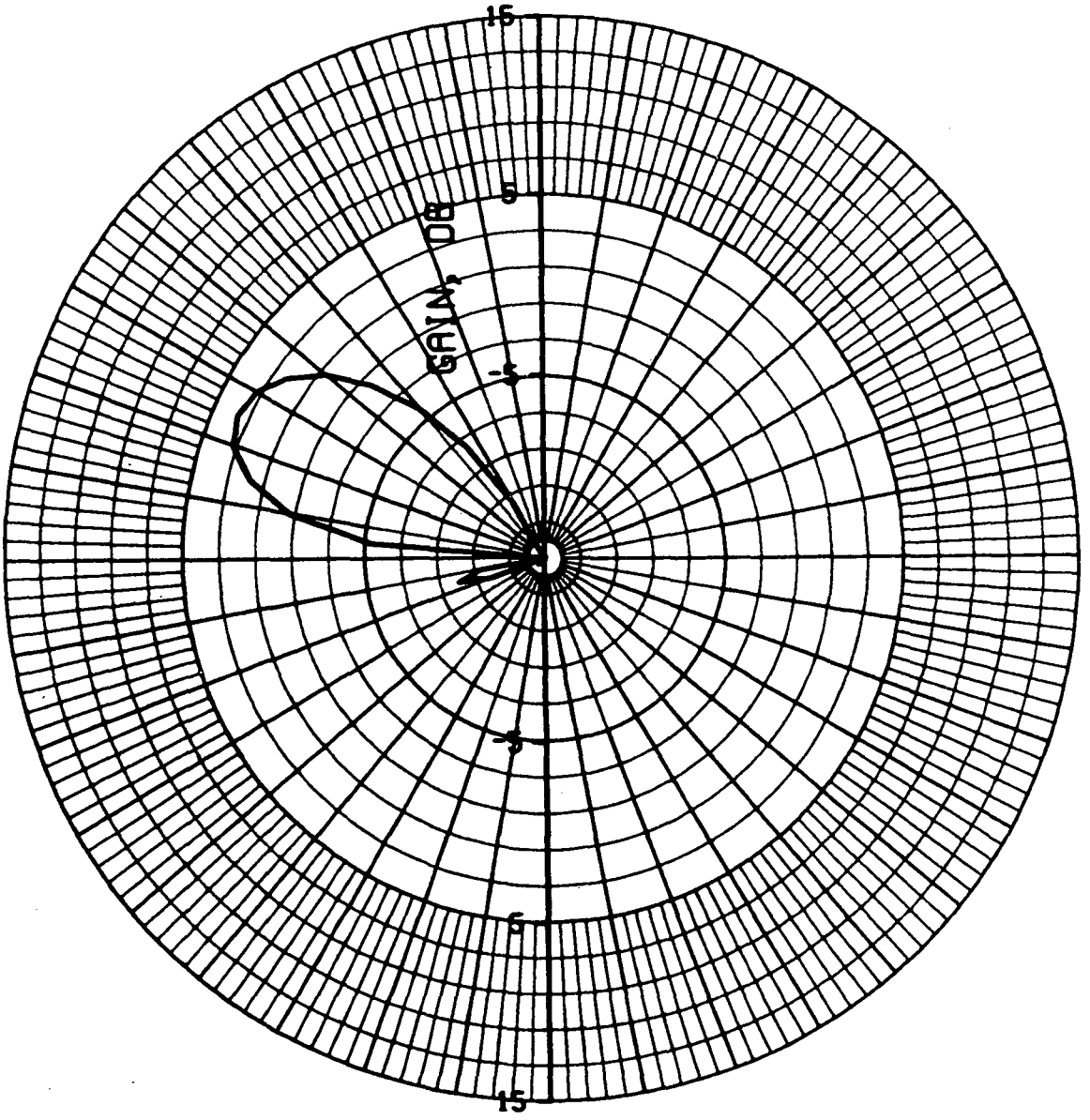

AVCO/SD
3.JUN.74

EPHI VS. ANGLE (PHI=0 DEG)

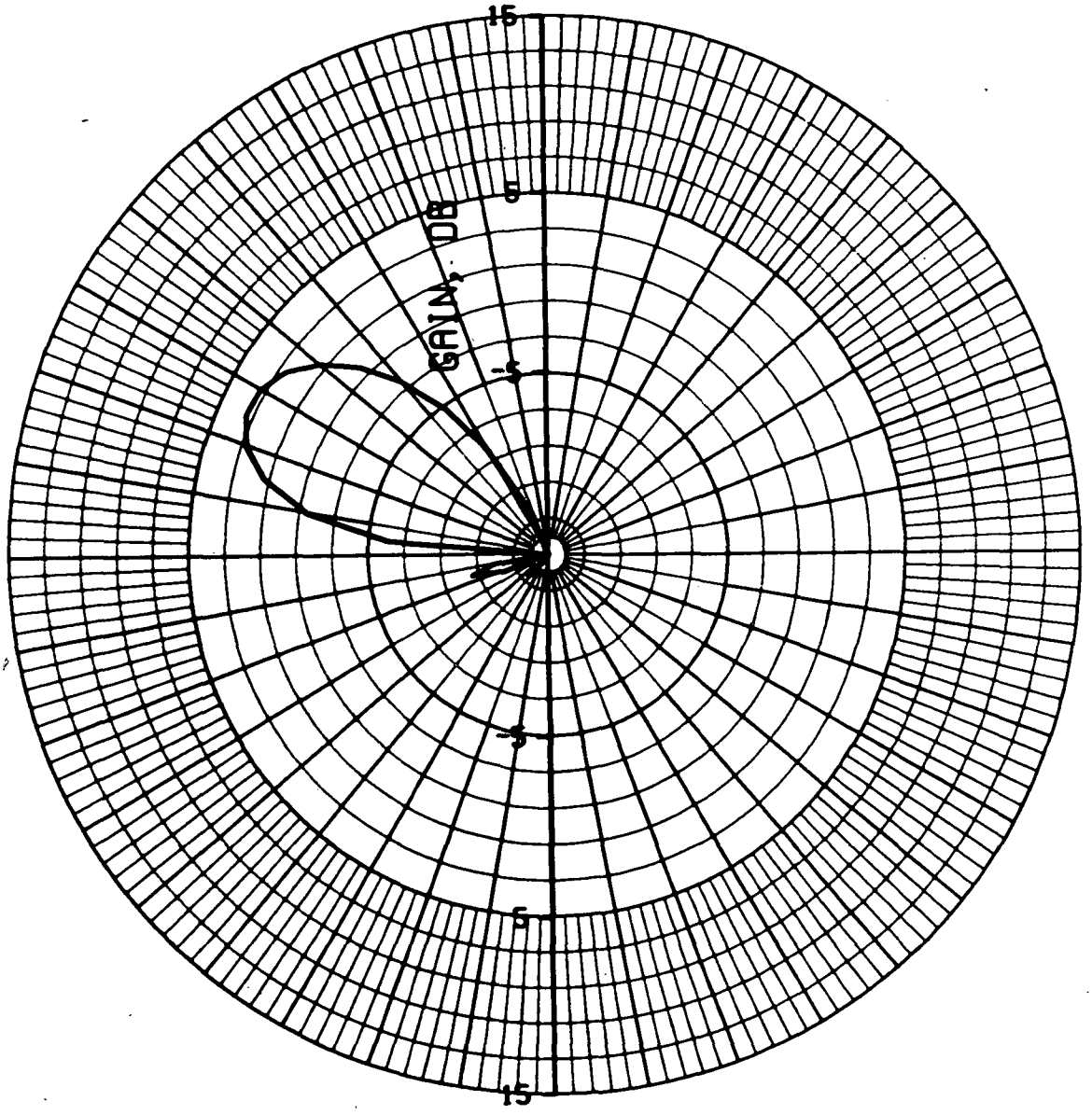

AVCO/SD
3.JUN.74

LEFT CIRCULAR POLARIZATION (PHI=0 DEG)

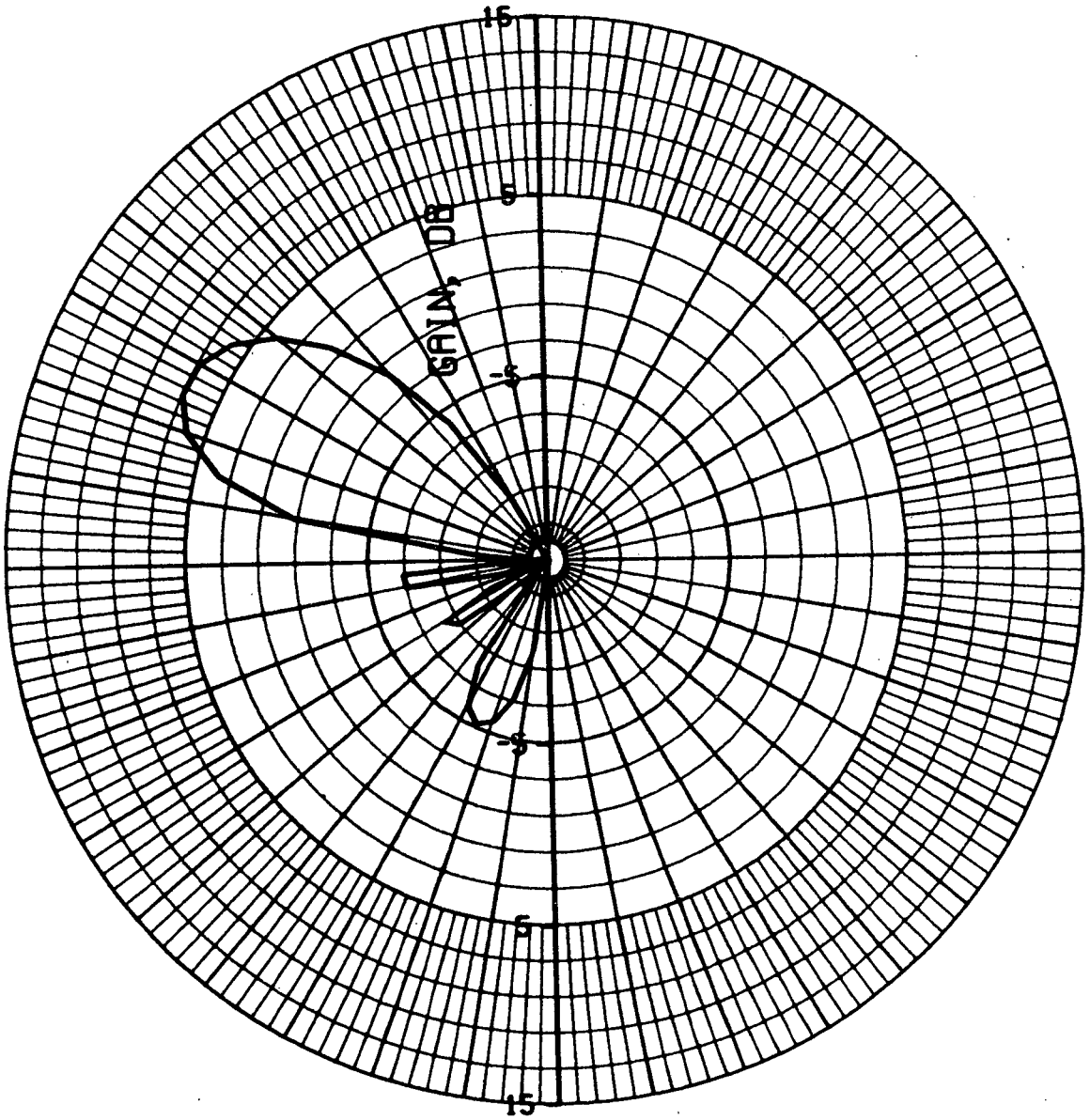

Gain = 6.88 db
Beamwidth = 25°
d/λ = .6

AVCO/SD
3.JUN.74

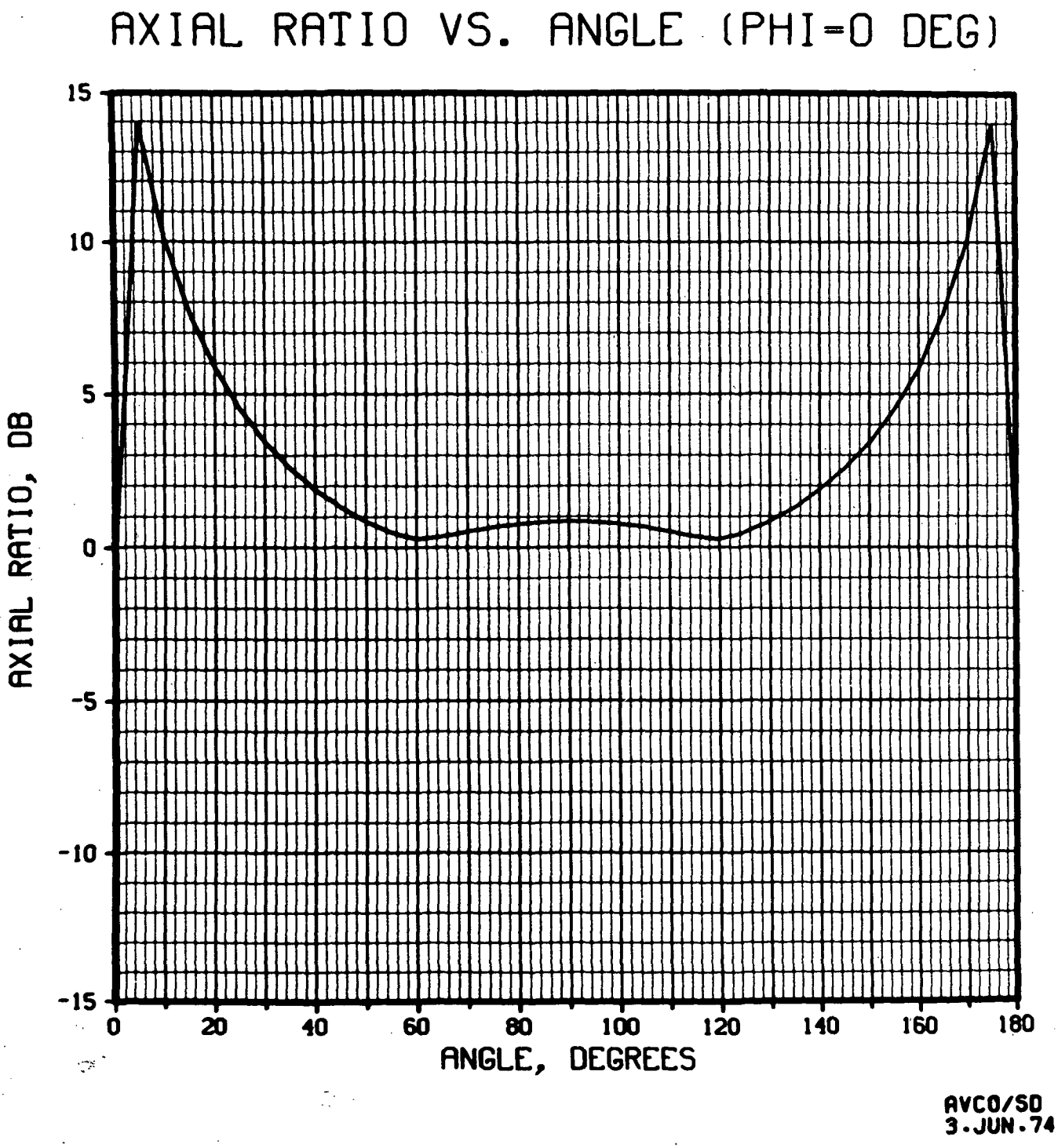
AXIAL RATIO VS. ANGLE (PHI=0 DEG)
AXIAL RATIO, DB
15
10
5
0
-5
-10
-15
0
20
40
60
80
100
120
140
160
180
ANGLE, DEGREES
AVCO/SD
3.JUN.74

ETHETA VS. ANGLE (PHI=0 DEG)

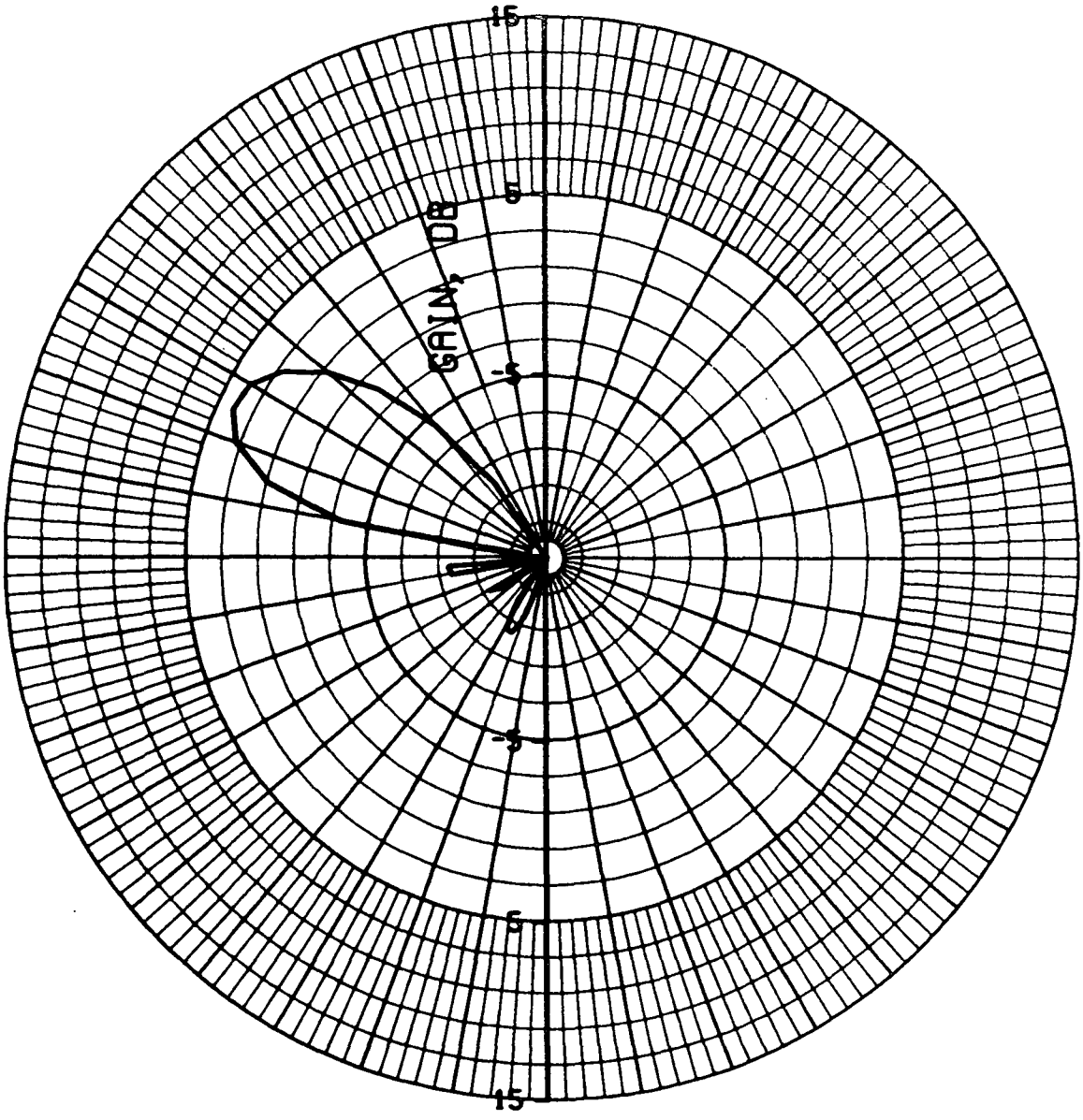

AVCO/SD
3.JUN.74

EPHI VS. ANGLE (PHI=0 DEG)

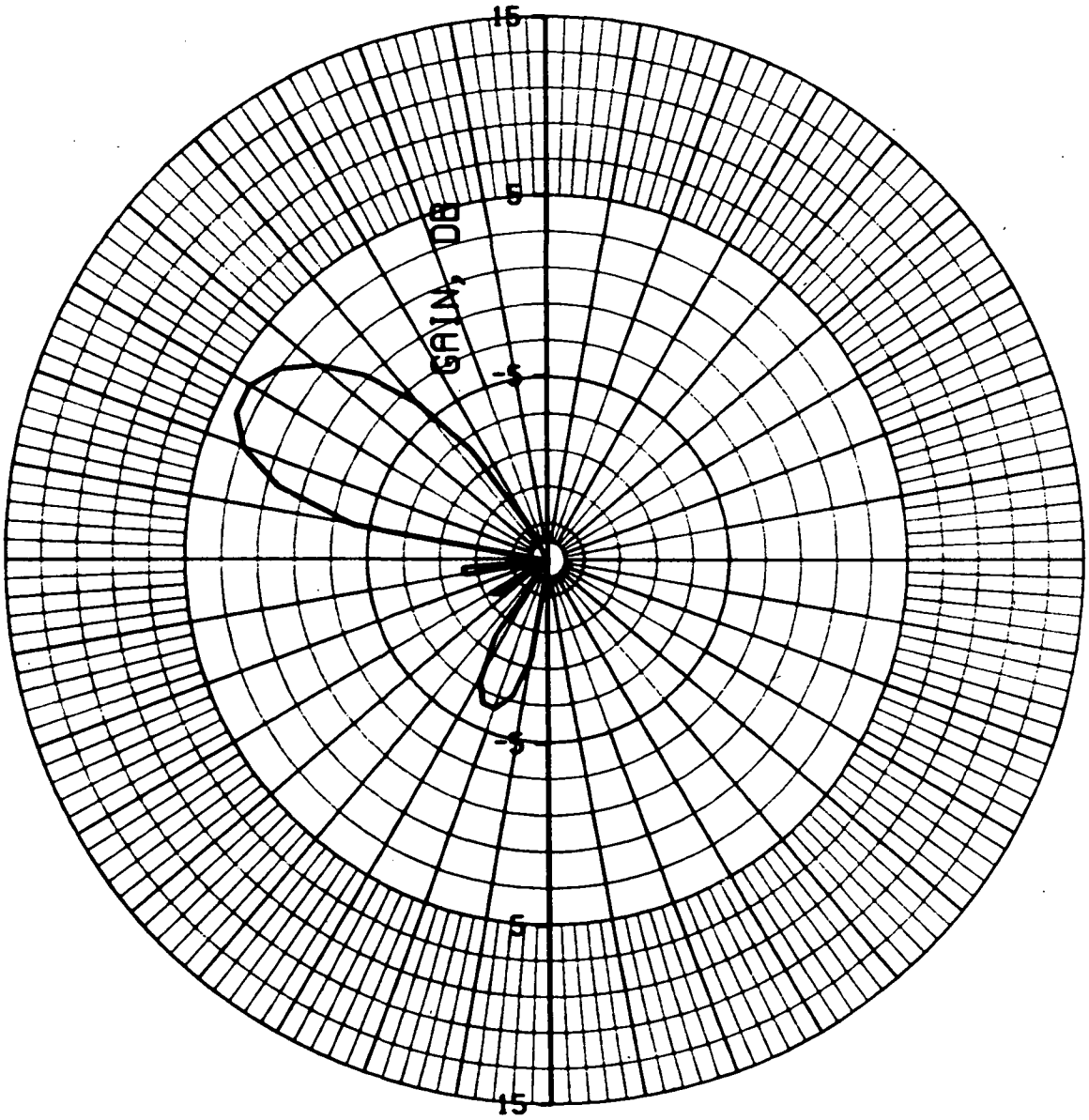

AVCO/SD
3.JUN.74

LEFT CIRCULAR POLARIZATION (PHI=0 DEG)

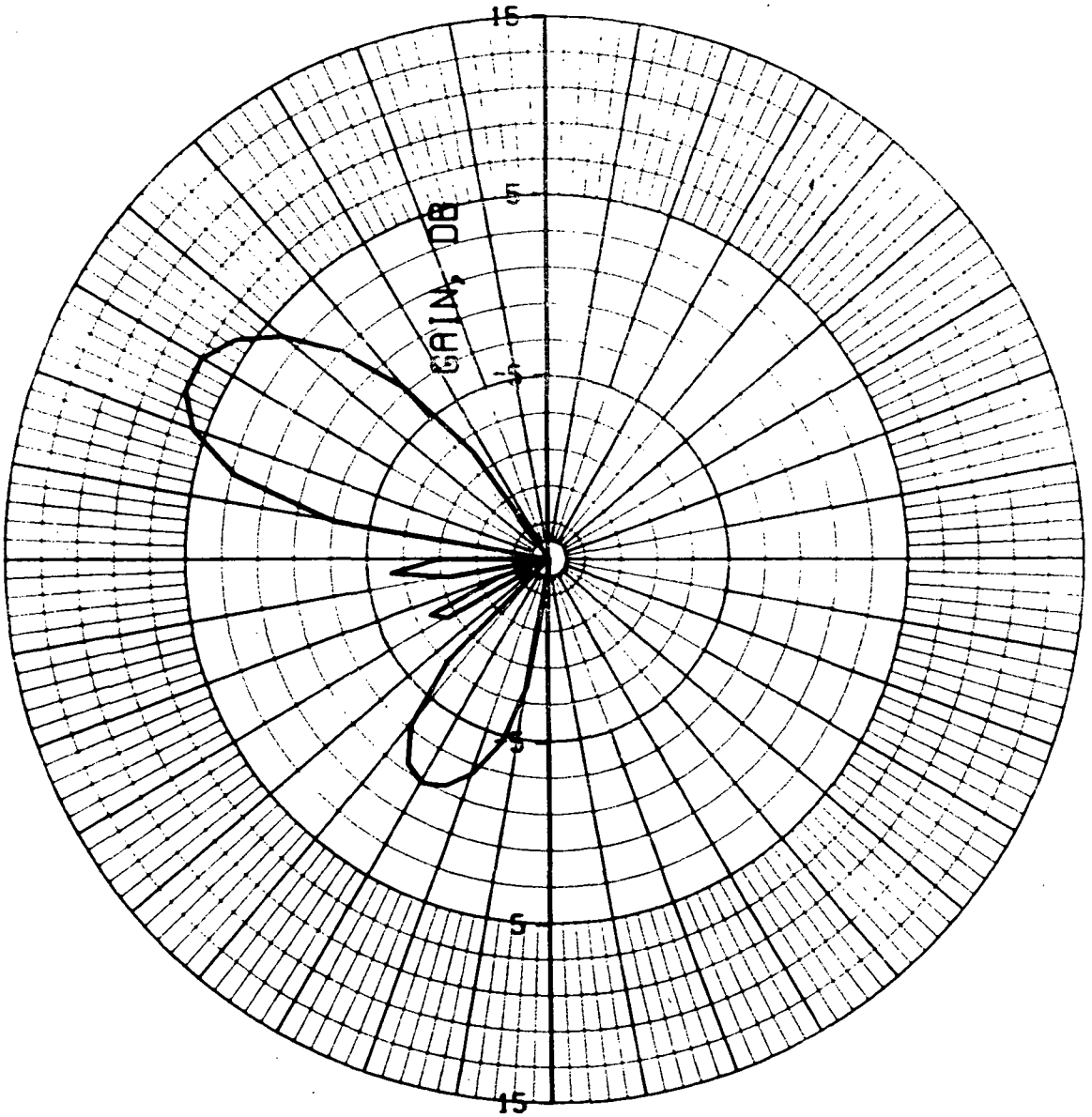

Gain = 6.92 db
Beamwidth = 21°
d/λ = .65

AVCO/SD
3.JUN.7

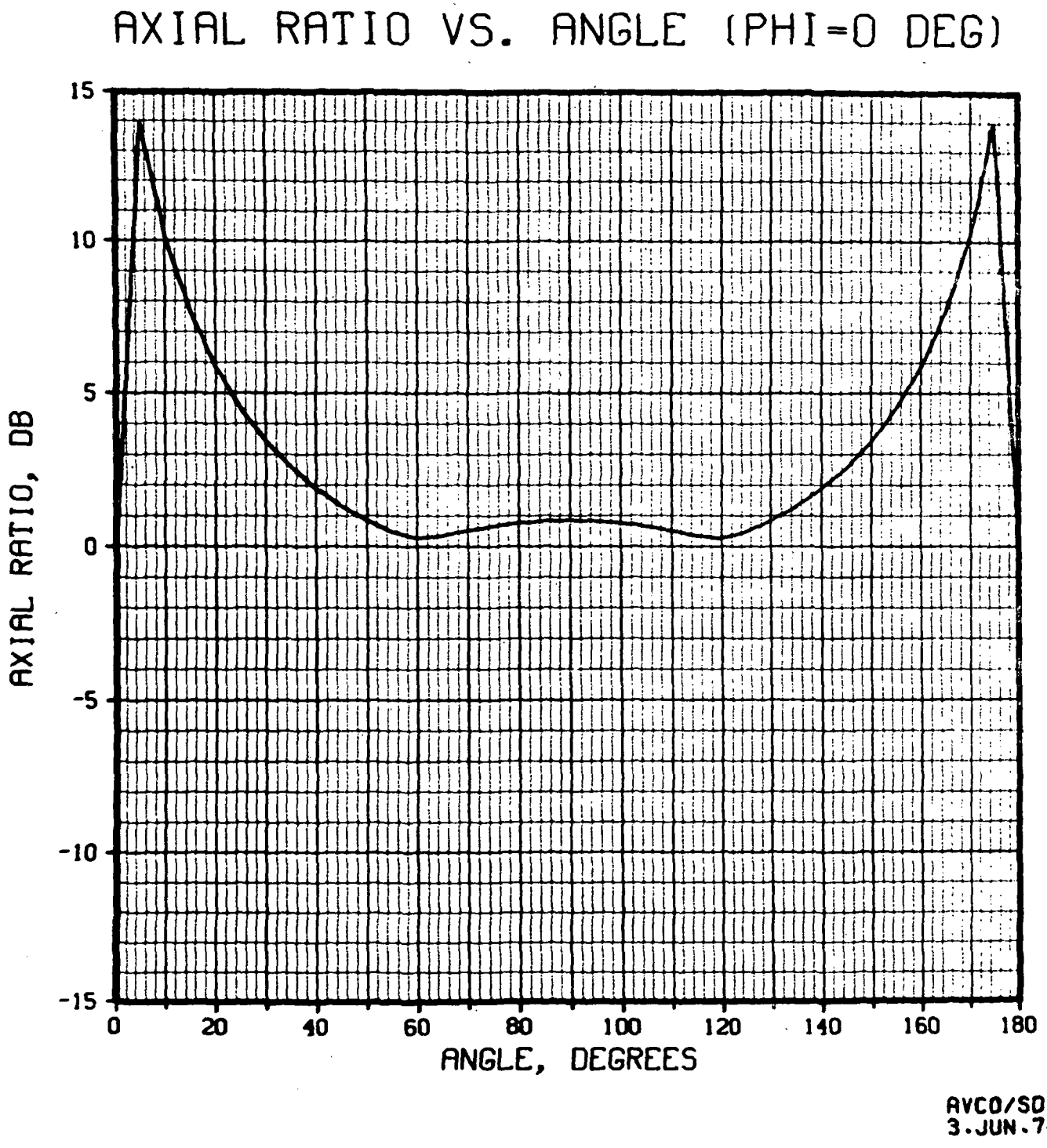
AXIAL RATIO VS. ANGLE (PHI=0 DEG)
AXIAL RATIO, DB
15
10
5
0
-5
-10
-15
0
20
40
60
80
100
120
140
160
180
ANGLE, DEGREES
AVCO/SD
3.JUN.7

ETHETA VS. ANGLE (PHI=0 DEG)

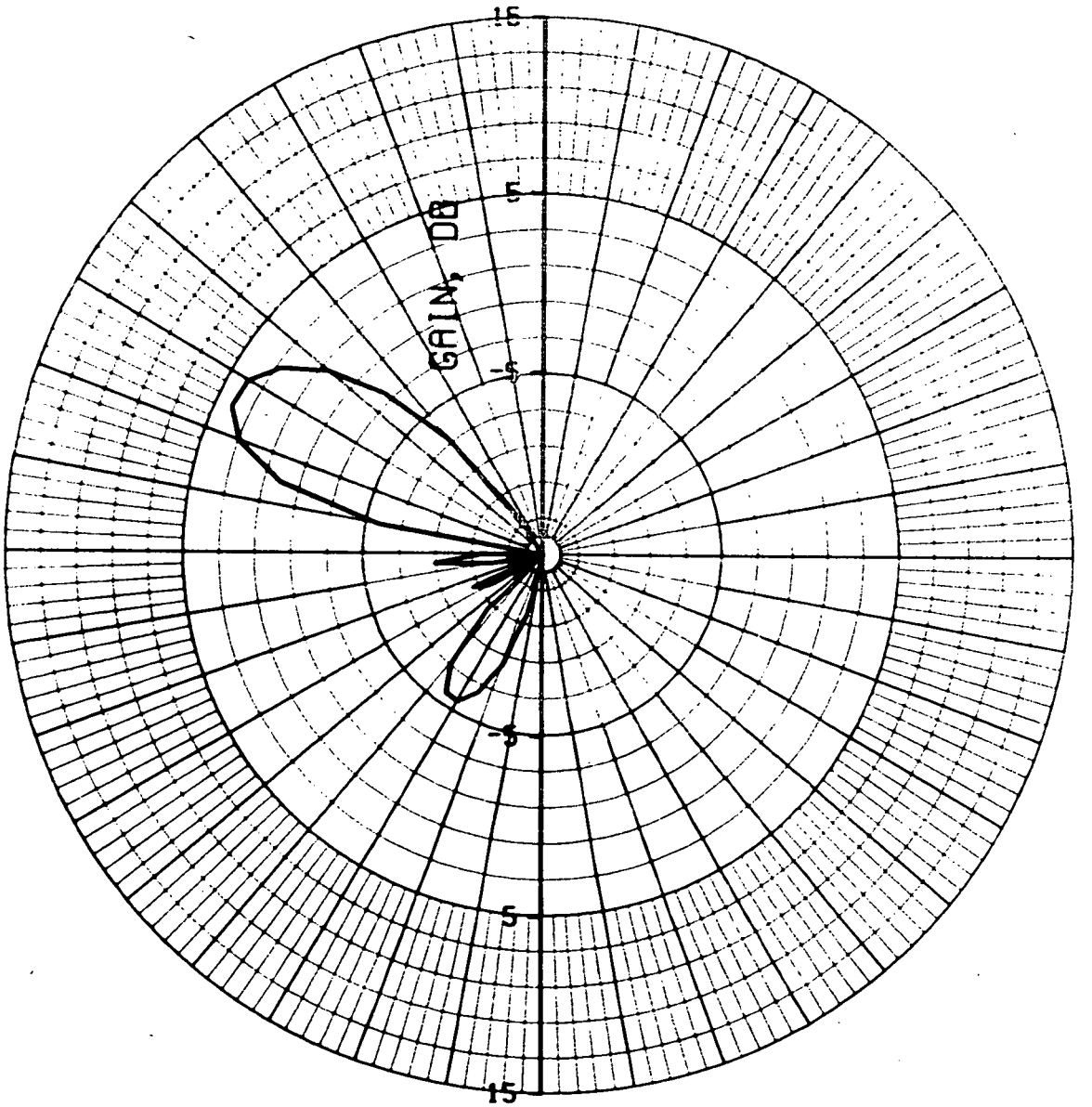

AVCO/SD
3.JUN.74

EPHI VS. ANGLE (PHI=0 DEG)

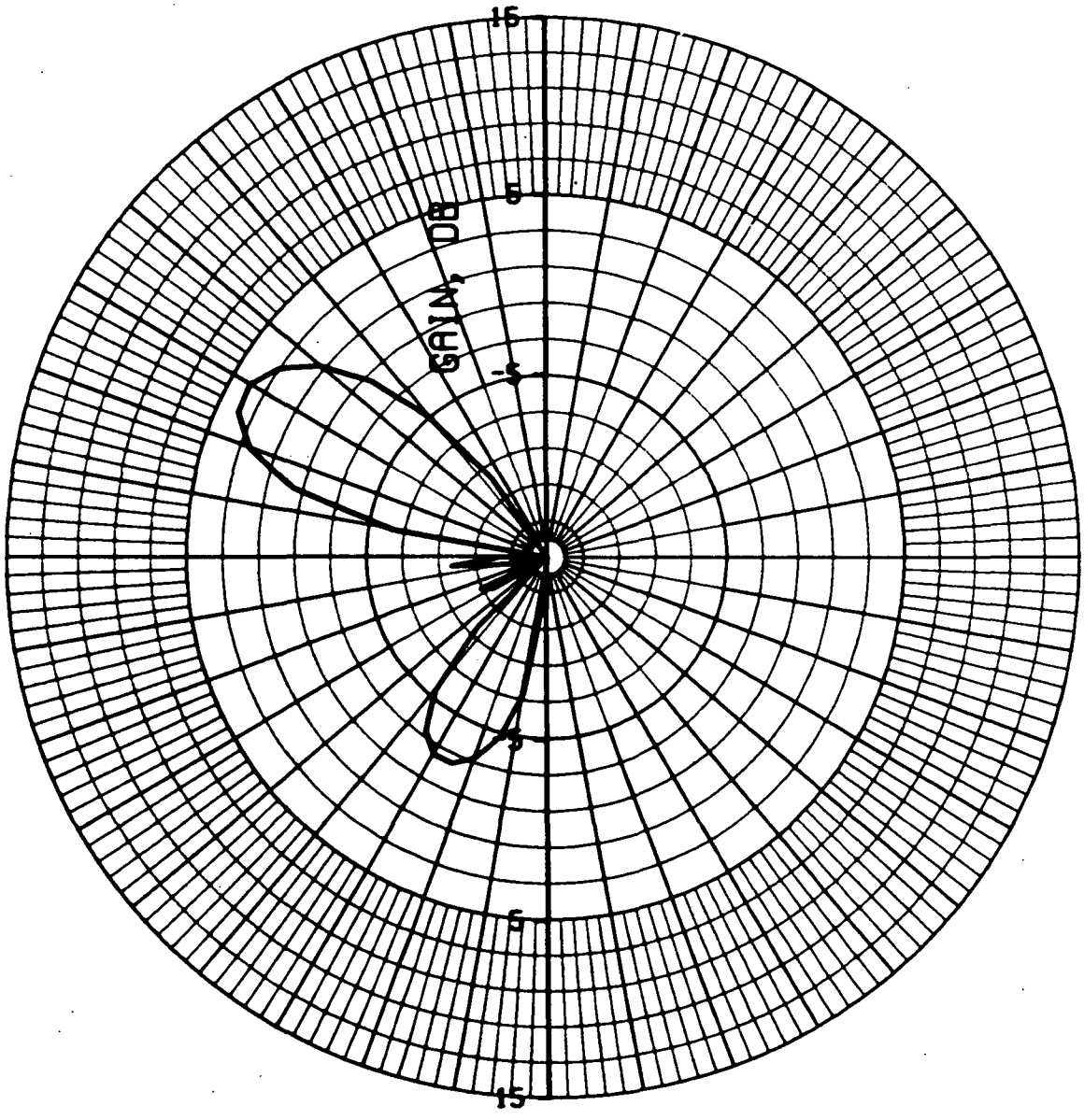

AVCO/SD
3.JUN.7

LEFT CIRCULAR POLARIZATION (PHI=0 DEG

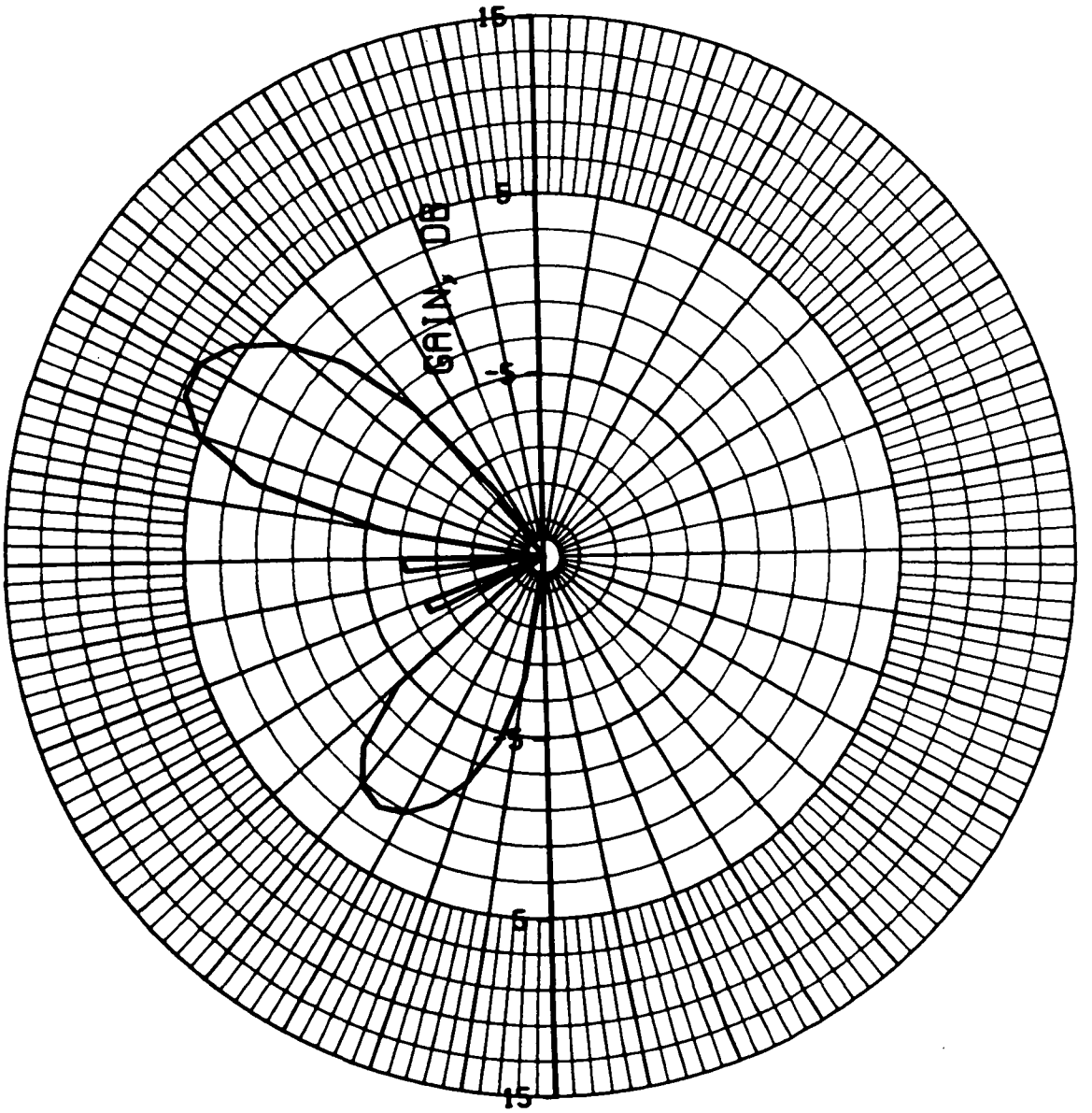

Gain = 7.0 db
Beamwidth = 16°
d/λ = .7

AVCO/S
5.JUN.

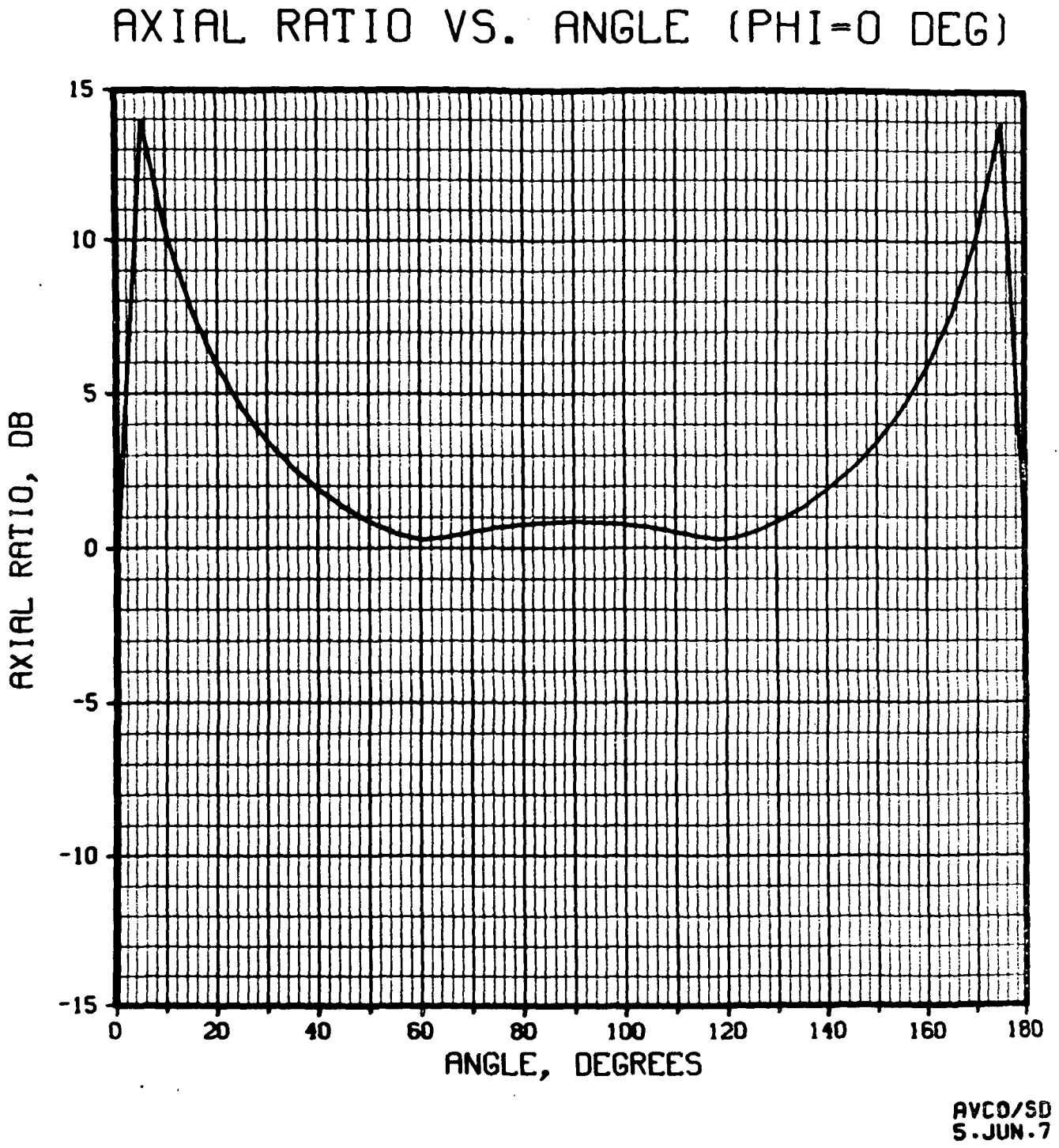
AXIAL RATIO VS. ANGLE (PHI=0 DEG)
AXIAL RATIO, DB
15
10
5
0
-5
-10
-15
0
20
40
60
80
100
120
140
160
180
ANGLE, DEGREES
AVCO/SD
5.JUN.7

ETHETA VS. ANGLE (PHI=0 DEG)

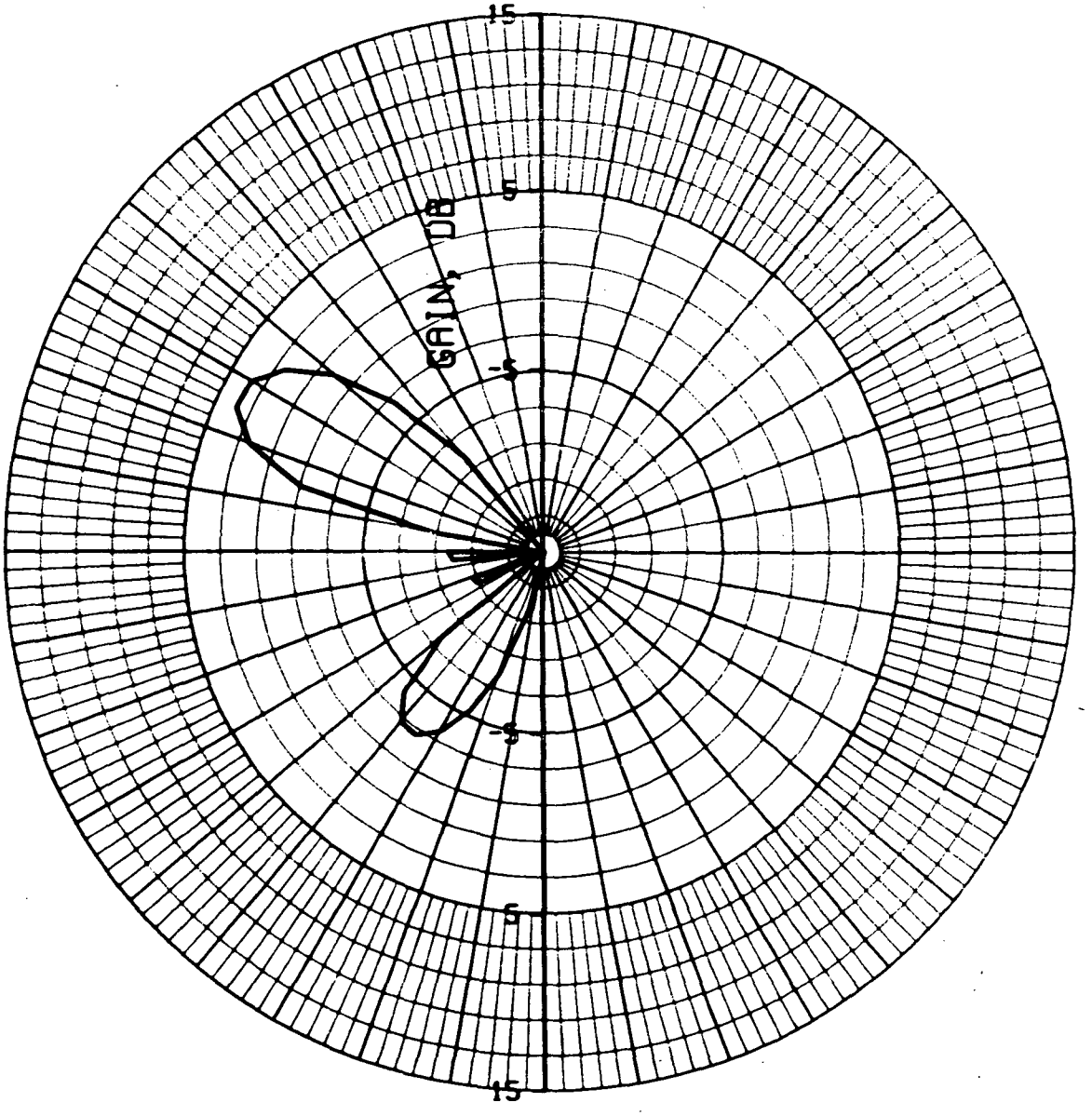

AVCO/SD
5.JUN.7

EPHI VS. ANGLE (PHI=0 DEG)

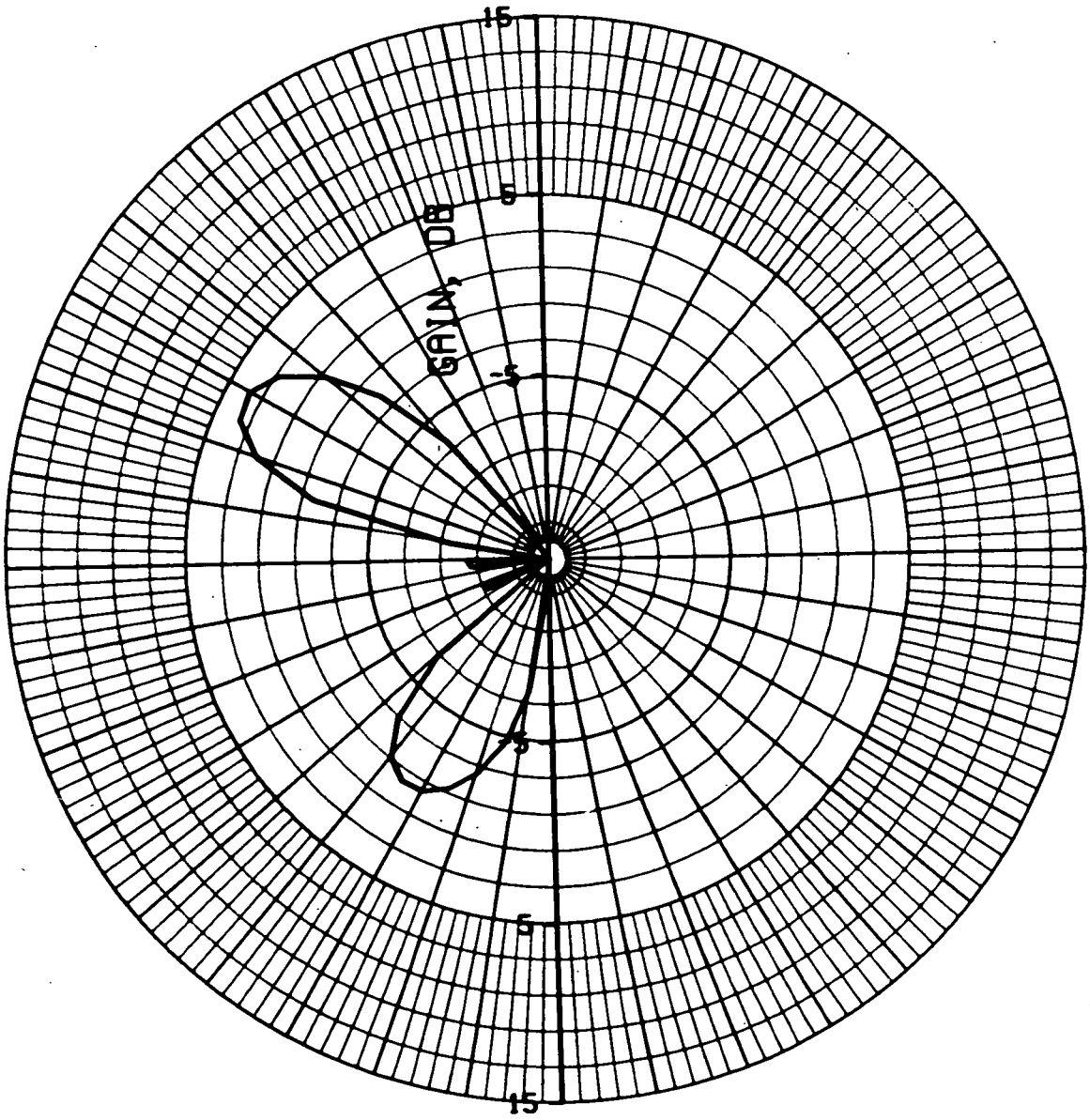

AVCO/S
5.JUN.

LEFT CIRCULAR POLARIZATION (PHI=0 DEG

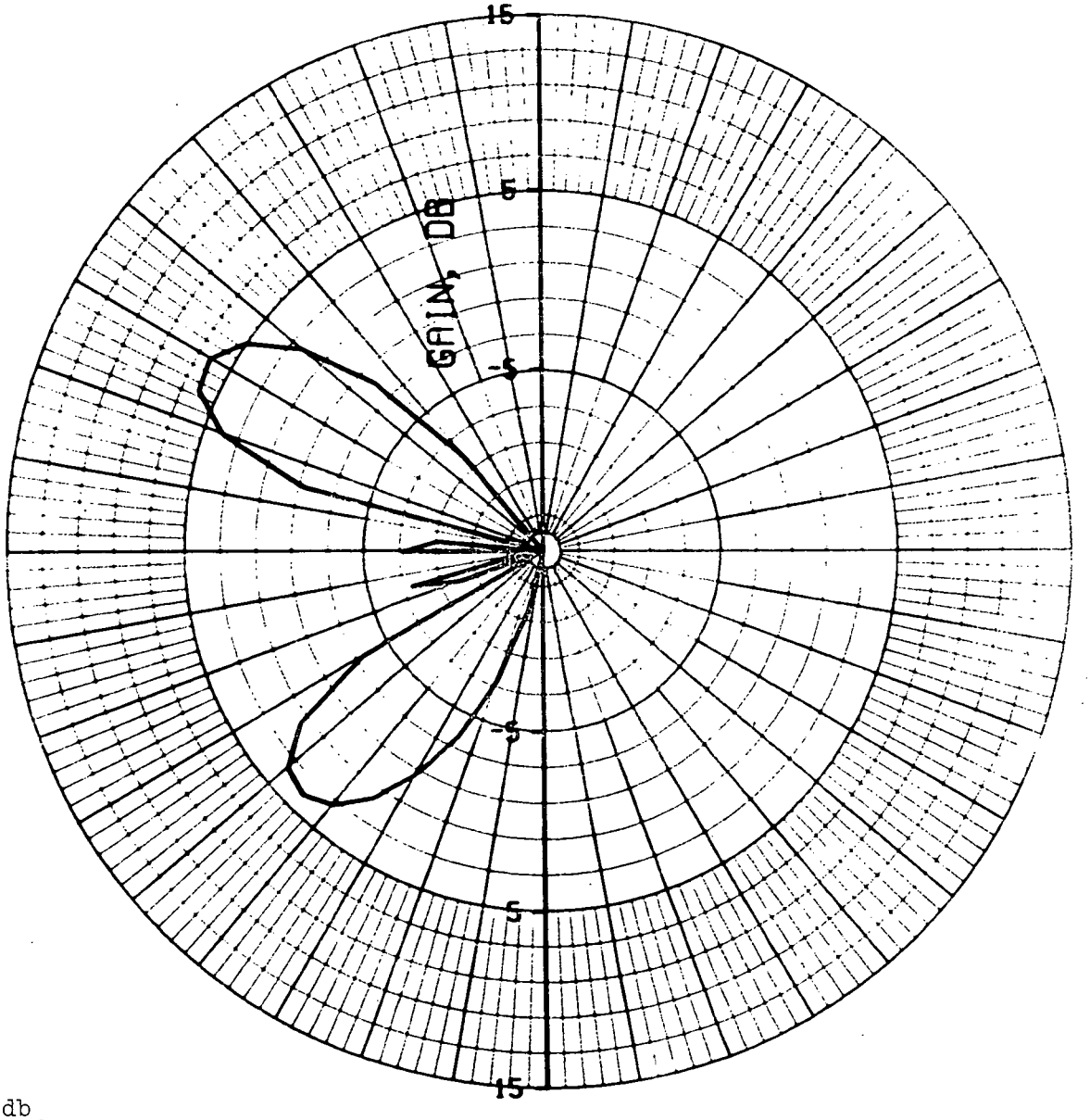

Gain = 6.30 db
Beamwidth = 18°
d/λ = .8

AVCO/SD
3.JUN.7

AXIAL RATIO VS. ANGLE (PHI=0 DEG)

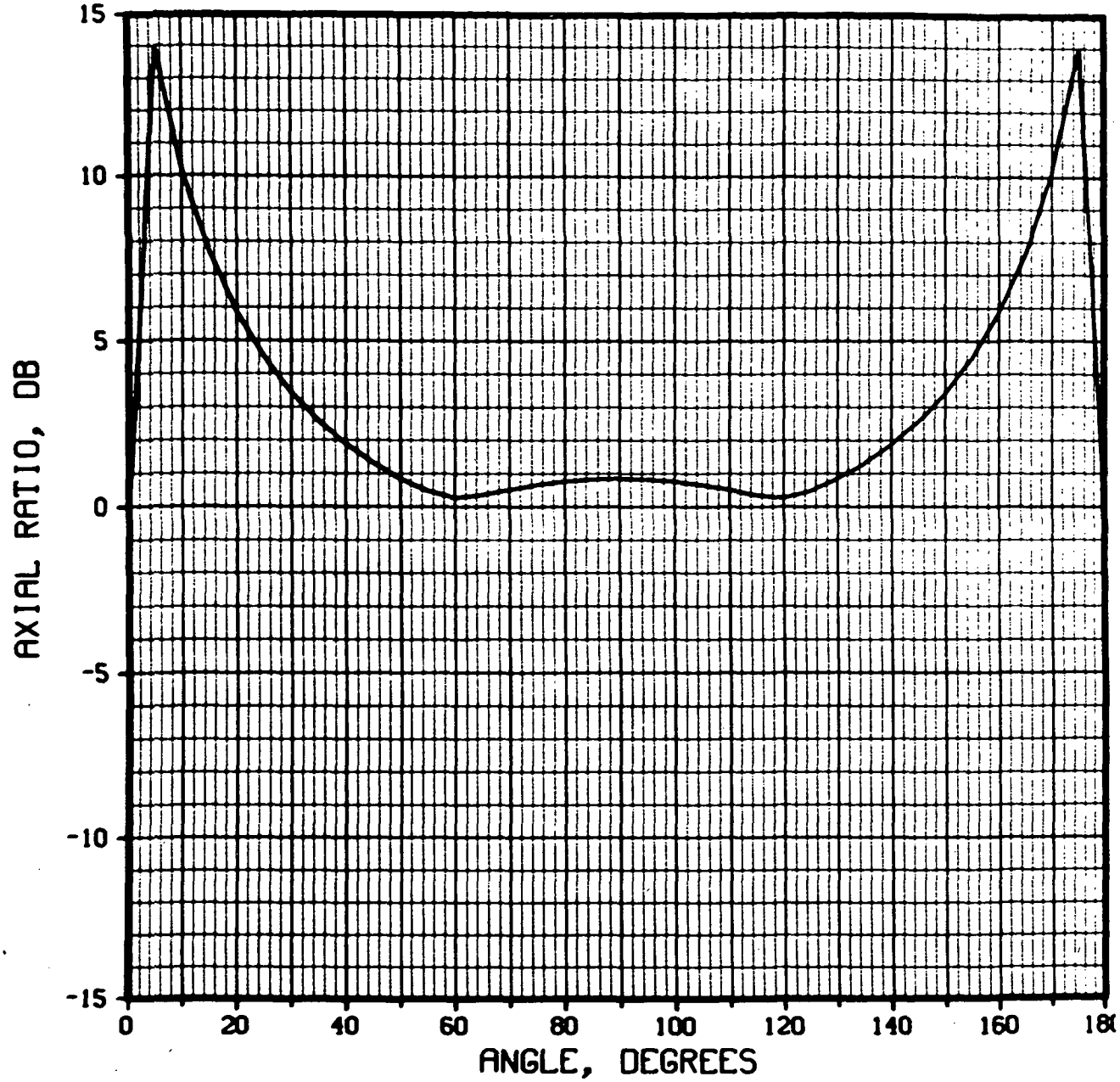

AVCO/S
3.JUN.

ETHETA VS. ANGLE (PHI=0 DEG)

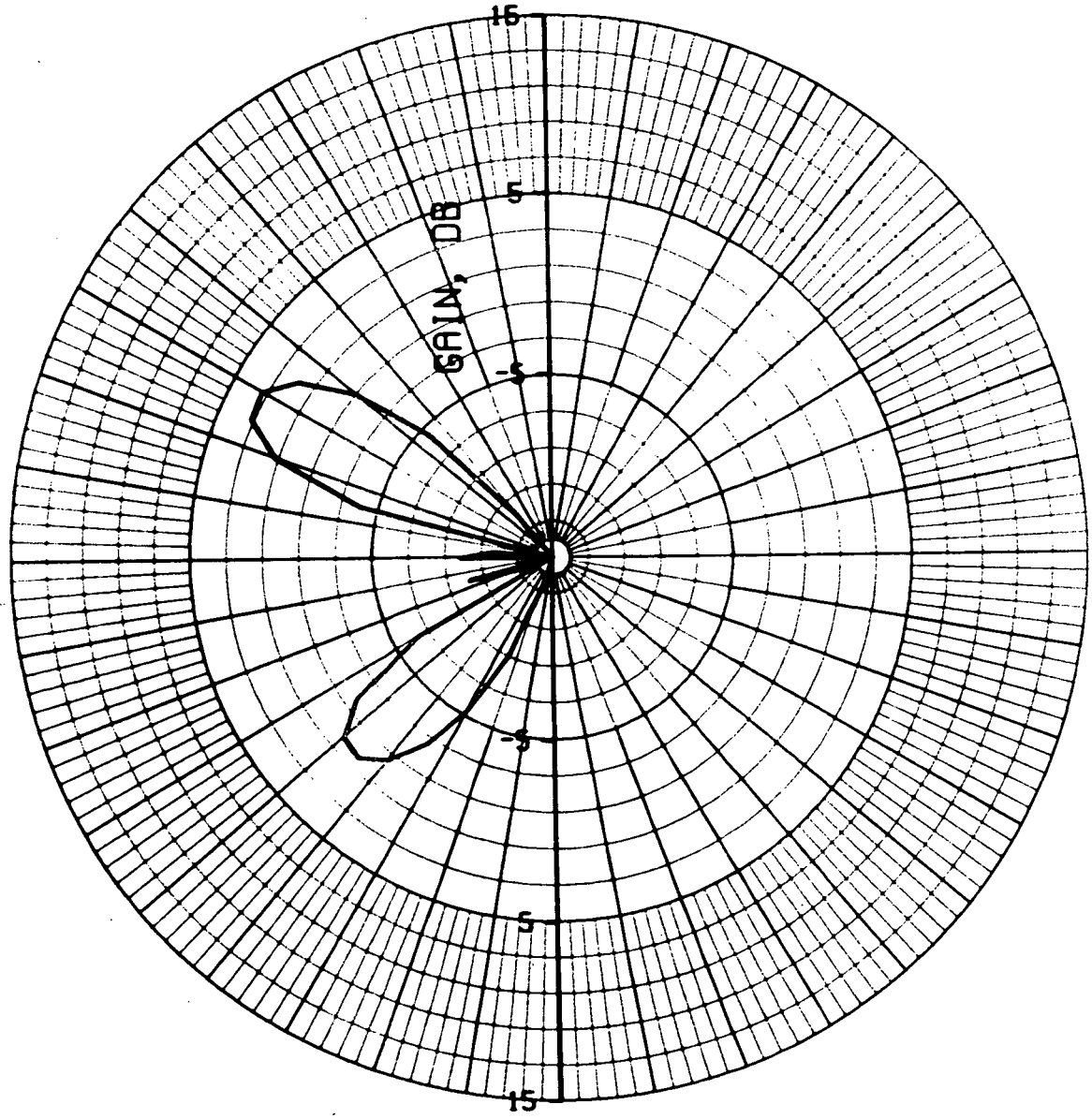

AVCO/S
3.JUN.

EPHI VS. ANGLE (PHI=0 DEG)

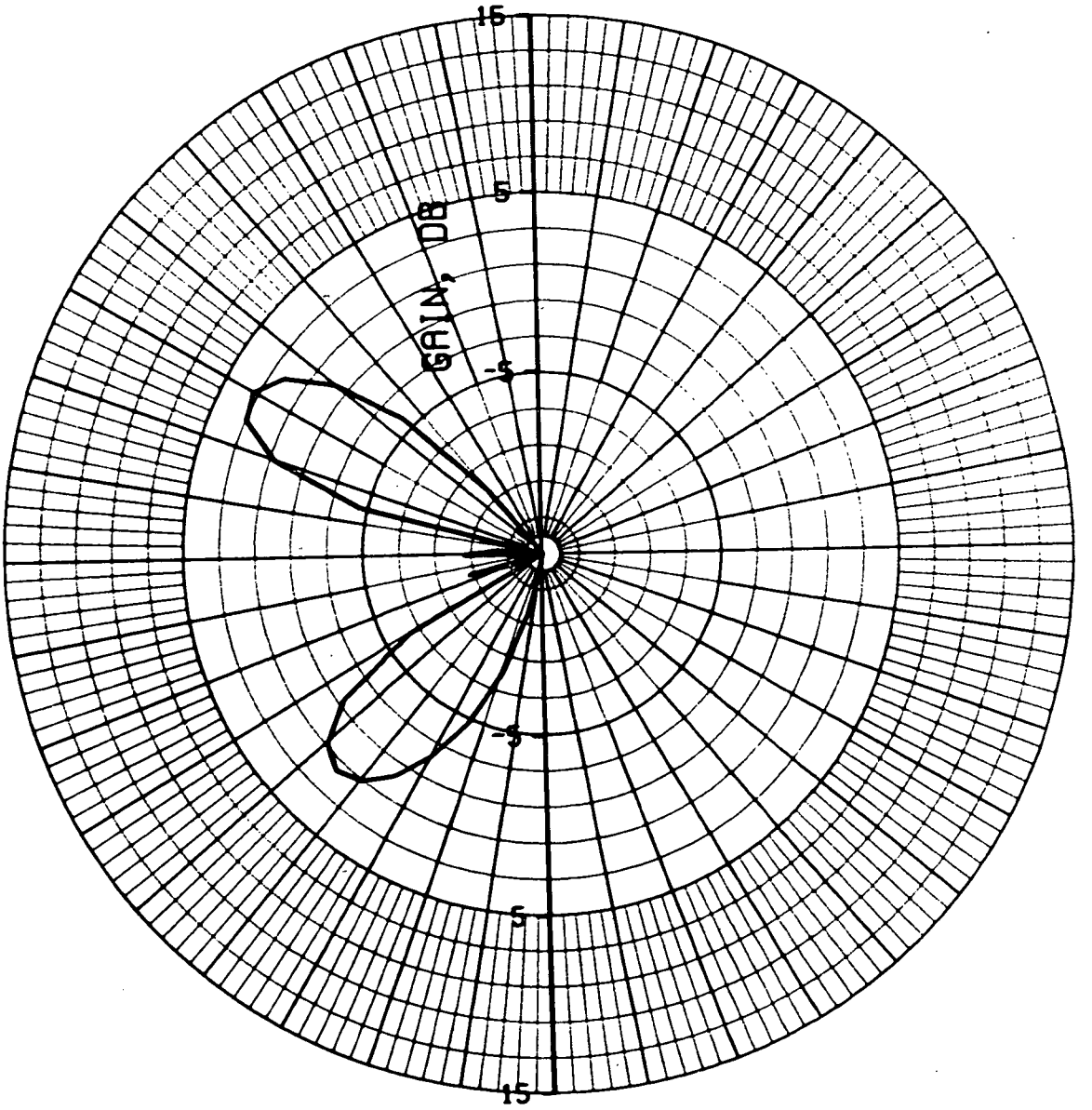

AVCO/SE
3.JUN.

Computed Radiation Patterns

Roll Plane

6 Element Circumferential Array

LEFT CIRCULAR POLARIZATION (THETA=90 DE

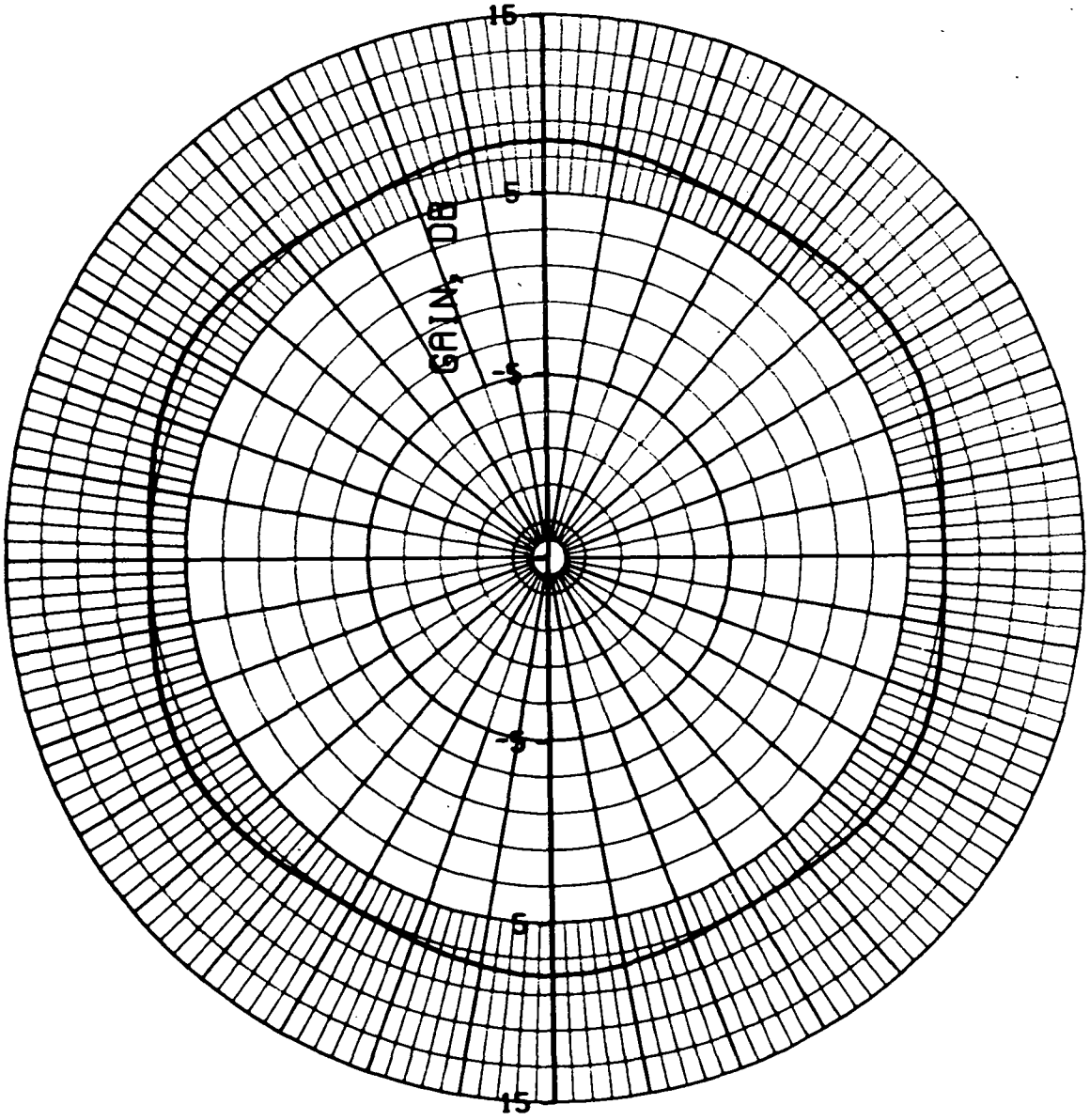

AVCO/SD
5.JUN.7

RIGHT CIRCULAR POLARIZATION (THETA=90 D

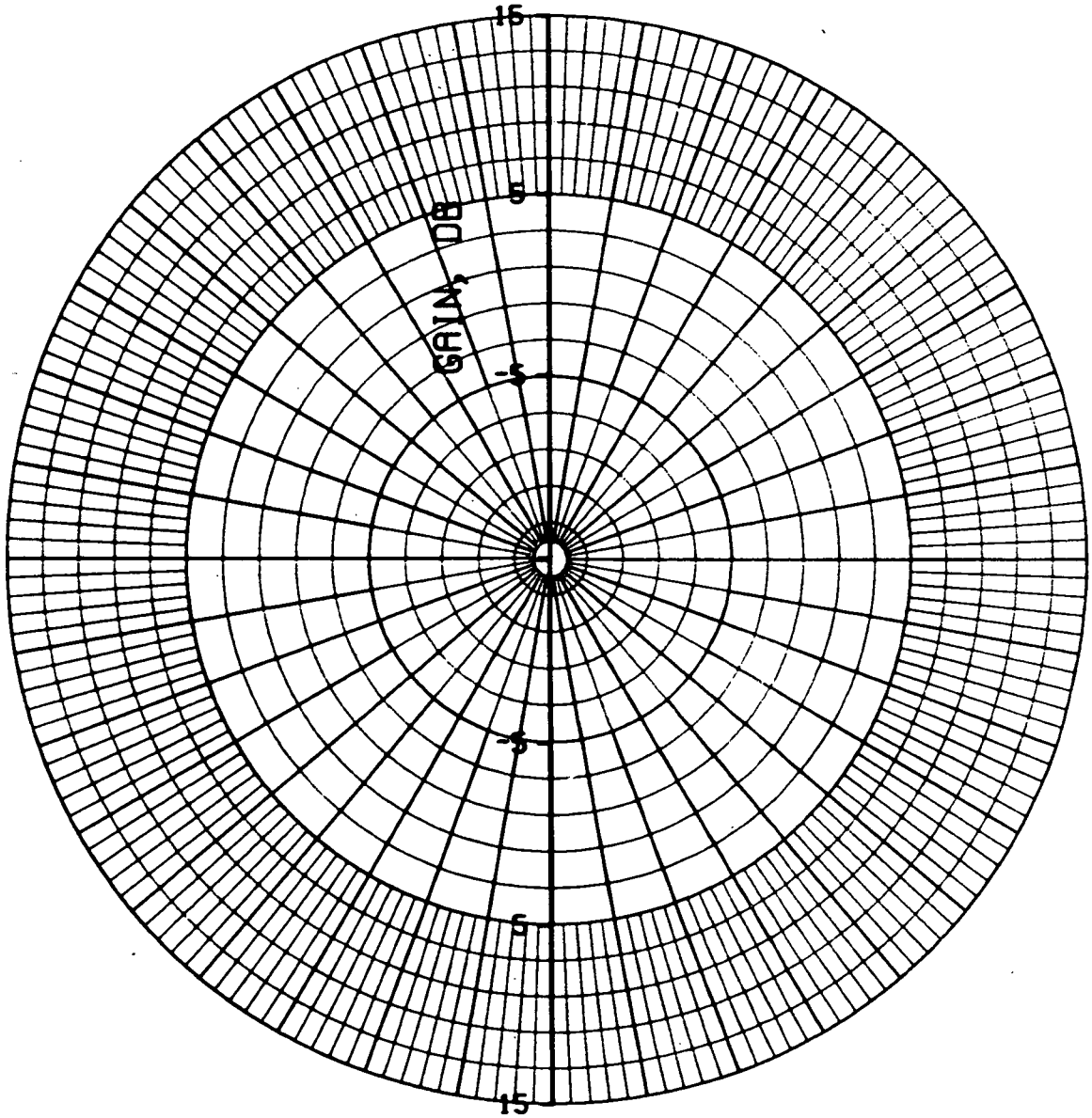

AVCO/S
5.JUN.

AXIAL RATIO VS. ANGLE (THETA=90 DEG

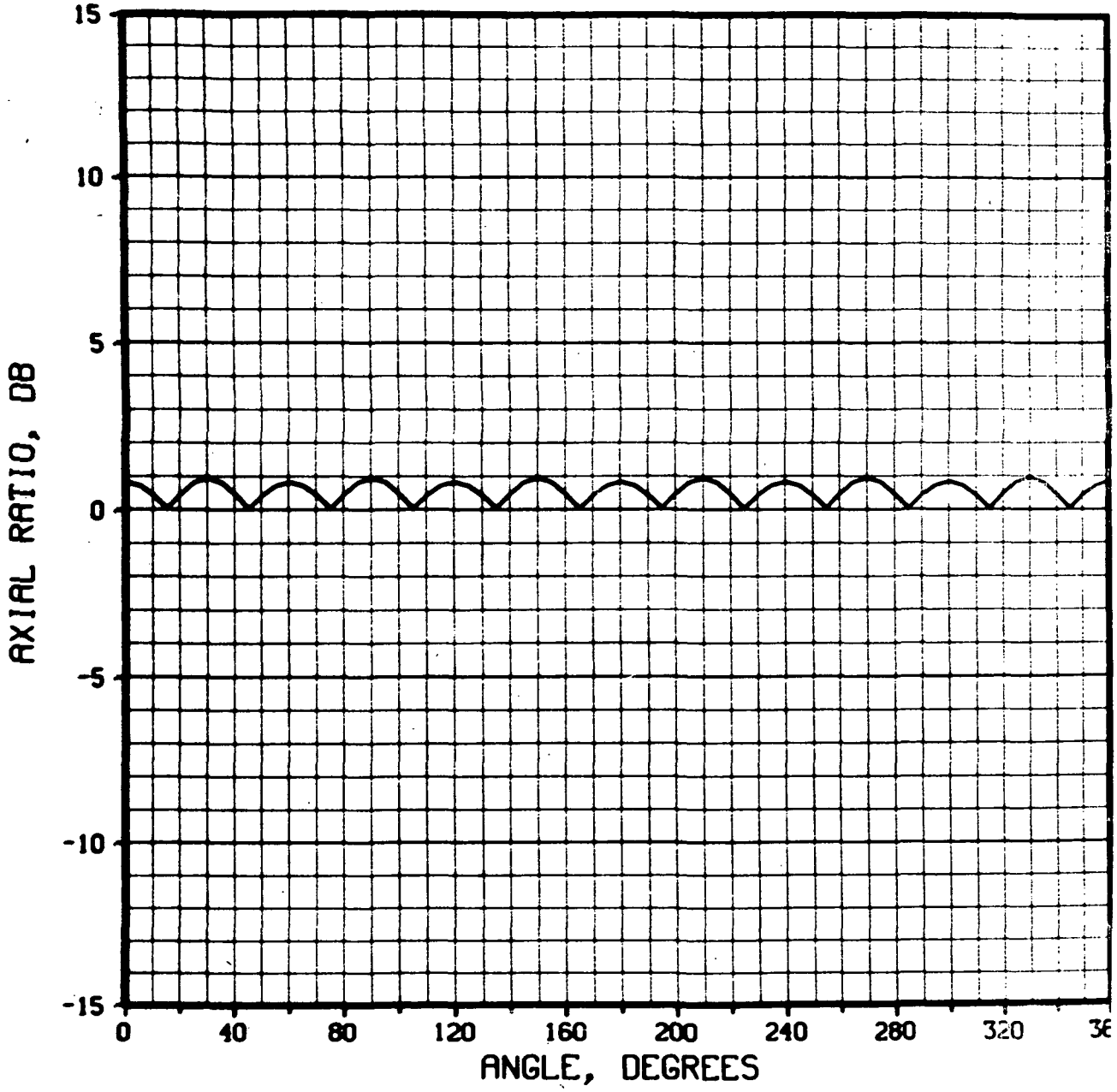

ETHETA VS. ANGLE (THETA=90 DEG)

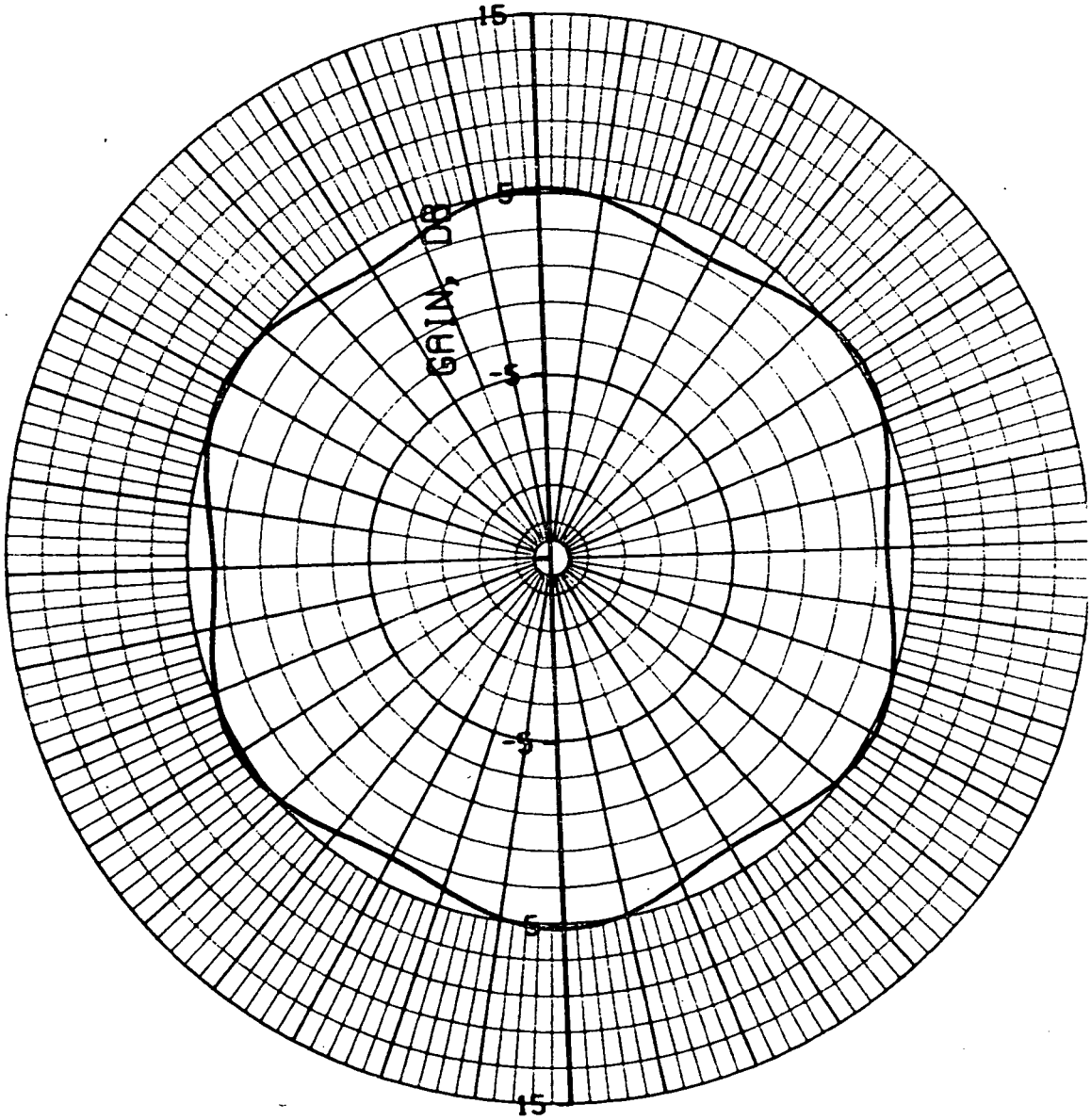

AVCO
5.JU

EPHI VS. ANGLE (THETA=90 DEG)

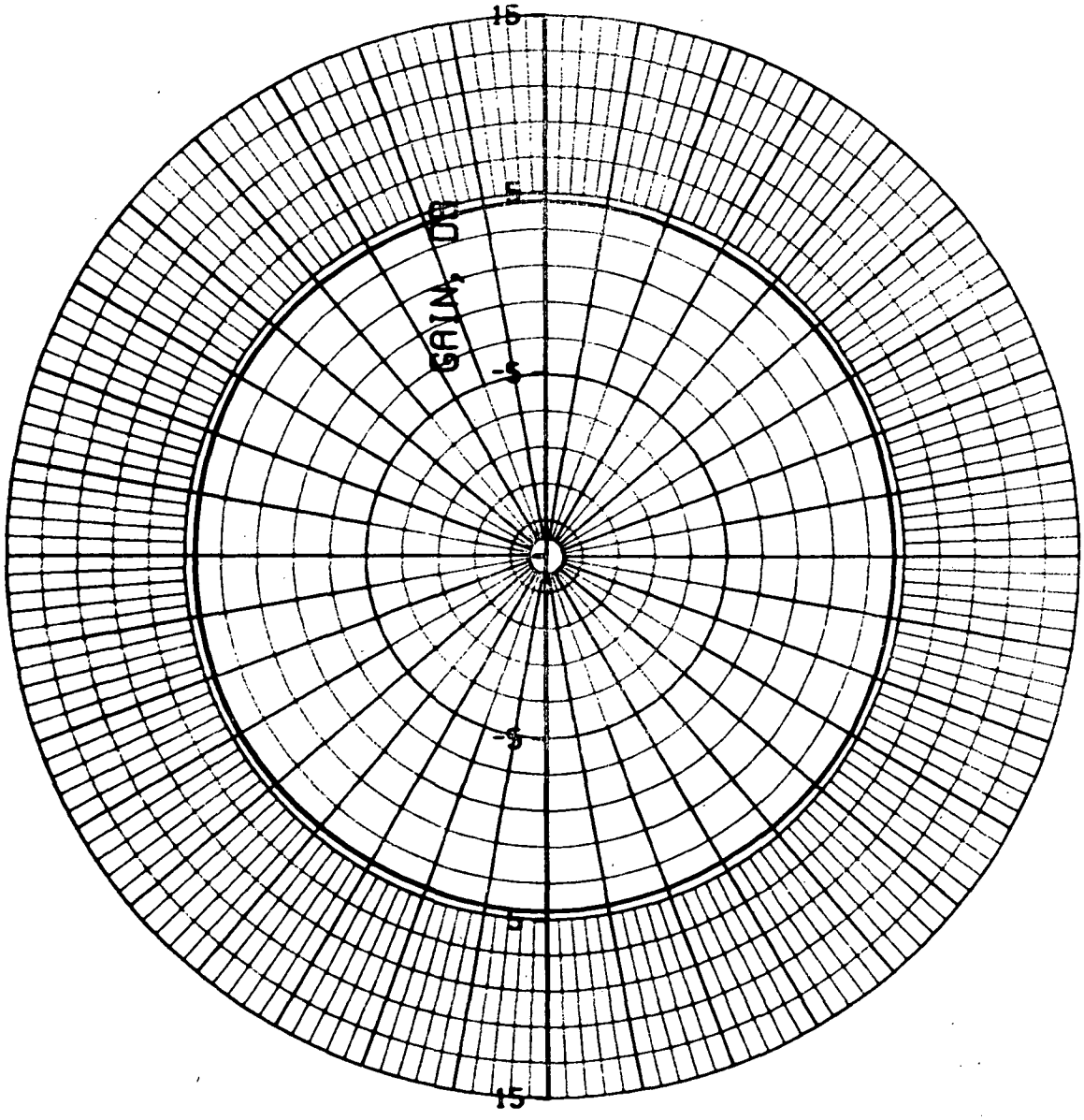

AVCO/
5.JUN